NATIONAL ENERGY TECHNOLOGY LABORATORY

Theoretical Review of the MFIX Fluid and Two-Fluid Models

February, 2020

U.S. DEPARTMENT OF ENERGY | NATIONAL ENERGY TECHNOLOGY LABORATORY

Office of Fossil Energy

DOE/NETL-2020/2100

Disclaimer

Keywords:
MFIX; Multiphase Flow; Computational Fluid Dynamics (CFD); Two-Fluid Model (TFM)

Suggested Citation: Jordan Musser and Janine Carney. *Theoretical Review of the MFIX Fluid and Two-Fluid Models*; DOE/NETL-2020/2100; NETL Technical Report Series; U.S. Department of Energy, National Energy Technology Laboratory: Morgantown, WV, 2020

Theoretical Review of the MFIX Fluid and Two-Fluid Models

Jordan Musser and Janine Carney

Research and Innovation Center, National Energy Technology Laboratory

---

DOE/NETL-2020/2100

February, 2020

NETL Contacts:

Jordan Musser, Principal Investigator

Jimmy Thornton, Associate Director, Computational Science & Engineering

Bryan Morreale, Executive Director, Research and Innovation Center

This page intentionally left blank

Table of Contents

Table of Contents ..... **i**

List of Figures ..... **iii**

List of Tables ..... **iv**

Nomenclature ..... **v**

Abbreviations and Acronyms ..... **vii**

Executive Summary ..... **viii**

Chapter 1 : Introduction **1**
1.1 Overview 1
1.2 Document Organization 2

Chapter 2 : Eulerian Fluid Phase Model **3**
2.1 Overview 3
2.2 Limitations 3
2.3 Volume Fraction Equation 3
2.4 Conservation Equations 4
2.4.1 Conservation of Mass 4
2.4.2 Conservation of Species Mass 4
2.4.3 Conservation of Momentum 5
2.4.4 Conservation of Internal Energy 6
2.5 Gas Phase Supplementary and Constitutive Equations 6
2.5.1 Gas Phase Equation of State 6
2.5.2 Gas Phase Stress 7
2.5.3 Porous Media / Semipermeable Surfaces 7
2.5.4 Turbulence 8
2.5.5 Diffusive Mass Transfer 9
2.5.6 Conductive Heat Transfer 9
2.5.7 Radiative Heat Transfer 9
2.5.8 Chemical Reaction Source Terms 10
2.6 Gas Phase Physical Properties 11
2.6.1 Mixture Molecular Viscosity 11
2.6.2 Mixture Molecular Weight 12
2.6.3 Mixture Specific Heat 12
2.6.4 Species Specific Enthalpy 12
2.6.5 Thermal Conductivity 13
2.6.6 Diffusivity 13

Chapter 3 : Eulerian Solids Phase Model (MFIX-TFM) **15**
3.1 Overview 15
3.2 Limitations 16
3.3 Conservation Equations 16
3.3.1 Conservation of Mass 16
3.3.2 Conservation of Species Mass 17

3.3.3 Conservation of Momentum 17
3.3.4 Conservation of Internal Energy 21
3.4 Solids Phase Supplementary and Constitutive Equations 22
3.4.1 Solids Phase Stress 22
3.4.2 Frictional Stress Models 25
3.4.3 Viscous Stresses 30
3.4.4 Momentum Transfer Between the Fluid and mth Phase 47
3.4.5 Momentum Transfer Between the mth and lth Dispersed Phases 50
3.4.6 Turbulence Effects 52
3.4.7 Diffusive Mass Transfer 52
3.4.8 Conductive Heat Transfer 52
3.4.9 Radiative Heat Transfer 53
3.4.10 Convective Heat Transfer 53
3.4.11 Chemical Reaction Source Terms 54
3.5 Solids Phase Physical Properties 56
3.5.1 Mixture Solids Density 56
3.5.2 Viscosity, Bulk Viscosity, and Pressure 57
3.5.3 Mixture Molecular Weight 57
3.5.4 Mixture Specific Heat 57
3.5.5 Species Specific Enthalpy 58
3.5.6 Thermal Conductivity 58
3.5.7 Diffusivity 61

References 62

Appendix A : Internal Energy Equations Derivation 81
A.1 Gas Phase Energy Equation. 81
A.2 Continuum Solids Phase Energy Equation. 84

Appendix B : Drag coefficients 87
B.1 Wen-Yu [146] 88
B.2 Gidaspow [73] 89
B.3 Gidaspow Blend [161] 90
B.4 Syamlal-O'Brien [167] 91

Appendix C : Nusselt Number Correlations 93
C.1 Gunn [137] 93
C.2 Ranz and Marshall [169] 93

Appendix D : Maximum Packing Correlations 94
D.1 Yu and Standish [172] 94
D.2 Fedors and Landel [173] 94

List of Figures

Figure 3-1: Schematic of the transition between the quasi-static/frictional regime and the kinetic regime [50]. 22

Figure 3-2: Schematic illustrating the instantaneous onset of frictional stresses when the solids packing surpasses a close pack condition. 25

Figure 3-3: Schematic illustrating the blending function around the critical void fraction (void fraction at maximum packing). 27

Figure 3-4: Bed thermal conductivity, $\boldsymbol{\kappa b}$ given by equation (3-83), is shown as a function of gas phase volume fraction. The gas phase thermal conductivity, $\boldsymbol{kg}$ is evaluated at several temperatures (300K – 2100K) using equation (2-26) and with all values shown as a single gray line. The constant solids material conductivity, $\boldsymbol{kp = 1.0\ W/(m.K)}$, is plotted as a dashed line. The bed conductivity is bounded above by $\boldsymbol{kp}$, for physical volume fractions ($\boldsymbol{\varepsilon g > 0.25}$), and decreases with increasing gas volume fraction. 61

List of Tables

Table 2-1: Default values for the MFIX k-ϵ model constants [26] 9

Table 2-2: Default values for Sutherland's Law model constants [29] 12

Table 2-3: Default values for temperature dependent thermal conductivity (See $8.B_1$ Computation of the Prandtl Number for Gases at Low Density, p263 [30]) 13

Table 2-4: Default values for temperature and pressure dependent diffusion based on CO_2 in N_2 (See Table 16.2-2 Experimental diffusivities of some dilute gas pairs, p503 [30]) 14

Table 3-1: Default values for Schaeffer model [55] 27

Table 3-2: Blending functions available in MFIX[1] 28

Table 3-3: Default values for Princeton Model constants [53, 67] 29

Table 3-4: Comparison of kinetic theory models available in MFIX 32

Table 3-5. Radial distribution functions at contact available in MFIX 40

Table C-1: Nusselt number heat transfer correlation availability in MFIX. 93

Nomenclature

Latin Symbols:

C_{pg}, C_{pm}	gas / m^{th} phase mixture specific heat
$\mathcal{D}_{gn}$, $\mathcal{D}_{mn}$	gas / m^{th} phase n^{th} species diffusion coefficient
d_m	diameter of m^{th} disperse phase particle
g	body force due to gravity
h_{gn}, h_{mn}	gas / m^{th} phase n^{th} species specific enthalpy
j_g, j_m	gas / m^{th} phase species mass flux
MW	molecular weight
P_g, P_m	gas / m^{th} phase pressure
q_g, q_m	gas / m^{th} phase conductive heat flux
R	gas constant (8314.56 $Pa \cdot m^3 \cdot kmol^{-1} \cdot K^{-1}$)
$\left[R_{gn}\right]_p$	gas phase n^{th} species rate of formation per unit volume from p^{th} reaction
$[R_{mn}]_p$	m^{th} phase n^{th} species rate of formation per unit volume from p^{th} reaction
R_{gn}, R_{mn}	gas / m^{th} phase n^{th} species rate of formation per unit volume
$\mathcal{R}_p$	user-defined reaction rate for the p^{th} reaction
S_g, S_m	gas / m^{th} phase general source term
S_{gij}, S_{mij}	gas / m^{th} phase deviatoric rate-of-strain tensor
T_g, T_m	gas / m^{th} phase temperature
T_{Rg}, T_{Rm}	gas / m^{th} phase radiative heat transfer temperature
U_g, U_m	gas / m^{th} phase velocity
X_{gn}, X_{mn}	gas / m^{th} phase n^{th} species mass fraction

Greek Symbols:

$\alpha_{n,p}$	signed stoichiometric coefficient of the n^{th} gas phase species for the p^{th} reaction
β	drag coefficient
δ_{ij}	Kronecker delta
γ_{Rg}, γ_{Rm}	gas / m^{th} phase radiative heat transfer coefficient
ε_g	fluid (gas) phase volume fraction, also commonly referred to as the 'void' fraction
ε_m	m^{th} disperse (solids) phase volume fraction
ε_s	total disperse phase volume fraction
Θ_m	m^{th} phase granular temperature
κ_g, κ_m	gas / m^{th} phase thermal conductivity

$\lambda_{g,eff}$	gas phase effective second viscosity
λ_m	m^{th} phase second viscosity
μ_{bm}	m^{th} phase bulk viscosity
μ_e	gas phase eddy viscosity
μ_g	gas mixture molecular viscosity
$\mu_{g,eff}$	gas phase effective dynamic viscosity
μ_m	m^{th} phase viscosity
ρ_g, ρ_m	gas / m^{th} phase density
τ_{gij}, τ_{mij}	gas / m^{th} phase stress tensor

Abbreviations and Acronyms

CFD	computational fluid dynamics
CI	continuous integration
CV	control volume
CVS	concurrent versioning system
DEM	discrete element model
DES	discrete element simulation
EE	Eulerian-Eulerian
GUI	graphical user interface
LES	large eddy simulation
METC	Morgantown Energy Technology Center
MFIX	Multiphase Flow with Interphase eXchanges
MFS	Multiphase Flow Science
MMS	method of manufactured solutions
MPPIC	multiphase particle in cell
NETL	National Energy Technology Laboratory
PIC	particle-in-cell
TFM	two-fluid method

Executive Summary

MFIX (Multiphase Flow with Interphase eXchanges) is a general purpose code that can be used for describing the hydrodynamics, chemical reactions, and heat transfer of dense or dilute multiphase fluid flows. MFIX calculations give detailed information on pressure, temperature, composition, and velocity distributions in the defined system. This report provides an overview of MFIX's expressions for single phase flow and continuous dispersed multiphase flow (i.e., the two-fluid model). In addition to the two fluid model (MFIX-TFM), MFIX contains a discrete element model (MFIX-DEM) and a multi-phase particle in cell model (MFIX-PIC) that are not reviewed within this document.

MFIX, developed at the National Energy Technology Laboratory (NETL), has the following capabilities: mass and momentum balance equations for a single continuous fluid phase and multiple dispersed solids phases; energy equations for each phase; an arbitrary number of species balance equations for each of phase; a user friendly chemistry; a three-dimensional Cartesian coordinate system with Cartesian cut cell application for complex geometry; nonuniform mesh size; impermeable and semipermeable internal surfaces; a user-friendly GUI (graphical user interface) for setting up the simulation; multiple, single-precision, binary, direct-access, output files that minimize disk storage and accelerate data retrieval; and extensive error reporting. For MFIX-TFM, the code also includes granular stress equations based on kinetic and frictional flow theory.

Chapter Two presents the continuous phase model which traditionally represents a gas or liquid phase. The continuous phase may be run by itself as single phase CFD or coupled with one of the disperse (e.g., solids) models for coupled multiphase flows. Chapter Three outlines the Eulerian two fluid model (MFIX-TFM), wherein the additional dispersed phases are inherently characterized as solids. The literature on the conservation equations and constitutive relations is briefly surveyed, and different parts of the model are highlighted.

Chapter 1: Introduction

MFIX is a general purpose code written in Fortran and used for describing the hydrodynamics, heat transfer, and chemical reactions in dense or dilute fluid-solids flows. The objective of the Multiphase Flow Science (MFS) group is to create a tool to aid in the understanding, design, optimization, and scale-up of multiphase systems such as gasifiers, carbon capture devices, and chemical looping reactors.

1.1 Overview

Development of MFIX started at the Morgantown Energy Technology Center (METC) in 1991 as a continuation of a multi-particle version [1] of the Eulerian-Eulerian (EE) code of Gidaspow and Ettehadieh [2]. The initial MFIX release was completed in 1993 and contained only the two-fluid model, MFIX-TFM. Public distribution was handled through the Energy Science and Technology Software Center starting in 1995. Afterwards the code underwent several revisions whereby high-resolution discretization methods were added, the source code was migrated from FORTRAN 77 to Fortran 90, and it was parallelized to run on shared memory and distributed memory systems [3]. Further advancements include the inclusion of a $k-\epsilon$ turbulence model [4], Cartesian cut cells for complex geometries [5], a stiff chemistry solver, variable solids density [6], and a number of kinetic theories for granular flows [7, 8, 9, 10, 11].

A Lagrangian solids model was implemented in 2004 whereby the position and trajectory of each solids particle is tracked through resolving all particle collisions via a soft-sphere spring-dashpot model [12]. The discrete element model, MFIX-DEM, is capable of pure granular simulations in addition to being coupled with an Eulerian (e.g., gas or liquid) phase model. DEM modeling uses fewer and less complex closures than the TFM and is therefore considered to contain less overall uncertainty. However, the computational intensity of tracking particles limits its application to small-scale devices. Recent efforts have included verification and validation studies [13, 14], dynamic solids inventory capabilities, and the inclusion of species and energy conservation equations [15]. Moderate-sized investigations containing tens of millions of particles were made possible by recent distributed [16] and shared memory [17] parallelization efforts.

A second Lagrangian solids model, MFIX-PIC, was implemented in 2013 [18] and has since undergone substantial revisions. The multiphase particle in cell (PIC) technique uses parcels for the solids where a parcel may represent a fraction of one particle or thousands of individual particles. This approach is more computationally efficient than other Lagrangian solids models because collisions are not resolved, but rather approximated using frictional stress model and averaged field quantities. Uncertainty in PIC models arises from the closure needed for the solids interaction terms, the need for accurate interpolation between the Eulerian and Lagrangian frames of reference, and a strong dependence on model implementation. However, this approach

offers the potential to shorten the time-to-solution making it ideal for initial design investigations for large multiphase devices where accuracy is not paramount.

MFIX development activities have been preserved through a concurrent versioning system (CVS) since 1999 to track source code changes. The CVS database was transferred to a Git® repository in 2014 to accommodate a more flexible development. Direct code access supports efforts to extend the reach of MFIX by encouraging greater community involvement in development and maintenance activities.

The integrity of the source code was originally maintained through nightly regression tests where a subset of tutorial and test cases was executed and the results compared to a fixed solution set [3]. This approach was replaced by a continuous integration (CI) server to expand the testing capabilities by running all tests and tutorials any time modifications are committed to the source code repository.

1.2 Document Organization

Chapter Two presents the continuous phase model which traditionally represents a gas or liquid phase. The continuous phase may be run by itself as single phase CFD or coupled with one of the disperse (e.g., solids) models for coupled multiphase flows. Chapter Three outlines the Eulerian two fluid model (MFIX-TFM), wherein the additional dispersed phases are inherently characterized as solids.

Chapter 2: Eulerian Fluid Phase Model

2.1 Overview

This chapter presents the MFIX Eulerian continuous fluid phase model. The fluid phase is referred to throughout this document as the *gas phase*, however it could also be a liquid. The fluid phase model presented here is done so in the context of a multiphase system. As a result, phasic volume fractions and interphase transfer terms arise in the governing equations. For single phase flow, the gas phase volume fraction is one and interphase transfer terms are generally zero[1]. The fluid phase model is consistent across the multiphase models, (MFIX-TFM, MFIX-DEM, and MFIX-PIC), unless specifically noted. It is also worth noting that here, and in the two fluid model section, the equations are presented in conservative form, however, in MFIX the equations are solved in non-conservative. The non-conservative form is obtained by subtracting the respective continuity equation from the conservative form.

2.2 Limitations

Limitations of the MFIX fluid phase model include:

- The fluid is incompressible (divergence free).
- The entire flow domain must contain the fluid phase such that the fluid phase volume fraction is always greater than zero.

2.3 Volume Fraction Equation

To derive the MFIX equations that describe multiphase flows, point variables are averaged over a region that is large compared with particle spacing but much smaller than the flow domain [19]. This results in phasic volume fractions that specify the fractions of the average volume occupied by each phase. The *volume fractions* are assumed to be continuous functions of space and time, and by definition, must sum to one. Therefore, for a system containing a gas phase and M disperse phases, the gas phase volume fraction, ε_g, is

$$\varepsilon_g = 1 - \varepsilon_s, \tag{2-1}$$

where, for later convenience, the notation ε_s is introduced representing the total volume fraction of the M dispersed phases (e.g., the total *solids* volume fraction):

[1] Here single phase flow generally implies that the gas volume fraction is one and no interphase transfer occurs. However, single phase flows through a porous media are permitted wherein the gas volume fraction may have values other than one and interphase transfer is possible.

$$\varepsilon_s = \sum_{m=1}^{M} \varepsilon_m \tag{2-2}$$

and ε_m is the m^{th} disperse phase volume fraction. The gas phase volume fraction is one in a single phase system (i.e., $\varepsilon_g = 1$ and $\varepsilon_s = \varepsilon_m = 0$).

2.4 Conservation Equations

This section presents the basic set of gas phase conservation equations solved by MFIX.[2] The equations, with the exception of the internal energy equation, are presented in conservative form, however, as already noted, the numerical implementation uses the non-conservative forms.

2.4.1 Conservation of Mass

The conservation of mass (i.e., the continuity equation) for the gas phase is

$$\frac{\partial}{\partial t}\left(\varepsilon_g \rho_g\right) + \frac{\partial}{\partial x_j}\left(\varepsilon_g \rho_g U_{gj}\right) = \sum_{n=1}^{N_g} R_{gn} + \mathcal{S}_g \tag{2-3}$$

where ρ_g is the gas phase density, ε_g is the gas phase volume fraction, U_{gj} is the j^{th} component of the gas phase velocity, N_g is the number of chemical species comprising the gas phase, R_{gn} is the rate of formation per unit volume of the n^{th} gas phase species, and $\mathcal{S}_g$ is a general user-defined gas phase mass source term.[3] The left hand side terms account for the rate of mass accumulation and the net rate of convective mass flux. The first term on the right hand side represents the production or consumption of mass attributed to interphase mass transfer from chemical reactions or physical processes, such as evaporation. Users may specify phase changes or heterogeneous chemical reactions that will subsequently give the first term on the right hand side a nonzero value. A user-defined mass source may also be specified to give the second term on the right hand side nonzero value. By default, however, the right hand side is zero in MFIX.

2.4.2 Conservation of Species Mass

The conservation equation for the n^{th} gas phase species mass is

$$\frac{\partial}{\partial t}\left(\varepsilon_g \rho_g X_{gn}\right) + \frac{\partial}{\partial x_j}\left(\varepsilon_g \rho_g U_{gj} X_{gn}\right) = \frac{\partial}{\partial x_j}\left(\varepsilon_g \jmath_{gj}\right) + R_{gn} + \mathcal{S}_{gn} \tag{2-4}$$

[2] The equations in this section describe flow in the laminar regime (low Reynolds number flow). Modeling of turbulent flows is examined in a later section.

[3] The general user-defined source term has not been propagated to the non-conservative form of the governing equations with respect to the numerical implementation.

where X_{gn} is the n^{th} gas phase species mass fraction, and $\mathcal{S}_{gn}$ is a general user-defined gas species mass source term. The left hand side terms account for the rate of species mass accumulation and the net rate of convective species mass flux. The first term on the right hand side is the diffusive species mass flux. The second term on the right hand side represents the production or consumption of species mass attributed to chemical reactions or phase changes. R_{gn} is zero by default in MFIX, however, users may specify phase changes or chemical reactions giving rise to nonzero values. The last term is a general user-defined species mass source, which is zero by default but may be specified to give the term value.

MFIX solves a conservation equation for each species comprising a phase. As such, ill-defined species mass source terms or poor numerical convergence may lead to the sum of mass fractions deviating from one.

2.4.3 Conservation of Momentum

The gas phase momentum balance is

$$\frac{\partial}{\partial t}\left(\varepsilon_g \rho_g U_{gi}\right) + \frac{\partial}{\partial x_j}\left(\varepsilon_g \rho_g U_{gj} U_{gi}\right) = -\frac{\partial P_g}{\partial x_i} + \frac{\partial \tau_{gij}}{\partial x_j} + \varepsilon_g \rho_g g_i + \mathcal{S}_{gi}. \tag{2-5}$$

where P_g is the gas pressure, τ_{gij} is the gas phase stress tensor, and g_i body force due to gravity. The first term on the left hand side represents the net rate of momentum accumulation while the second term is the net rate of momentum transferred by convection. The first three terms on the right hand side are the pressure force, viscous stress, and gravitational force. Finally, $\mathcal{S}_{gi}$ is a general gas phase momentum source term. For single phase flow defined by $\varepsilon_g = 1$, this latter term is generally zero, however, exceptions exists.[4] A user-defined gas phase momentum source may be specified to add to this term. Later sections present models that also contribute to this term, including interphase momentum transfer[5] and resistance due to flow through a porous media[6].

Recall the fluid phase transport equations presented here are done so in the context of a multiphase system, and are the result of an averaging process that is based on the work of Anderson and Jackson [19] for a fluidized system of particles. Consequently, the fluid phase equation may still be written as shown in equation (2-5) upon introduction of a total fluid-particle interaction force (i.e., interphase momentum transfer) as a separate term encompassed here in $\mathcal{S}_{gi}$. However, once traditional closures for this interphase transfer term are incorporated,

[4] For single phase flow through a porous media, ε_g may have values other than unity and $\mathcal{S}_{gi}$ may become non-zero.
[5] Interphase momentum transfer due to mass transfer is zero in this formulation [205].
[6] Here resistance due to flow through a porous media specifically refers to the use of the internal surface feature in MFIX. However, a porous media approach may also be established by specifying a stationary, secondary phase (multiphase), and then a resistance to flow occurs through the associated interphase momentum transfer term.

the form of the governing equation is also altered. This term is discussed in more detail in the chapter on the two fluid model (TFM).

2.4.4 Conservation of Internal Energy

The conservation of internal energy is presented in terms of temperature. The derivation of the temperature form of the equation in non-conservative form obtained from the internal energy formulation is presented in Appendix A along with simplifying assumptions.

The equation for the gas phase internal energy [20, 21] is

$$\varepsilon_g \rho_g C_{pg} \left[\frac{\partial T_g}{\partial t} + U_{gj} \frac{\partial T_g}{\partial x_j} \right] = -\frac{\partial}{\partial x_j} \left(\varepsilon_g q_{gj} \right) + \mathcal{S}_g \tag{2-6}$$

where T_g is the gas phase temperature, and C_{pg} is the gas phase mixture specific heat. The left hand side terms account for the accumulation and convection of thermal energy. The first term on the right hand side is the conductive heat flux, and the last term, $\mathcal{S}_g$, is a general source term. For single phase flow defined by $\varepsilon_g = 1$, it includes heat transfer due to radiation.[7] However, user-defined gas phase energy sources may also be specified which add to this term. The source term contribution arising from the production or consumption of gas phase species is presented in section 2.5.8.2. For multiphase flows, additional contributions may include interphase convective heat transfer and enthalpy transfer accompanying interphase mass transfer. Models for these terms are presented in the chapter on the two fluid model.

2.5 Gas Phase Supplementary and Constitutive Equations

This section presents the additional relationships and constitutive equations used by MFIX to fully close the gas phase presented conservation equations presented above.

2.5.1 Gas Phase Equation of State

The gas phase density, ρ_g, is either specified as constant, calculated using a user-defined function[8], or calculated from the ideal gas law:

$$\rho_g = \frac{P_g \mathrm{MW}_g}{R T_g} \tag{2-7}$$

[7] For single phase flow through a porous media, ε_g may have values other than unity.

[8] MFIX ensures that the continuity equation is satisfied by solving a pressure correction equation which, to improve stability of mildly compressible flows, relies on the derivative of density with respect to pressure, $\partial \rho_g / \partial P_g$ [213]. The implementation uses the derivative of equation (2-7) which may lead to inconsistencies when user-defined functions are employed to specify the equation of state.

Here, MW_g is the gas phase *mixture* molecular weight, R is the gas constant, and the other quantities are as before. The equation of state provides a linkage between the energy equation and mass and momentum equations [22]. For constant density fluids, no linkage occurs and the energy equation only needs to be solved if the problem involves heat transfer.

2.5.2 Gas Phase Stress

The gas phase is assumed to be an isotropic Newtonian fluid so that the viscous stress tensor, τ_{gij}, is given by[9]

$$\tau_{gij} = \mu_{g,eff}\left(\frac{\partial U_{gi}}{\partial x_j} + \frac{\partial U_{gj}}{\partial x_i}\right) + \lambda_{g,eff}\left(\frac{\partial U_{gk}}{\partial x_k}\right) \tag{2-8}$$

where $\mu_{g,eff}$ is the effective dynamic viscosity and $\lambda_{g,eff}$ is an effective second viscosity, modeled as

$$\lambda_{g,eff} = -\mu_{g,eff}\frac{2}{3} \tag{2-9}$$

By default, the effective viscosity in MFIX is taken as the mixture molecular viscosity, μ_g, defined in section 2.6.1. However, the effects of turbulence are incorporated though the additional of an eddy viscosity, μ_e, if one of the turbulence models available in MFIX is used (see section 2.5.4).

$$\mu_{g,eff} = \mu_g + \mu_e \tag{2-10}$$

2.5.3 Porous Media / Semipermeable Surfaces

Resistance due to flow through a porous media specifically refers to the semipermeable surface feature in MFIX.[10] Homogeneous porous media are modeled by the addition of a momentum source term, $S_{gi,pm}$, to the gas phase momentum equation (2-5).

$$S_{gi,pm} = -\frac{\mu_g}{C_1}U_{gi} - \frac{1}{2}C_2\rho_g\varepsilon_g\left|U_{gi}\right|U_{gi} \tag{2-11}$$

where μ_g, ρ_g, and ε_g are the mixture molecular viscosity, density, and volume fraction of the gas phase, and C_1 and C_2 are use defined constants. The first term represents viscous losses while the

[9] MFIX assumes the fluid phase bulk (or volume) viscosity is zero. Recall, the bulk viscosity is the proportionality constant relating pure volumetric-rate-of strain to the normal stress. Here it is also implicit that viscosity is independent of the rate of shear.

[10] A porous media approach may also be established by specifying a stationary, secondary phase (multiphase) so that resistance to flow occurs through the associated interphase momentum transfer term.

second term captures inertial losses. The porous media source term is added in the gas phase momentum equation (2-5) through the general source term, $\mathcal{S}_{gi}$.

2.5.4 Turbulence

Turbulence is modeled in MFIX using the Boussinesq hypothesis which relates Reynolds stresses to mean rates of deformation of fluid elements [22]. This technique is implemented by using an effective viscosity in the gas phase viscous stress tensor that combines the mixture molecular viscosity with a turbulent mixing coefficient, commonly referred to as *eddy viscosity*. Although eddy viscosity has the same units as molecular viscosity, it is not a property of the fluid; instead it is a function of both fluid properties and flow conditions [23]. By default, eddy viscosity is zero in MFIX, however two eddy viscosity models are available and are presented the following sections.

2.5.4.1 Mixing Length Model

Prandtl's mixing length hypothesis [24] is an algebraic (zero-equation) turbulence model that relates turbulent fluctuations to a user-defined length scale, l_{mix}, and velocity gradient [25].

$$\mu_e = 2l_{mix}^2 \rho_g \sqrt{I_{g2D}} \tag{2-12}$$

Here, I_{g2D} is the second invariant of the deviatoric strain rate tensor[11].

$$I_{g2D} = \frac{1}{2}\left(S_{gij}S_{gji}\right) \tag{2-13}$$

2.5.4.2 k-ε Model

A modified version of the two-equation k-ϵ model [4] relates the turbulent eddy viscosity to the turbulent kinetic energy, k_g, and turbulent dissipation, ϵ, by a constant, $C_{1\mu}$.

$$\mu_e = \rho_g C_{1\mu} \frac{k_g^2}{\epsilon_g} \tag{2-14}$$

[11] The second invariant of a general second order tensor (T_{ij}) is given by $\frac{1}{2}(T_{ii}T_{jj} - T_{ij}T_{ji})$. In regard to the deviatoric rate-of strain tensor, however, $S_{mii} = 0$. So the magnitude of the second invariant of S_{mij} reduces as shown.

The kinetic energy and dissipation are given by

$$\varepsilon_g \rho_g \left[\frac{\partial k_g}{\partial t} + U_{gj}\frac{\partial k_g}{\partial x_j}\right] = \varepsilon_g \tau_{gij}\frac{\partial U_{gi}}{\partial x_j} - \varepsilon_g \rho_g \epsilon_g + \frac{\partial}{\partial x_j}\left(\varepsilon_g \frac{\mu_e}{\sigma_k}\frac{\partial k_g}{\partial x_j}\right) + \mathcal{S}_{k_g} \quad (2\text{-}15)$$

$$\varepsilon_g \rho_g \left[\frac{\partial \epsilon_g}{\partial t} + U_{gj}\frac{\partial \epsilon_g}{\partial x_j}\right] = \frac{\partial}{\partial x_j}\left(\varepsilon_g \frac{\mu_{gt}}{\sigma_\epsilon}\frac{\partial \epsilon_g}{\partial x_j}\right) + \varepsilon_g \frac{\epsilon_g}{k_g}\left(C_{1\epsilon}\,\tau_{gij}\frac{\partial U_{gi}}{\partial x_j} - \rho_g C_{2\epsilon}\epsilon_g\right) + \mathcal{S}_{\epsilon_g} \quad (2\text{-}16)$$

where σ_k, σ_ϵ, $C_{1\epsilon}$, and $C_{2\epsilon}$ are model constants provided in Table 2-1. $\mathcal{S}_{k_g}$ and $\mathcal{S}_{\epsilon_g}$ are interphase turbulent exchange terms which are zero for a single phase simulation. Closures for the interphase turbulent exchange terms are specific to particular kinetic theory models implemented in the MFIX two-flow model.

Table 2-1: Default values for the MFIX k-ϵ model constants [26]

Constant	σ_k	σ_ϵ	$C_{1\epsilon}$	$C_{2\epsilon}$	$C_{1\mu}$
MFIX Default	1.0	1.3	1.44	1.92	0.09

2.5.5 Diffusive Mass Transfer

Species mass flux through the gas phase is based on Fick's First Law of diffusion [27]:

$$j_{gj} = \rho_g \mathcal{D}_{gn}\frac{\partial X_{gn}}{\partial x_j} \quad (2\text{-}17)$$

where $\mathcal{D}_{gn}$ is the n^{th} gas phase species diffusion coefficient described in section 2.6.6 and the other quantities are defined as before.

2.5.6 Conductive Heat Transfer

Conductive heat flux through the gas phase is described by Fourier's Law [27]:

$$q_{gj} = -\kappa_g \frac{\partial T_g}{\partial x_j} \quad (2\text{-}18)$$

where κ_g is the gas phase thermal conductivity described in section 2.6.5 and the other quantities are defined as before.

2.5.7 Radiative Heat Transfer

Gas phase radiative heat transfer is modeled by the simple relation,

$$S_{g,rad} = \gamma_{Rg}\left(T_{Rg}^4 - T_g^4\right) \quad (2\text{-}19)$$

where T_{Rg} and γ_{Rg} are the radiative temperature and heat transfer coefficient. By default radiative heat transfer is not considered, that is, T_{Rg} and γ_{Rg} are taken as zero. The gas phase radiation source term is added in the gas phase internal energy equation (2-6) through the general source term, $\mathcal{S}_{g,I}$.

2.5.8 Chemical Reaction Source Terms

Source terms associated with chemical reactions are zero by default in MFIX. To incorporate chemical reactions, users must define chemical equations (stoichiometry) in the input deck, in addition to specifying reaction rates via user-defined functions[12]. Subsequent subsections present how user-provided information is used to calculate source terms that contribute to the species mass and internal energy conservation equations.

2.5.8.1 Production and Consumption of Species Mass

The rate of production per unit volume of the n^{th} gas phase species due to the p^{th} chemical reaction is given by[13]

$$\left[R_{gn}\right]_p = \frac{\alpha_{n,p}\mathcal{R}_p}{\mathrm{MW}_{gn}} \tag{2-20}$$

where MW_{gn} is the molecular weight of the n^{th} gas phase species (not to be confused with MW_g the gas phase mixture molecular weight defined in section 2.6.2). $\mathcal{R}_p$ is the user-defined reaction rate for the p^{th} reaction[14] and $\alpha_{n,p}$ is the signed stoichiometric coefficient of the n^{th} gas phase species for the p^{th} reaction. The sign of the stoichiometric coefficient is positive for products (e.g., the n^{th} species is produced by the p^{th} reaction) and negative for reactants (e.g., the n^{th} species is consumed by the p^{th} reaction). The total rate of production (or consumption), R_{gn}, is obtained by summing the contributions from all reactions

$$R_{gn} = \sum_p \left[R_{gn}\right]_p \tag{2-21}$$

and substituted into equations (2-3) and (2-4).

---

[12] Details on how to specify chemical equations and reaction rates is provided in the MFIX User Guide available online at https://mfix.netl.doe.gov/doc/mfix/latest

[13] *Intraphase* and *interphase* species mass transfer terms are evaluated identically; specifically, user-defined reaction rates and signed stoichiometric coefficients are combined to determine the net rate of production (or consumption) of each species within the gas mixture. As a result, similar descriptions are provided in subsequent chapters in the context of multiphase heterogeneous chemical reactions and/or phase changes.

[14] The unit systems adopted in MFIX are not consistent with the general definitions, and as such, MFIX uses units of $kmole/kg$ for molecular weight in SI and $mole/gram$ in CGS units. A consequence of these units is that user-defined reaction rates have units of $kmole/m^3sec$ in SI and $mole/m^3sec$ in CGS units.

2.5.8.2 Energy Change Due to Mass Production and/or Consumption

The p^{th} chemical reaction contributes to the general source term in the gas phase internal energy equation due to the production or consumption of gas phase species. This contribution may be specified[15] or computed as

$$\left[\mathcal{S}_{g,I}\right]_p = -\sum_{n=1}^{N_g} h_{gn}\left[R_{gn}\right]_p \tag{2-22}$$

N_g is the total number of species comprising the gas phase mixture, and h_{gn} is the specific enthalpy of the n^{th} gas species, defined in section 2.6.4. The total source term arising from intraphase enthalpy change is added in the gas phase internal energy equation (2-6) through the general source term, $\mathcal{S}_g$:

$$\mathcal{S}_{g,I} = \sum_p \left[\mathcal{S}_{g,I}\right]_p \tag{2-23}$$

2.6 Gas Phase Physical Properties

This section defines physical properties for the gas phase.

2.6.1 Mixture Molecular Viscosity

The gas phase mixture molecular viscosity, μ_g, is either specified as constant, calculated using a user-defined function, or calculated based on Sutherland's formula [28]. The latter is the default model and is given as

$$\mu_g = \mu_{ref}\left(\frac{T_g}{T_{ref}}\right)^{3/2}\left(\frac{T_{ref}+C}{T_g+C}\right) \tag{2-24}$$

where C is the Sutherland constant for the gas, T_{ref} is a reference temperature, and μ_{ref} is a reference viscosity at the reference temperature. The constant and reference values for the default model correspond to air and are provided in Table 2-2.

[15] If a constant heat of reaction is specified, then the evaluation of enthalpy defined in equation (2-27) is not performed so that the sensible heat contribution is not incorporated. Additionally, the partitioning of the specified heat of reaction between phases must also be provided.

Table 2-2: Default values for Sutherland's Law model constants [29]

	μ_{ref}	T_{ref}	C
Unit	$Pa \cdot s$	K	K
Air	1.7×10^{-5}	273	110

2.6.2 Mixture Molecular Weight

The gas phase *mixture* molecular weight, MW_g, is either specified as constant or calculated as

$$\frac{1}{\mathrm{MW}_g} = \sum_{n=1}^{N_g} \frac{X_{gn}}{\mathrm{MW}_{gn}} \tag{2-25}$$

where X_{gn} and MW_{gn} are the mass fraction and elemental molecular weight of the n^{th} gas phase chemical species.

2.6.3 Mixture Specific Heat

The gas phase mixture specific heat, C_{pg}, is either specified as constant[16] or calculated as

$$C_{pg} = \sum_{n=1}^{N_g} X_{gn} C_{pgn} \tag{2-26}$$

where $C_{pgn}$is the specific heat of the n^{th} gas phase species. The species specific heat is obtained from either the BURCAT database [30] or from a user provided entry following the same format.

2.6.4 Species Specific Enthalpy

The specific enthalpy each species is calculated by combining the heat of formation, $H_{fn}^{\circ}(T_{ref})$,0 and integrating the specific heat of that species from the reference temperature, T_{ref}, to the gas phase temperature.

$$h_{gn} = H_{fn}^{\circ}(T_{ref}) + \int_{(T_{ref})}^{T_g} C_{pgn}(T)\, dT \tag{2-27}$$

The species heat of formation is obtained from either the BURCAT database [30] or as a user provided entry following the same format.

[16] Specifying a constant specific heat for the gas phase is only permissible for non-reacting flows.

2.6.5 Thermal Conductivity

The gas phase thermal conductivity, κ_g, is either specified as constant, calculated using a user-defined function, or calculated using a temperature dependence model that has basis in kinetic theory for dilute monatomic gases [27]. The latter is the default model and is given as:

$$\kappa_g = \kappa_{ref}\sqrt{\frac{T_g}{T_{ref}}} \tag{2-28}$$

where T_{ref} is a reference temperature and κ_{ref} is a reference conductivity evaluated at the reference temperature. The reference values for the default model correspond to air and are provided in Table 2-2 [31].

Table 2-3: Default values for temperature dependent thermal conductivity (See 8.B$_1$ Computation of the Prandtl Number for Gases at Low Density, p263 [31])

	κ_{ref}	T_{ref}
Unit	$W/(mK)$	K
Air	0.0252	300

2.6.6 Diffusivity

The gas phase species diffusivity, $\mathcal{D}_{gn}$, is either specified as constant, calculated using a user-defined function, or calculated based on a correlation by Fuller, Schettler and Giddings (FSG). In their effort, the temperature dependence was determined from fitting a generalized function with theoretical foundations to experimental data [32]. The FSG correlation is used to form the default model:

$$\mathcal{D}_{gn} = D_{n,ref}\left(\frac{T_g}{T_{ref}}\right)^{7/4}\left(\frac{P_{ref}}{P_g}\right) \tag{2-29}$$

Here T_{ref} and P_{ref}, are a reference temperature and pressure, respectively, while $D_{n,ref}$ is a reference diffusion coefficient for species *n* defined at the reference temperature and pressure. The reference values for the default model correspond to the diffusivity of CO_2 and N_2 with values provided in Table 2-4. A dilute mixture approximation for multicomponent diffusion [33] is available to evaluate $D_{n,ref}$. This approximation is based on the binary diffusion coefficient of all gas pairs in the mixture as:

$$D_{n,ref} = \left(\sum_{\substack{n'=1\\ n'\neq n}}^{N_g} X_{gn'}\right) \Bigg/ \left(\sum_{\substack{n'=1\\ n'\neq n}}^{N_g} \frac{X_{gn'}}{D_{n'n}}\right) \tag{2-30}$$

Here $D_{n\prime n}$ is the binary diffusion coefficient for gas phase species n and n', which is given in Table 2-4 for CO_2 and N_2.

Table 2-4: Default values for temperature and pressure dependent diffusion based on CO_2 in N_2 (See Table 16.2-2 Experimental diffusivities of some dilute gas pairs, p503 [31])

	P_{ref}	T_{ref}	$D_{n,ref}$
Unit	Pa	K	m^2/sec
$CO_2 - N_2$	1.01	298.2	1.65×10^{-5}

Chapter 3: Eulerian Solids Phase Model (MFIX-TFM)

MFIX-TFM (two-fluid model), also referred to as the gas-solids continuum model, the Euler-Euler model, or the multi-fluid model, describes the motion of a mixture of a continuous phase and one or more dispersed phases. The continuous phase was presented in Chapter 2 and is commonly referred to throughout this chapter as the *gas phase*, however it may be taken to represent other fluids.[17] The gas phase is identified as the *continuous phase* because its volume fraction must always be greater than zero. A dispersed phase is generally referred to throughout this chapter as a *solids phase*, but it could be liquid droplets or gas bubbles. Elements of a dispersed phase, referred to as *particles*, are assigned to separate phases that delineate size, density, and chemical species composition; a total of M dispersed phases may be defined. Like the continuous phase, a dispersed phase is described as a continuum. However, volume fractions may be zero. Specifically, a dispersed phase may be absent in regions of the domain (e.g., the freeboard of a dense bubbling bed), whereas the continuous phase must always be present. Here the equations are presented in conservative form, however, in MFIX the equations are solved in non-conservative form by subtracting the respective phase continuity equation.

3.1 Overview

Many approaches have been used to derive the governing equations of motion for multiphase flow. Two broad categories for such attempts include the mixture (drift-flux) approach [34, 26, 35] that treats the mixture as a whole, and a multiphase averaging approach [19, 36, 37, 38, 39, 40, 41, 42, 43]. This section focuses on the latter. The Eulerian multiphase model allows for the modeling of multiple separate interacting materials called phases. In the Eulerian approach, each *phase* is described as a continuum occupying the same region of space.

Application of an averaging process to the continuum equations describing the exact motion of each material at each point establishes a connection with the corresponding exact or microscopic description. Two well-known averaging techniques include ensemble averaging and volume averaging. In general terms, ensemble averaging involves averaging over each point in space over an ensemble of macroscopically equivalent systems. Volume averaging, on the other hand, involves a local spatial average taken over regions small in extent compared to macroscopic scales of interest. For further details the reader is referred to Chapter 2 of [39]. Regardless, the formal process of averaging leads to equations with a number of terms whose form is not determined[18]; that is, a closure problem remains. Expressing these quantities in well-defined terms that reflect the behavior at the microscopic level is a difficult task. Here, well-defined

[17] When the continuous phase is no longer considered gaseous, then additional physics may become important that MFIX does not currently consider. For example, virtual mass may become important in liquid-solid or bubbly flows.

[18] Namely, terms involving integrals of point properties over the microscopic domain remain.

refers to having closure relationships for unknown terms written explicitly in terms of the same averaged variables (e.g., locally averaged velocity or phase concentration) as in the governing equations.

Developing the corresponding constitutive equations remains a formidable task. In particular, what form they should take and what approximations may be implied in their use is not always clear. The existence of interfaces between phases and the discontinuities associated with them is especially challenging in terms of experimentation and modeling. Thus constitutive equations for the interfacial terms are often considered the weakest link in multifluid model formulation [44]. An alternate approach to the formal averaging process still models the system as interpenetrating continuous fluids. However, the equations are formulated based more on intuitive ideas, and constrained by general principles of continuum mechanics. This may lead to similar equations, but it does not reveal how the macroscopic relations arise from appropriate microscopic considerations [39].

The following sections outline the equations that comprise the MFIX-TFM dispersed phase model. Recall the MFIX-TFM continuous phase model is as presented in Chapter 2 unless otherwise indicated.

3.2 Limitations

Limitations of MFIX-TFM include:

- The continuous, or fluid, phase volume fraction (ε_g) is always greater than zero such that the dispersed, or solids, phase volume fractions (ε_m) cannot sum to one.

3.3 Conservation Equations

This section presents the m^{th} phase conservation equations solved by MFIX. To solve this set of equations requires specifying additional closures, which includes, among others, the interphase momentum transfer and stress terms. Modeling of these terms must proceed carefully as discussed in the sections following.

3.3.1 Conservation of Mass

The conservation of mass (or continuity equation) for the m^{th} phase is

$$\frac{\partial}{\partial t}(\varepsilon_m \rho_m) + \frac{\partial}{\partial x_j}\left(\varepsilon_m \rho_m U_{mj}\right) = \sum_{n=1}^{N_m} R_{mn} + \mathcal{S}_m \tag{3-1}$$

where, ε_m is the m^{th} phase volume fraction, ρ_m is the m^{th} phase material density, U_{mj} is the j^{th} component of the m^{th} phase velocity, N_m is the number of chemical species comprising the m^{th} phase, R_{mn} is the rate of production/consumption of the m^{th} phase n^{th} chemical species, and $\mathcal{S}_m$

is a general user-defined m^{th} phase mass source term. The left hand side terms account for the rate of mass accumulation and the net rate of convective mass flux. The first term on the right hand side is the interphase mass transfer attributed to chemical reactions or physical processes, such as evaporation. Users may specify sources due to phase changes or chemical reactions that will give this first term on the right hand side value. A user-defined mass source may also be specified to give the second term on the right hand side value. By default, however, the right hand side is zero in MFIX.

3.3.2 Conservation of Species Mass

The n^{th} species mass conservation equation for the m^{th} phase is

$$\frac{\partial}{\partial t}(\varepsilon_m \rho_m X_{mn}) + \frac{\partial}{\partial x_j}(\varepsilon_m \rho_m U_{mj} X_{mn}) = \frac{\partial}{\partial x_j}(\varepsilon_m \jmath_{mj}) + R_{mn} + \mathcal{S}_{mn} \tag{3-2}$$

where X_{mn} is the m^{th} phase n^{th} species mass fraction, and $\mathcal{S}_{mn}$ is a general user-defined m^{th}phase species mass source term. The left hand side terms account for the rate of species mass accumulation and the net rate of convective species mass flux. The first term on the right hand side is the diffusive species mass flux. The second term on the right hand side is the rate of production of species mass attributed to chemical reactions or physical processes. R_{mn} is zero by default in MFIX, however, users may specify phase changes or chemical reactions giving rise to nonzero values (see section 3.4.11). The last term is a general user-defined species mass source, which is by default zero but may be specified to give the term value. Properties of the m^{th} phase are discussed later in this chapter, however, it is worth noting that $\mathcal{D}_{mn}$ is zero by default in MFIX (i.e., no species diffusion occurs within the m^{th} *solids* phase). As a result, the right hand side is also by default zero in MFIX.

MFIX solves a conservation equation for each species comprising each phase. As such, ill-defined species mass sources, poor convergence, or inappropriate numerical techniques can lead to the sum of mass fractions deviating from unity.

3.3.3 Conservation of Momentum

This section presents the gas and m^{th} phase momentum equation formulations available in MFIX-TFM.

3.3.3.1 Default Formulation

The default MFIX-TFM gas and momentum balances are

$$\frac{\partial}{\partial t}(\varepsilon_g \rho_g U_{gi}) + \frac{\partial}{\partial x_j}(\varepsilon_g \rho_g U_{gj} U_{gi}) = -\frac{\partial P_g}{\partial x_i} + \frac{\partial \tau_{gij}}{\partial x_j} + \varepsilon_g \rho_g g_i + \mathcal{S}_{gi} \tag{3-3}$$

$$\frac{\partial}{\partial t}(\varepsilon_m \rho_m U_{mi}) + \frac{\partial}{\partial x_j}(\varepsilon_m \rho_m U_{mj} U_{mi}) = -\frac{\partial P_m}{\partial x_i} + \frac{\partial \tau_{mij}}{\partial x_j} + \varepsilon_m \rho_m g_i + \mathcal{S}_{mi} \tag{3-4}$$

where P_m is the m^{th} phase pressure, τ_{mij} is the m^{th} stress tensor and $\mathcal{S}_{mi}$ is a general m^{th} phase momentum source term. The other terms are as before in the presentation of the fluid phase governing equations, that is, P_g is the gas pressure, τ_{gij} is the gas phase stress tensor, g_i is the body force due to gravity and $\mathcal{S}_{gi}$ is a general gas phase momentum source term. The source terms include contributions from interphase momentum transfer, such as, gas-solids drag. User-defined momentum sources may also be specified. Note that the gas phase momentum balances given by Equations (2-5) and (3-3) are identical. As noted in presentation of the Eulerian fluid phase model, the above set of Eulerian multiphase governing equations are the result of an averaging process that is chiefly based on the work of Anderson and Jackson [19] for a fluidized system of particles.[19]

This section more closely examines the form of the interphase momentum transfer term and how its definition impacts the overall form of the governing equations when inserted. For convenience $\mathcal{S}_{gi}$ and $\mathcal{S}_{mi}$ are redefined to specifically distinguish the contribution(s) due to interphase momentum transfer between the gas and m^{th} phase:

$$\mathcal{S}_{gi} = -\sum_{m=0}^{M} I_{gmi} + \mathcal{S}_{gi}' \tag{3-5}$$

$$\mathcal{S}_{mi} = I_{gmi} + \mathcal{S}_{mi}' \tag{3-6}$$

Here I_{gmi} represents contributions to the gas-m^{th} phase interphase momentum transfer term, M represents the number of additional phases beyond the fluid phase, and $\mathcal{S}_{gi}'$ and $\mathcal{S}_{mi}'$ are general gas and m^{th}phase momentum source terms excluding that due to gas-m^{th} phase interphase momentum transfer. The default form for this interphase transfer term in MFIX is presented here for quick reference but discussed in more detail later[20].

$$I_{gmi} = -\varepsilon_m \frac{\partial P_g}{\partial x_i} + \beta_{gm}(U_{gi} - U_{mi}) \tag{3-7}$$

[19] Following Anderson and Jackson [19] the default momentum balances shown in (3-3) and (3-4) involve some mathematical manipulation wherein similarities are leveraged between 1) the definition for the force exerted on a single particle by the surrounding fluid (i.e., the surface integral of the fluid stress tensor over the particles' surface) and 2) a surface integral term that arises from averaging the point wise fluid stress tensor.

[20] Additional gas-solids interaction terms are possible, such as, virtual mass and the Basset force. However, these are not incorporated into the default model.

The corresponding default form of the governing equations are obtained upon introduction of this force and they are shown here for context and comparison with other available options in MFIX.

$$\frac{\partial}{\partial t}\left(\varepsilon_g \rho_g U_{gi}\right) + \frac{\partial}{\partial x_j}\left(\varepsilon_g \rho_g U_{gj} U_{gi}\right) = -\varepsilon_g \frac{\partial P_g}{\partial x_i} + \frac{\partial \tau_{gij}}{\partial x_j} + \sum_m^M \beta_{gm}\left(U_{mi} - U_{gi}\right) + \varepsilon_g \rho_g g_i + \mathcal{S}_{gi}' \tag{3-8}$$

$$\frac{\partial}{\partial t}\left(\varepsilon_m \rho_m U_{mi}\right) + \frac{\partial}{\partial x_j}\left(\varepsilon_m \rho_m U_{mj} U_{mi}\right) = -\varepsilon_m \frac{\partial P_g}{\partial x_i} - \frac{\partial P_m}{\partial x_i} + \frac{\partial \tau_{mij}}{\partial x_j} + \beta_{gm}\left(U_{gi} - U_{mi}\right) + \varepsilon_m \rho_m g_i + \mathcal{S}_{mi}' \tag{3-9}$$

Multiphase flow equations have been derived from formal averaging of the microscopic description by both Anderson and Jackson [19] and Ishii [45]. The authors employed different averaging methods (volume versus time) and applied their technique to differing multiphase flow systems. In particular, Ishii's formulation considers both phases to be a fluid and as such the interphase term is treated the same. While in Jackson's formulation the fluid and solids phases are treated differently and as a result the interphase interaction term appears differently in the fluid and solids phases' momentum equation [46]. Regardless, the assumptions inherent in their treatment suggest the types of multiphase flows to which they can be most appropriately applied [46]. In addition to the default form presented above, multiphase momentum equation formulations based on each of these works is also available in MFIX as discussed subsequently.

3.3.3.2 Jackson Formulation

Anderson and Jackson [19, 38, 39] presented a formal averaging procedure for fluid-particle systems and examined the impact of different definitions of the gas-solids interphase momentum transfer term. Shown below is their interpretation of the total interaction force and the corresponding form of the governing equations:[21]

$$I_{gmi} = -\varepsilon_m \left(\frac{\partial P_g}{\partial x_i} - \frac{\partial \tau_{gij}}{\partial x_j}\right) + \beta_{gm}\left(U_{gi} - U_{mi}\right) \tag{3-10}$$

[21] Anderson and Jackson [19] and Jackson [36] acknowledge additional gas-solids interaction terms including added mass and the Basset force. Discussion of such additional terms is reserved until section 3.4.4 on the gas-solids momentum transfer.

This form of the interaction force follows a series of arguments building first on a single particle in an undisturbed fluid, to a single particle in a fluid with diverging streamlines to fluid flow through an assembly of particles. The resulting momentum equations are shown here.[22].

$$\frac{\partial}{\partial t}\left(\varepsilon_g \rho_g U_{gi}\right) + \frac{\partial}{\partial x_j}\left(\varepsilon_g \rho_g U_{gj} U_{gi}\right) = -\varepsilon_g \frac{\partial P_g}{\partial x_i} + \varepsilon_g \frac{\partial \tau_{gij}}{\partial x_j} + \sum_m^M \beta_{gm}\left(U_{mi} - U_{gi}\right) + \varepsilon_g \rho_g g_i + \mathcal{S}_{gi}' \tag{3-11}$$

$$\frac{\partial}{\partial t}\left(\varepsilon_m \rho_m U_{mi}\right) + \frac{\partial}{\partial x_j}\left(\varepsilon_m \rho_m U_{mj} U_{mi}\right) = -\varepsilon_m \frac{\partial P_g}{\partial x_i} + \varepsilon_m \frac{\partial \tau_{gij}}{\partial x_j} - \frac{\partial P_m}{\partial x_i} + \frac{\partial \tau_{mij}}{\partial x_j} + \beta_{gm}\left(U_{gi} - U_{mi}\right) + \varepsilon_m \rho_m g_i + \mathcal{S}_{mi}' \tag{3-12}$$

The above form of the multiphase momentum equations is also available in MFIX. The default formulation in MFIX for the multiphase momentum equations (equations 3-8 and 3-9) closely mirrors Jackson's formulation with two primary differences. First, Jackson's m^{th} phase momentum balance contains the gas phase volume fraction multiplied by the gas phase shear stress tensor. This term is wholly absent from the *default* MFIX formulation. Second, in Jackson's gas phase momentum balance, the divergence of the gas phase shear term is also multiplied by the gas phase volume fraction.

3.3.3.3 Ishii Formulation

Ishii [45] presented a formal averaging procedure for fluid-fluid systems. The resulting multiphase formulation of Ishii, as presented by van Wachem [46], is reproduced here[23]:

$$\frac{\partial}{\partial t}\left(\varepsilon_g \rho_g U_{gi}\right) + \frac{\partial}{\partial x_j}\left(\varepsilon_g \rho_g U_{gj} U_{gi}\right) = -\varepsilon_g \frac{\partial P_g}{\partial x_i} + \frac{\partial}{\partial x_j}\left(\varepsilon_g \tau_{gij}\right) + \sum_m^M \beta_{gm}\left(U_{mi} - U_{gi}\right) + \varepsilon_g \rho_g g_i + \mathcal{S}_{gi}' \tag{3-13}$$

[22] These equations shown here differ slightly from Anderson and Jackson [19] as their derivation is based on a monodisperse gas-solids system. As a result, gas-solids interphase momentum transfer is the only source term present in the formal equation set. Recall, however, that the MFIX-TFM implementation includes extensions for polydispersity, hence the summation over M.

[23] As noted by van Wachem et al. [43] a few terms in Ishii's interphase momentum transfer model have been neglected in this presentation, including an interfacial shear term and a term due to pressure differences between the bulk and the interface.

$$\frac{\partial}{\partial t}(\varepsilon_m \rho_m U_{mi}) + \frac{\partial}{\partial x_j}(\varepsilon_m \rho_m U_{mj} U_{mi}) = -\varepsilon_m \frac{\partial P_g}{\partial x_i} + \frac{\partial}{\partial x_j}(\varepsilon_m \tau_{mij}) + \beta_{gm}(U_{gi} - U_{mi}) + \varepsilon_m \rho_m g_i + \mathcal{S}_{mi}' \quad (3\text{-}14)$$

The above form of the multiphase momentum equations is also available in MFIX. As evident by comparison, the default formulation for the multiphase momentum equations in MFIX is slightly different from this modified version of the multiphase momentum equations of Ishii. For example, the default gas-phase momentum equation in MFIX is similar to those based on Ishii except the latter has the gas phase volume fraction multiplying the gas phase shear term. Differences are also evident in the m^{th} phase momentum equations.

This form of the m^{th} phase momentum balance, presented above, is modified further when applied to gas-solids systems in MFIX. Specifically, the solids-phase stress tensor is *not* multiplied by the solids volume fraction as its functionality is accounted for in the solids phase model description (e.g. kinetic theory model). Moreover, a solids pressure term is included (see [46]) in the solids phase momentum balance. Note that the m^{th} phase momentum equation shown above do not reflect these modifications, but in MFIX they are incorporated into the m^{th} phase solids momentum equation when applied to gas-solids systems with a kinetic theory description for solids. This formulation based on Ishii [45] is more appropriate for a dispersed phase consisting of a fluid material (e.g., fluid droplets) as opposed to solids particles [46].

3.3.4 Conservation of Internal Energy

The conservation of internal energy is presented in terms of temperature. The derivation of the temperature form of the equation, obtained from the internal energy formulation [20, 21], is presented in Appendix A along with simplifying assumptions.

The m^{th} phase energy equation is

$$\varepsilon_m \rho_m C_{pm}\left[\frac{\partial T_m}{\partial t} + U_{mj}\frac{\partial T_m}{\partial x_j}\right] = -\frac{\partial(\varepsilon_m q_{mj})}{\partial x_j} + \mathcal{S}_m \quad (3\text{-}15)$$

where T_m is the m^{th} phase temperature, and C_{pm} is the m^{th} phase mixture specific heat. The left hand side terms account for the accumulation and convection of thermal energy. The terms on the right hand side include the conductive heat flux, and a general source term, $\mathcal{S}_m$. A user-defined m^{th} phase energy source may be specified to add to this term. Other contributions may include heat transfer due to radiation, interphase heat transfer, and enthalpy transfer accompanying intra- and interphase mass transfer.

3.4 Solids Phase Supplementary and Constitutive Equations

This section presents the additional relationships and constitutive equations used by MFIX to fully close the m^{th} phase conservation equations presented above. As evident below, these relationships assume a granular basis, that is, the m^{th} phase is a *solids* phase with a characteristic diameter and density.

3.4.1 Solids Phase Stress

As noted earlier MFIX was originally designed to model multiphase gas-solids flows. Accordingly, MFIX-TFM characterizes the m^{th} phase as a granular material wherein individual particles are not resolved. Granular flows are often classified into two limiting flow regimes, quasi-static (referred to here as frictional) and kinetic, as shown in Figure 3-1 [47, 48].[24] Stresses in the quasi-static/friction regime are the result of the internal structure of the granular material (quasi-linear structures or chains), which supports the bulk internal stress within the material [49, 50]. These quasi-static materials demonstrate apparent frictional behavior in that the shear and normal stresses are related; the stresses can be related through the compressive force acting on the structure and the angle of the structure, which generally does not vary significantly. In a shearing material, these chains are dynamic structures that may collapse and form new ones. Stresses in the kinetic regime are considered the result of collisional and streaming momentum transfer of particles wherein it is generally assumed that particle contacts occur instantaneously. Therefore, constitutive equations for particle-particle interactions must consider the fundamentally different modes of force transmission across flow regimes.

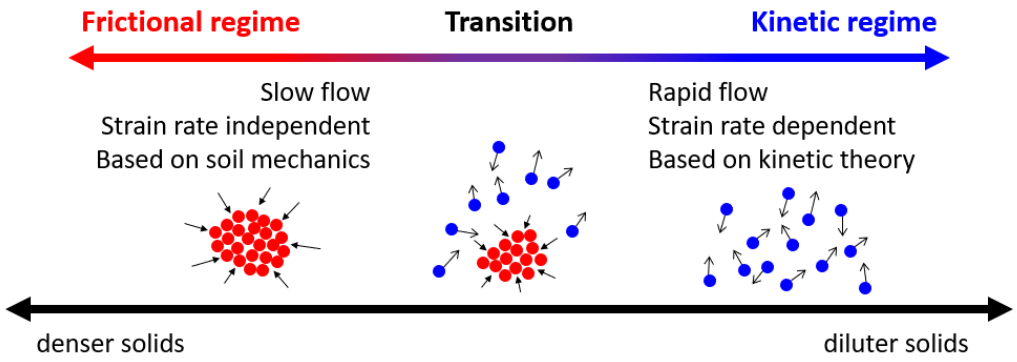

Figure 3-1: Schematic of the transition between the quasi-static/frictional regime and the kinetic regime [51].

[24] The term frictional may be somewhat misleading as these relations refer to the internal behavior of a *collection* of particles, that is, the behavior of the internal structure of the granular material [46]. It is not a simple function of friction between grains (e.g., consider deformation). In other words, stresses are not necessarily simply the result of particles sliding over one another (classic frictional picture) Nevertheless, this terminology is used here.

A general continuum mechanics theory for computational purposes that is capable of simultaneously capturing these different rheological behaviors is lacking. However, constitutive equations describing all flow regimes are needed, since all may exist at any time at various locations in a granular flow system. Moreover, the transition between the two limiting regimes, where particle-particle contacts are of intermediate duration is difficult to describe [48, 52]. Therefore, the results taken from both limiting regimes are typically stitched together to describe all flow situations. That is, the frictional and kinetic regime contributions to the solids pressure and solids stress tensor are combined through addition [53, 52, 48] While this *superposition principle* is ad hoc, it has been used to investigate a wide range of slow and rapid granular flows [54]. For further discussion see section 3.4.2.1.1.

Since the rheological behavior of the granular phase varies depending on the regime, the form of the constitutive equations may also be expected to differ. Nevertheless, the stresses are cast in the same general form for computational purposes. For context in the following, refer back to the governing m^{th} phase momentum equation: equation 3-4 or equivalently equation 3-9. The general formulation for the total m^{th} phase solids stress tensor is given by

$$\tau_{mij} = 2\mu_m D_{mij} + \lambda_m D_{mkk}\delta_{ij} \tag{3-16}$$

where μ_m is the viscosity, λ_m is referred to as the second viscosity[25] and D_{mij} is the rate-of-strain tensor. The latter two quantities are defined as

$$D_{mij} = \frac{1}{2}\left(\frac{\partial U_{mi}}{\partial x_j} + \frac{\partial U_{mj}}{\partial x_i}\right) \tag{3-17}$$

$$\lambda_m = \mu_{bm} - \frac{2}{3}\mu_m \tag{3-18}$$

where μ_{bm} is the bulk viscosity of the m^{th} phase. For completeness, it should also be noted that some publications present the solids stress tensor in terms of the deviatoric rate-of-strain tensor, S_{mij}.

$$\tau_{mij} = 2\mu_m S_{mij} + \mu_{bm} D_{mkk}\delta_{ij} \tag{3-19}$$

$$S_{mij} = \frac{1}{2}\left(\frac{\partial U_{mi}}{\partial x_j} + \frac{\partial U_{mj}}{\partial x_i}\right) - \frac{1}{3}\frac{\partial U_{mk}}{\partial x_k}\delta_{ij} \tag{3-20}$$

This representation illustrates that the bulk viscosity is the proportionality constant relating pure volumetric-rate-of-strain to the normal stress. The two definitions of the stress tensor, (3-16) and

[25] The second viscosity is employed to facilitate computations and is a composite parameter representing the combination of all the viscous effects associated with the volumetric-rate-of-strain.

(3-19), are identical. The motivation in providing both definitions is to establish a connection between the equations modeled in MFIX and common variants found in literature.

Using the superposition principle, the solids stress tensor is obtained by summing solids stress contributions from frictional and kinetic models for granular material:

$$\tau_{mij} = \tau_{mij}^{fric} + \tau_{mij}^{kin} \tag{3-21}$$

This may also be accomplished through its components. That is, the m^{th} phase solids viscosity and solids second viscosity are obtained by summing the viscosity and second viscosity contributions from the frictional and kinetic models.

$$\mu_m = \mu_m^{fric} + \mu_m^{kin} \tag{3-22}$$

$$\lambda_m = \lambda_m^{fric} + \lambda_m^{kin} \tag{3-23}$$

Specific models for the frictional and kinetic contributions are provided in the subsequent sections. Like solids stress, the total m^{th} phase solids pressure is obtained by summing solids pressure contributions from frictional, P_m^{fric}, and kinetic, P_m^{kin}, models for granular material.

$$P_m = P_m^{fric} + P_m^{kin} \tag{3-24}$$

Specific models for the frictional and kinetic contributions are provided in the subsequent sections 3.4.2 and 3.4.3, respectively.

Under the assumption that the stresses can be treated in an additive manner, each contribution is evaluated independently as if it acted alone. This ad hoc formulation provides a mechanism to describe each regime within the same framework. A well-established quantitative methodology for characterizing the two limiting flow conditions (kinetic and frictional) or their transition is not available [55].[26] In early efforts [48, 53], the stresses from each regime were simply summed regardless of the flow conditions. Alternatively, Syamlal et al. [56] introduced a switch function where the frictional stresses are included only when a critical solids volume fraction is reached. This approach is followed here. Namely, the frictional models only contribute to the solids pressure and solids viscosity when the gas phase volume fraction falls below some value representative of close pack or frictional conditions (section 3.4.2 equations 3-25 and 3-28 or

[26] More recently, simulations (e.g., [184, 208, 210, 209]) based on Discrete Element Methods have been used to investigate the rheology of granular materials. Using these tools flow regime maps have been described, however, they rely on material properties (e.g., elasticity), which are not found in the typical frictional and kinetic models employed in the Eulerian Method (current Chapter). Therefore, their usefulness for specifying a transition criteria in the context of these continuum approaches remains uncertain.

3-32 and 3-34) as shown in Figure 3-2. Under the currently implemented frictional models (section 3.4.2), this approach also results in a step transition or discontinuity in the solids pressure and viscosity.

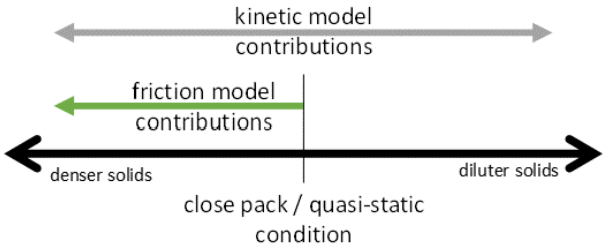

Figure 3-2: Schematic illustrating the instantaneous onset of frictional stresses when the solids packing surpasses a close pack condition.

3.4.2 Frictional Stress Models

When particles undergo long enduring contacts in which the bulk material exhibits a solid-like behavior (e.g. soil mechanics, silos), the system is considered to be in the quasi-static or slow-flow regime. A few options are available in MFIX to describe the motion of particles in this flow regime, which are discussed in the following. The condition under which these physics are functioning depends on the invoked model (see below for the specific criteria), but generally the fluid volume (void) fraction must be lower than some specified void fraction representing close-pack ($\varepsilon_g < \varepsilon^*$) or frictional conditions ($\varepsilon_g < 1 - \varepsilon_f^{min}$). The theories used here for the frictional contribution are largely based on the critical state theory of soil mechanics (e.g., [57]), but as indicated by Johnson and Jackson [48] such efforts are largely empirical.

3.4.2.1 Schaeffer Model [56]

Syamlal *et al*. [56] developed a constitutive model for the quasi-static flow regime where the shear viscosity is adapted from Schaeffer [58] and Pitman and Schaeffer [59] who examined the equations for compressible and incompressible granular flow, respectively. Originally written for a single phase, here it adapted for M phases:

$$\mu_m^{fric} = \begin{cases} \min\left\{\dfrac{P_c \sin(\phi)}{\sqrt{4 I_{m2D}}}\dfrac{\varepsilon_m}{\varepsilon_s}, \mu_s^{max}\right\} & \varepsilon_g < \varepsilon^* \\ 0 & \varepsilon_g \geq \varepsilon^* \end{cases} \tag{3-25}$$

where ϕ is the angle of internal friction, μ_s^{max} is a specified maximum granular viscosity[27], P_c represents the solids pressure in the quasi-static flow regime, ε_m is the m^{th} phase volume

[27] An upper limit is specified to help stabilize the calculation as the calculated values are large and become unbounded as $I_{m2D} \to 0$.

fraction, ε_s represents the total volume fraction of M dispersed phases, that is, the total *solids* volume fraction ($\varepsilon_s = \sum_{m=1}^{M} \varepsilon_m$), and ε^* is the void fraction at close packing [60, 51] described below.[28] The quantity I_{m2D} is the *magnitude* of the second invariant of the deviatoric rate-of-strain tensor:[29]

$$I_{m2D} = \frac{1}{2}\left(S_{mij}S_{mji}\right). \tag{3-26}$$

This quantity may be expressed in terms of components of the rate-of-strain tensor as follows:

$$I_{m2D} = \frac{1}{6}[(D_{m11} - D_{m22})^2 + (D_{m22} - D_{m33})^2 + (D_{m33} - D_{m11})^2] + D_{12}^2 + D_{23}^2 + D_{33}^2 \tag{3-27}$$

As indicated by [48, 54], the pressure in this quasi-static regime is expected to increase rapidly with volume fraction and diverge on approaching some close packed value. This critical or close-pack pressure is given here by an arbitrary expression related to the void fraction that allows some compressibility in the solids phase [56]:

$$P_c = \begin{cases} A_{pc}\left(\varepsilon^* - \varepsilon_g\right)^{n_{pc}} & \varepsilon_g < \varepsilon^* \\ 0 & \varepsilon_g \geq \varepsilon^* \end{cases} \tag{3-28}$$

The model constants are given in Table 3-1. As before ε^* is the void fraction at close packing.[30] As shown, the critical pressure only has value when the void fraction falls below a critical void fraction (the void fraction at close packing).

For uniformly sized particles the close-pack void fraction is a specified constant, whereas for polydisperse mixtures it can estimated from correlations or also simply specified as a constant. Note the void fraction at close packing is related to the maximum volume fraction at close packing ε_s^{max} as:

$$\varepsilon^* = 1 - \varepsilon_s^{max} \tag{3-29}$$

Correlations available in MFIX for the maximum volume fraction at close packing are presented in Appendix D.

The close-pack solids pressure, P_c, contributes to the total solids phase pressure (3-24) through the frictional solids pressure term by taking $P_m^{fric} = P_c$ in this case. While the frictional flow

[28] If stress blending is used (section 3.4.2.1.1) then ε^* is replaced with ε_u^*.

[29] The second invariant of a general second order tensor (T_{ij}) is given by $\frac{1}{2}(T_{ii}T_{jj} - T_{ij}T_{ji})$. In regard to the deviatoric rate-of strain tensor, however, $S_{mii} = 0$. So the magnitude of the second invariant of S_{mij} reduces as shown.

[30] If stress blending is used (section 3.4.2.1.1) then ε^* is replaced with ε_u^*.

shear viscosity, μ_m^{fric}, is added to the total solids viscosity in equation (3-22). Note that, this model does not contribute to the solids second viscosity in equation (3-23).[31]

Table 3-1: Default values for Schaeffer model [56]

Constant	n_{pc}	A_{pc} [barye]
MFIX Default	10	10^{25}

3.4.2.1.1 Stress Blending

While rapid transition between these two regimes may be expected in many gas-solid flow applications (i.e. bubbling bed, spouted bed), the physics of this transition is not well understood [48]. The current step transitioning (see section 3.4.1 Figure 3-2) leads to slow convergence due to numerical instabilities [61, 62]. To circumvent this issue, a blending function is introduced to obtain a smooth but rapid transition between the frictional and kinetic regimes depending on the void fraction as indicated here [61, 63].

$$P_m = f(\varepsilon_g)P_m^{kin} + \left(1 - f(\varepsilon_g)\right)P_m^{fric} \tag{3-30}$$

$$\tau_{mij} = f(\varepsilon_g)\tau_{mij}^{kin} + \left(1 - f(\varepsilon_g)\right)\tau_{mij}^{fric} \tag{3-31}$$

More precisely, blending of solids stress is achieved by blending the kinetic and frictional contributions to solids viscosity as indicated in section 3.4.1; the model based on Schaeffer [58] does not contribute to solids second viscosity. Two options for the blending function are available as shown in Table 3-2 and illustrated in Figure 3-3.

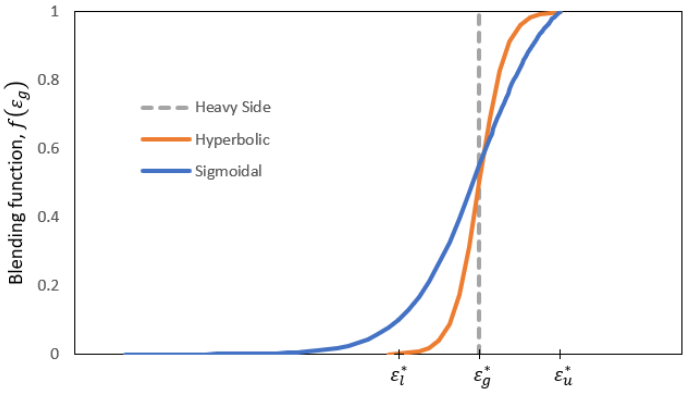

Figure 3-3: Schematic illustrating the blending function around the critical void fraction (void fraction at maximum packing).

[31]The stress model of Schaeffer does not match the total stress formula given by 3-16 and so not all terms in the latter are represented. Recall, it was re-written and cast in this form for computational reasons.

Table 3-2: Blending functions available in MFIX[1]

Type	Function	ε_l^*	ε_u^*
Hyperbolic Tangent	$f(\varepsilon_g) = \begin{cases} \frac{1}{2}\left[\tanh\left(2\pi\frac{\varepsilon_g - 0.5(\varepsilon_u^* + \varepsilon_l^*)}{\varepsilon_u^* - \varepsilon_l^*}\right) + 1.0\right] & \varepsilon_l^* < \varepsilon_g < \varepsilon_u^* \\ 1.0 & \varepsilon_u^* \le \varepsilon_g \\ 0.0 & \varepsilon_g \le \varepsilon_l^* \end{cases}$	$0.99\varepsilon^*$	$1.01\varepsilon^*$
Truncated Sigmoidal	$f(\varepsilon_g) = \begin{cases} \frac{\varphi(\varepsilon_g)}{\varphi(\varepsilon_u^*)} & \varepsilon_g < \varepsilon_u^* \\ 1.0 & \varepsilon_u^* \le \varepsilon_g \end{cases}$ where $\varphi(\alpha) = \left[1.0 + 0.01^{\frac{\alpha - \varepsilon^*}{\varepsilon_u^* - \varepsilon_l^*}}\right]^{-1}$	$0.99\varepsilon^*$	$1.01\varepsilon^*$

1) As indicated earlier, ε^* is the void fraction at close packing [60, 51] (see 3.4.2.1 for more detail).

3.4.2.2 Srivastava Friction Model [54]

Srivastava *et al*. [54, 64] proposed a constitutive model for the frictional regime that follows a rigid-plastic rheological model based on the works of Schaeffer [58], Tardos [65], and Prakash and Rao [66].

$$\mu_m^{fric} = \begin{cases} \dfrac{\sqrt{2}P_f \sin\phi}{\sqrt{\Theta_m/d_m^2 + S_{mij}S_{mji}}}\left(n - (n-1)\left(\dfrac{P_f}{P_c}\right)^{\frac{1}{n-1}}\right)\left(\dfrac{\varepsilon_m}{\varepsilon_s}\right) & \varepsilon_g < 1 - \varepsilon_f^{min} \\ 0 & \varepsilon_g \ge 1 - \varepsilon_f^{min} \end{cases} \quad (3\text{-}32)$$

Here ϕ is the angle of internal friction, d_m represents the diameter of particles in the m^{th} phase, and Θ_m is the m^{th} phase granular temperature (see section 3.4.3). Based on arguments of Savage [52], Srivastava introduced the term Θ_m/d_m^2 in the denominator to eliminate a numerical singularity appearing in regions of little to no flow. Here Θ_m has dimensions of square of velocity (see section 3.4.3.3.2). The conditional criteria is based on ε_f^{min} which represents the minimum total solids volume fraction required for the onset of frictional stresses. The last term in 3-32, $(\varepsilon_m/\varepsilon_s)$, is an ad-hoc extension of the original model for polydisperse mixtures where ε_m is the m^{th} phase volume fraction and ε_s represents the total volume fraction of M dispersed phases, that is, the total *solids* volume fraction ($\varepsilon_s = \sum_{m=1}^{M} \varepsilon_m$).
The exponent (n) is determined on whether the granular assembly is dilating or compacting.

$$n = \begin{cases} \dfrac{\sqrt{3}}{2\sin\phi} & D_{mkk} \ge 0; \text{ dilation} \\ 1.03 & D_{mkk} < 0; \text{ compaction} \end{cases} \quad (3\text{-}33)$$

P_c and P_f are the critical state and frictional pressures:

$$P_c = \begin{cases} 0 & \left(1-\varepsilon_f^{min}\right) \le \varepsilon_g \\ \mathrm{Fr}\dfrac{\left(\left(1-\varepsilon_g\right)-\varepsilon_f^{min}\right)^r}{\left(\varepsilon_g-\varepsilon^*\right)^s} & \varepsilon^*+\delta \le \varepsilon_g < \left(1-\varepsilon_f^{min}\right) \\ L_{\varepsilon_g^*+\delta}(\varepsilon_g) & \varepsilon_g < \varepsilon^*+\delta \end{cases} \tag{3-34}$$

$$\frac{P_f}{P_c} = \left(1 - \frac{D_{mkk}}{n\sqrt{2}\sin\phi\sqrt{S_{mij}S_{mji}+\Theta_m/d_m^2}}\right)^{n-1}\left(\frac{\varepsilon_m}{\varepsilon_s}\right) \tag{3-35}$$

As communicated in [67], the expression for P_f/P_c is correctly expressed with an exponent as $n-1$ rather than as $1/(n-1)$ shown in [54]. Here the expression for P_C is based on that proposed in Johnson *et al.* [68], who also provides values for the model constants, Fr, r, and s, as they are cited in [54] and listed here in Table 3-3. D_{mkk} and S_{mij} are given by equations (3-17) and (3-20), respectively. As in the Schaeffer Model (section 3.4.2.1), ε_g^* is the void fraction at close packing. Similar to the viscosity term in 3-32, the last term in 3-35 ($\varepsilon_m/\varepsilon_s$) represents an ad-hoc extension of the original model for polydisperse mixtures. To avoid a discontinuity in P_c when ε_g equals that of ε^*, while also providing a stable and continuous function, the third conditional criteria is introduced. Here, $L_{\varepsilon_g^*+\delta}(\varepsilon_g)$ is the linearization of $P_c(\varepsilon_g)$ at void fraction approaching that of close packing, that is, for $\varepsilon_g = \varepsilon^*+\delta$ where and δ represents a small constant deviation whose value is also listed in Table 3-3.

$$\begin{aligned} L_{\varepsilon_g^*+\delta}(\varepsilon_g) = \ \mathrm{Fr}\Bigg\{ & \frac{\left(1-\varepsilon^*-\delta-\varepsilon_f^{min}\right)^r}{\delta^s} + \frac{r\cdot\left[1-\varepsilon^*-\delta-\varepsilon_f^{min}\right]^{r-1}}{\delta^s} \\ & + \frac{s\cdot\left[1-\varepsilon^*-\delta-\varepsilon_f^{min}\right]^r}{\delta^{s-1}}\Bigg\}\cdot\left(\varepsilon^*+\delta-\varepsilon_g\right) \end{aligned} \tag{3-36}$$

Table 3-3: Default values for Princeton Model constants [54, 68]

Constant	ε_f^{min}	Fr [barye]	r	s	δ
MFIX Default	0.5	0.5	2.0	5.0	0.01

The frictional solids pressure, P_m^{fric}, contributes to the total solids phase pressure in equation (3-24). Similarly, the frictional flow shear viscosity, μ_m^{fric}, is added to the total solids viscosity in equation (3-22), while the frictional second viscosity, λ_m^{fric}, contributes to the total second viscosity in equation (3.25) through its definition given in equation (3-18).

3.4.3 Viscous Stresses

When the particles move freely and interact via nearly instantaneous collisions, then the system is considered in the rapid-flow regime and is commonly referred to as either collision-dominated flow, a rapid flow or a granular gas. Several kinetic theory based options are available in MFIX to describe the motion of particles in this flow regime, which are discussed in the following.

For reference, granular flows generally refer to systems where the interstitial fluid does not play a significant role in determining the overall mechanics and therefore can be ignored (also referred to as dry granular gas). In such a case, the physical picture of a granular gas is viewed analogously to that of a molecular gas; both are composed of many individual entities interacting through collisions. The key difference is that particles undergo dissipative collisions. Thus to maintain the motion, kinetic energy must be continually added (e.g., shaking, vibrating, shearing). Nevertheless, the fluctuating velocity in a granular gas (corresponding to the random motion of the particles) is viewed similarly to the thermal velocity in a molecular gas. Thus, the kinetic energy in a granular system is referred to as granular temperature (Θ). A complete thermodynamic analogy, however, is not applicable as granular 'gases' are inherently non-equilibrium systems. Still, this parallel has provided a useful framework for discussing the behavior of granular systems. In particular, dense-gas kinetic theory [69] modified to account for grain inelasticity provides one of the more sophisticated methods for modeling such systems.

The hydrodynamic equations, including constitutive relations, can be derived from a fundamental basis in kinetic theory. In this approach, the *closures* follow as mathematical consequence of the theory, and not phenomenologically as from experiment or intuitive argument (see section 3.1). Generally, this analyses involves some constraints although development in the area of kinetic-theory based models for granular flows has evolved over time. Savage & Jeffrey [70] were the first to place the problem of developing a model for granular gases in the more formal context of dense-gas kinetic theory. However, Lun [71] was the first to incorporate the kinetic contribution to momentum transport (previously only collisional transfer was considered). Each subsequent iteration has generally incorporated more representative physics and/or less assumptions. Such inclusions, however, give rise to greater complexity of the calculations in the derivation. The remainder of this section is intended to provide a short introduction to the various kinetic theory based models that are currently available in MFIX and highlight their essential differences. For further details on various kinetic theory based treatments and their implications, see references [10, 72].

Briefly, kinetic theory based models for granular flows may be differentiated from one another based on a number of conditions that may restrict their application or expected accuracy. Some of these are listed here for convenience and are discussed below in more detail: number of components or phases (i.e., monodisperse vs polydisperse systems); the specific starting kinetic equation; the solution method and assumptions/technicalities used in the subsequent derivation process. Table 3-4 lists the current kinetic theory based models available in MFIX along with

some of their various limitations and differences in derivation. Of the kinetic theory based models available in MFIX, several standard simplifying assumptions are used: 1) particles are smooth, frictionless spheres; and 2) particle collisions are instantaneous, binary and characterized by a constant coefficient of restitution. In addition, the Knudsen numbers of the continuum variables are also small (i.e., the theory is of Navier-Stokes-order).

Essentially the hydrodynamic equations derived from kinetic theory for the granular material are combined with those that describe the fluid phase resulting in the two-fluid equations and closure relations for the solids-phase stresses [48, 73, 56, 74, 75, 39, 76]. At a basic level, interaction forces, such as drag, were then typically included to account for transfer of momentum between the phases. However, incorporating the role of a fluid phase on a more fundamental level has also received more recent attention. Generally speaking, two things happen when the equations are combined: (1) the solids stress τ_{mij}^{kin} in two-fluid model is taken as the granular stress in the kinetic theory of granular gases; (2) a granular energy equation(s) is added to the two-fluid model. The precise details, however, depend on the kinetic theory model.

Table 3-4: Comparison of kinetic theory models available in MFIX

Reference	Year	Number of Phases[1]	Restitution Ceofficient[2]	Velocity Distribution	Hydro-dynamic Variables[3]	Fluid Effects[4]
Lun et al. [71]	1984	$1 \overset{mod}{\Longrightarrow} M$	e~1	non-Maxwellian	n_1, U_{1i},Θ_1	not inherently
Cao and Ahmadi [77]	1995	$1 \overset{mod}{\Longrightarrow} M$	e~1	non-Maxwellian	n_1, U_{1i}, Θ_1	influence of gas velocity fluctuations due to turbulence considered in solids phase description through a heuristic approach
Simonin [78] and Balzer [79]	1996	$1 \overset{mod}{\Longrightarrow} M$	e~1	non-Maxwellian	n_1, U_{1i}, Θ_1	influence of gas velocity fluctuations due to turbulence considered in solids phase description through a heuristic approach
Garzo and Dufty [7]	1999	1	inelastic	non-Maxwellian	n_1, U_{1i}, Θ_1	not inherently
Iddir and Arastoopour [8]	2005	M	e_{ml}~1	Maxwellian (unlike) non-Maxwellian (like)	n_m, U_{mi}, $\Theta_{m,IA}$	not inherently
Garzo et al. [9, 10]	2007	M	inelastic	non-Maxwellian	n_m, U_{Mi}, Θ_M	not inherently
Garzo et al. [11]	2012	1	inelastic	non-Maxwellian	n_1, U_{1i},Θ_1	influence of gas phase effects in solids phase description are incorporated on a fundamental level

1) The number of phases considered in the original derivation is given along with an indication of whether any ad hoc modifications have been included to extend the theory in the MFIX implementation.
2) Here, e~1 refers to theory based on an expansion about a nearly-elastic state and "inelastic" to one based on expansion about a homogenous cooling system. While no formal restriction on dissipation may exist in the latter, strong dissipation may lead to breakdown of the Enskog equation with regard to the assumption of molecular chaos.
3) While no subscripts are generally necessary in the monodisperse case, here the subscript 1 is kept for consistency with MFIX notation. It refers to the case $M = 1$ so $m = 1$. For Garzo et al. (2007) the subscript M refers to the *mixture* value as opposed to an m^{th} phase value. For Iddir and Arastoopour (2005) the subscript IA on granular temperature refers to m^{th} phase temperature defined in terms of velocity fluctuations relative to the mean *phase* velocity instead of a *mixture* velocity as is often used by polydisperse kinetic theories.
4) For reference see discussion of incorporating an interstitial fluid in section 3.4.3.3.8. While fluid effects may not be inherent to the indicated kinetic theory, the influence of a fluid phase has been incorporated at various levels depending on the kinetic theory model. Such details are reserved for the discussion for each available kinetic theory based model. Otherwise, a mean drag force is added into the momentum balance that effectively results in the basic two fluid model formulation.

3.4.3.1 Kinetic Theory in Brief

Kinetic-theory-based models for granular gases generally starts with a kinetic equation which describes the evolution of the single particle velocity distribution function (f). Models based on the Boltzmann kinetic equation are limited to dilute systems (e.g., [80, 81]). However, extensions to moderately dense systems are possible by employing the Enskog(-Boltzmann) kinetic equation (e.g., [71, 7, 8, 9, 10]). In the latter, the collisional term involves finite-volume effects (which are important in dense systems), whereas the former treats the particles as points. More precisely, the difference between these equations essentially stems from the treatment of the two particle distribution function (f_2) which appears in the collisional integral. The theories available in MFIX employ the Enskog equation (either revised or standard Enskog Theories; see next), and none are based on the Boltzmann equation.

In the Boltzmann equation, the two particle distribution function is assumed equal to the product of two single-particle distribution functions evaluated at the same location. In contrast, the Enskog equation (or Enskog kinetic theory), incorporates the pair correlation function (i.e., a quantity related to the radial distribution function or RDF) as a factor and the single particle distribution functions are evaluated at different locations (accounting for the finite distance between touching particles). The difference between the revised Enskog Theory (RET) and Standard Enskog Theory (SET) concerns the treatment of the radial distribution function during the derivation. In the latter, the RDF is taken as a function of the component densities, while in RET, it is taken as functionals [82][32]. SET is found to be inconsistent with irreversible thermodynamics [82]. Generally speaking, using RET is more important for mixtures and states far from equilibrium.[33] It is worth noting that in either case, the Enskog equation *neglects* velocity correlations between particles that are about to collide (molecular chaos assumption). So that, strictly speaking, multiparticle collisions, including recollision events ("ring" collisions) are not described.

3.4.3.2 Solution Method

The hydrodynamic (continuum) equations may be obtained by taking moments of the kinetic equation (i.e., they follow from the corresponding moments of the kinetic equation and the definition of the hydrodynamic fields in terms of integrals of the distribution function). This

[32] In a nonuniform equilibrium state the local RDF may involve gradients in the local density, higher powers of those gradients and higher order space derivatives than the first. This cannot be properly expressed based on a local value only (SET) but can be expressed as a functional of the local density (RET), that is, as a function of local density and its gradients (non-local dependence on the field at all points).

[33] For monodisperse systems ($M = 1$), SET and RET yield the same Navier-Stokes equations [79]. However, Burnett and high-order hydrodynamic equations will not be properly described based on SET. For polydisperse systems ($M > 1$), different Navier-Stokes transport coefficients are obtained.

leads to the constitutive terms as functionals of the single particle velocity distribution function (see [83]). An exact analytic solution for the single particle distribution function is itself not practical [9], however, finding even an approximation for the single particle distribution function is nontrivial. While exact balance equations for the hydrodynamic fields can be obtained, they are not closed until the constitutive equations are also expressed as functions of the hydrodynamic fields and their gradients[34]. Ultimately a solution for the single particle velocity distribution function as a functional of the hydrodynamic fields is sought, and this is referred to as the "normal" solution.[35]

Generally speaking, two different approaches have been used to solve the kinetic equation for the single particle velocity distribution function: Grad's method of moments and its generalizations [71, 84, 85] or the Chapman-Enskog (CE) expansion [7, 8, 9, 10, 86]. Alternatively, a form of the single particle velocity distribution may simply be conjectured and then substituted into the balance equations. Such studies do not involve a direct or systematic analysis of the starting kinetic equation. Several of the theories available in MFIX are based on the CE expansion, and so, the following short discussion focuses on this method. The CE expansion involves a perturbative expansion about the zeroth order solution to the kinetic equation (e.g., Boltzmann-Enskog equation). Approximate methods are used to obtain a solution and different simplifying assumptions can further distinguish the various kinetic theories models available. The solution is then used to obtain explicit expressions for the constitutive equations in terms of the hydrodynamic variables.

3.4.3.2.1 *Order of Expansion (CE)*

As noted above, CE expansion is a method for solution to the Enskog equation (RET) and it involves a perturbative expansion. More specifically, this expansion is about *low* Knudsen (Kn) numbers which is defined as the ratio of the mean free path to the characteristic length scale of mean-flow gradients (spatial variation in hydrodynamic variable). A low Knudsen number generally corresponds to small variation in the flow on a scale of the mean free path. Granular flows are often characterized by lack of separation of length and time scales. In particular, clusters can produce regions of high mean free paths and large Knudsen number based on velocity gradients. As a result the appropriateness of a continuum description based on such an assumption is a topic of debate (e.g., [87, 88, 89] ref). Mitrano *et al*. [89] demonstrated that kinetic-theory-based continuum models are accurate even at large Knudsen-numbers. The expansion order refers to how many terms are used in the perturbative expansion. For reference, a first order expansion yields the Navier-Stokes equation and the next are the Burnett and super-

[34] All space and time dependence of the single particle distribution function is made to occur through functionals of the hydrodynamic fields.
[35] For polydisperse systems, the solution for each component, or phase in MFIX terms, is needed.

Burnett orders. As indicated, the Navier-Stokes equations can, in principle, be refined by expanding to high order in Kn, however, the approach is non-trivial (e.g. [81]).[36] As noted earlier, the theories available in MFIX are of Navier-Stokes order.

3.4.3.2.2 *Base State (CE)*

Several theories a priori assume a form of the *zeroth* order distribution function in an effort to simplify the analysis (e.g., [81]). However, this base state should be determined as a solution to the kinetic equation to zeroth order gradient expansion. For classic molecular systems (i.e., purely elastic), the zeroth order corresponds to a state of local equilibrium (Maxwellian distribution). That is, it is a solution of the pertinent kinetic equation. In contrast, granular systems are inherently dissipative so that no such "equilibrium" state exists (i.e. energy must be added to maintain motion). Nonetheless, this same zeroth order solution has been used to derive theories for granular systems (e.g., [8, 81, 90]). Strictly speaking, such theories are restricted to nearly elastic systems; they *should* not only involve an expansion about small Kn, but also about small degree of inelasticity ($1 - e^2$; where e is the restitution coefficient).[37] The zeroth order solution for *inelastic* systems is found to correspond to the local homogenous cooling state. Theories based on the homogenous cooling system as the zeroth-order solution (e.g., [7, 9, 10, 80]), do not have such formal restrictions on inelasticity (see Table 3-4).

3.4.3.2.3 *Order of Sonine Polynomial Expansion (CE)*

A truncated Sonine polynomial expansion is employed to allow analytic evaluation of the collision integrals. Generally speaking all applicable theories available in MFIX employ the lowest, nonzero order, (1^{st}) order of the polynomial expansion. The interested reader is referred to Dufty and Baskaran [83] for further details and additional references on the topic.

3.4.3.3 Additional Comments and Considerations

3.4.3.3.1 Number of Phases

The earliest theoretical models for granular gases were limited to monodisperse systems (i.e. systems composed of identical particles) (e.g., [71, 7]). However, most industrially relevant systems will be polydisperse wherein particles may differ by size, density and/or some other factor. More recently, kinetic theory based models for polydisperse systems have been developed with varying degrees of sophistication and rigor. Jenkins and Mancini [86] were one

[36] Burnett equations also require higher-order boundary conditions, which is an active area of research (see Hrenya [69]).

[37] Many early kinetic theories failed to perform a systematic expansion about both parameters; they assume the single particle distribution function to be Maxwellian with an added perturbation about small *Kn* but not about $(1 - e)$ (for further clarification see Sela and Goldhirsch [78]).

of the first to develop a complete kinetic-theory based model for a binary granular mixture in a general flow field. Some recent theories have been derived for a more general system of M distinct phases (e.g., [8, 9, 10]). A polydisperse kinetic theory is generally largely analogous to a monodisperse theory, however, several items are worth discussing.

While a monodisperse theory is insufficient for most realistic systems, polydisperse theories were not available at first. Thus, some monodisperse theories were generalized in an ad hoc manner so that they can be used for polydisperse systems (e.g., [91]). In MFIX, such a technique was used to extend the monodisperse theory of Lun *et al*. [71] to polydisperse systems; the details of which are discussed in the corresponding 3.4.3.5. As indicated by Mathiesen *et al*. [91] the generalized multiphase model should be consistent, that is, the model description for an arbitrary number of identical phases reduces to the model description for a single phase (discussed in more detail below). That said, such a generalized monodisperse theory will miss contributions found in a polydisperse theory that has been systematically developed.

Polydisperse theories are expected to reduce to a monodisperse theory under equivalent limiting conditions. For example, one expects the same results if the number of phases is equal to one ($M = 1$) or if multiple identical phases are used ($M > 1$ with $d_m = d_1 = d_2 = \cdots$, $m_m = m_1 = m_2 = \cdots$) and compared to a monodisperse system of the same total solids volume fraction ($\varepsilon_1 = \varepsilon_s \equiv \sum_{m=1}^{M} \varepsilon_m$). Some polydisperse theories have been found to fail this monodisperse limit [92]. For example, in the theory of Iddir and Arastoopour [8] the sum of the kinetic stresses of two identical phases (or components) do not add to that of an equivalent monodisperse system. To ensure the monodisperse limit is correctly reached an ad hoc modification to this theory was proposed [92].

3.4.3.3.2 Granular Temperature Definition

Generally speaking the definition of the m^{th} solids phase granular temperature is given as follows:

$$\Theta_m = \frac{1}{3} m_m < V_{mi}^2 > \tag{3-37}$$

Here, m_m is the mass of a particle from the m^{th} solids phase and V_{mi} is the peculiar or fluctuating velocity. The latter is defined as $V_{mi} = v_{mi} - U_{Mi}$, where v_{mi} is the instantaneous velocity of the m^{th} solids phase, and U_{Mi} is the mass-averaged mixture velocity.

$$U_{Mi} = \frac{\sum_{m=1}^{M} \rho_m \varepsilon_m U_{mi}}{\sum_{m=1}^{M} \rho_m \varepsilon_m} \tag{3-38}$$

Here it is worth noting that $\rho_m \varepsilon_m = m_m n_m$, where n_m is the m^{th} phase number density. The other quantities are as before. For monodisperse theories mass is often not included in the definition of granular temperature (e.g., [71]), in which case, granular temperature has

dimensions of velocity squared. Furthermore, not all polydisperse kinetic theories employ this definition of granular temperature. For example, Iddir and Arastoopour [8] define the peculiar velocity relative to the average phase velocity (U_{mi}) instead of the mass-averaged mixture velocity (U_{Mi}). For reference see Table 3-4.

3.4.3.3.3 Equipartition of Energy

Equipartition of energy assumes the granular temperature of each phase is equal ($\Theta = \Theta_1 = \Theta_2 = \cdots$). While this assumption has been used in the derivation of several early polydisperse kinetic theories [86, 85], it is not used by either of the *polydisperse* theories available in MFIX.[38] Such an assumption would restrict the validity of the theory to nearly elastic systems and systems without mass disparities (i.e., unlike particles have equal masses).[39]

3.4.3.3.4 Single Particle Velocity Distribution Function

Evaluation of the collision integrals is challenging. To ease the calculations, the form of the single particle velocity distribution has often been assumed to be Maxwellian. This assumption is only valid for perfectly elastic systems in equilibrium. Most of the theories available in MFIX incorporate a non-Maxwellian distribution. However, the polydisperse theory of Iddir and Arastoopour [8] assumes a Maxwellian distribution when evaluating the collision integrals between unlike particles and a non-Maxwellian distribution to evaluate collision integrals between like particles.

3.4.3.3.5 Hydrodynamic Variables

In developing a hydrodynamic description, the relevant hydrodynamic fields are first identified and the subsequent balance equations are then derived. These equations reflect the macroscopic description corresponding to the behavior on the microscopic scale. The selection of these fields is not necessarily clear and their choice will impact that resulting set of balance equations. Ideally, these fields have long time and length scales that exceed those of the transient microscopic dynamics [83, 10]. A locally conserved quantity will demonstrate this property; it will approach a constant as the system becomes uniform. Thus, for an elastic gas, species number densities (mass), total momentum (velocity) and total energy density (temperature) are selected as the hydrodynamic fields. Note that the number density is related to the solids volume fraction as follows: $n_m = \varepsilon_m / \mathcal{V}_m$ where $\mathcal{V}_m$ is the volume of a particle from the m^{th} solids

[38] The notion of equipartition of energy is not relevant when considering the ad-hoc modifications to extend the monodisperse kinetic theory of Lun et al. [68] to polydisperse systems.

[39] The theory of Garzo et al. [9, 10] use Θ_M as a hydrodynamic variable but allows for a non-equipartition of energy. The granular temperature of each phase (Θ_m) are obtained through solution of the cooling rate as opposed to solving a conservation balance equation.

phase (i.e., $\mathcal{V}_m = \pi d_m^3/6$ or equivalently $n_m m_m = \varepsilon_m \rho_m$ where m_m is the mass of a particle from the m^{th} solids phase). In a granular gas, the *granular* energy is not conserved (recall section 3.4.3). However, the cooling rate may be slow compared to the microscale dynamics and therefore granular energy may be considered a relevant slow variable.

For monodisperse systems, number density, average velocity and granular temperature (n_1, U_{1i} , Θ_1, respectively, here $m = 1$ for $M = 1$) become the set of hydrodynamic variables. For polydisperse kinetic systems, however, various sets of hydrodynamic variables have been used as indicated in Table 3-4. Namely, Iddir and Arastoopour [8] utilize the number density, average velocity and granular temperature associated with each phase present (n_m, U_{mi}, and Θ_m, respectively), whereas Garzo *et al*. [10] use the phasic number density, mixture average velocity, and mixture granular temperature (n_m, U_M, Θ_M, respectively, where the subscript M refers to a mixture quantity as opposed to that associated with a specific phase). This choice of a mixture granular temperature (Θ_M) is observed to be the more appropriate [10, 72].

In regard to polydisperse theories, the choice of hydrodynamic variables will not only influence the form of the resulting balance equations but also dictate the total number of balance equations that are required to describe the system (see [72] for details). Namely, a theory using n_m, U_{mi}, and Θ_m, will have $3M$ differential balances (M mass balances, M momentum balances and M granular energy balances), whereas a theory using n_m, U_{Mi}, and Θ_M will have M+2 balances (M mass balances, a mixture momentum balance and a mixture granular energy balance). That said, the one polydisperse theory available in MFIX which uses this latter set of hydrodynamic variables [10] involves closures which are largely implicit in form as opposed to explicit. That is, for a given values of the hydrodynamic variables a set of algebraic equations must be solved to find the constitutive quantity. Thus, while the number of balance equations may be less, additional computational effort is required to determine the corresponding constitutive quantities.

3.4.3.3.6 Radial Distribution Function at Contact

Recall that the Enskog equation employs a factor that encompasses the spatial correlations arising from volume exclusion effects (i.e. finite volume) which can be related to the radial distribution function at contact [82, 93]. In the revised Enksog theory (RET), this factor is treated as a functional of species densities, while in the "standard" Enskog theory (SET), this factor is treated as a function of species densities at a single position (i.e., a constant value) [83]. The latter results in equations that are inconsistent with irreversible thermodynamics (see section 3.4.3.1 for more detail).

In the dilute limit, the radial distribution function (RDF) at contact has a value of one since no spatial correlations exist.[40] The value of the RDF then increases with increases in concentration to reflect the development of spatial correlations due to volume exclusion effects.

A number of different RDF at contact have been proposed and several area available in MFIX as listed in Table 3-5. The radial distribution function can be obtained experimentally, numerically from computer simulation techniques, or theoretically based on an appropriate intermolecular potential [94, 95].[41] Of those listed, Lebowitz [96] provides the earliest contribution and it is based on a generalization of the Percus-Yevick integral equation for the radial distribution function of a hard sphere fluid to that of a general mixture. An explicit relation for the radial distribution function is given. Carnahan and Starling [97] provided an equation of state (EOS) for a hard sphere fluid (monodisperse), which can be used to construct an expression for the hard-sphere radial distribution function [98, 99]. The radial distribution function has been employed in numerous works describing the behavior of hard spheres (e.g., [70, 71]) The equation of state was also generalized to mixtures [99, 100], the latter whom also presents the corresponding radial distribution function.

The RDF/EOS cited above [96, 97, 99, 100] yield a finite value as the solids volume fraction approaches that of maximum close packing diverging only when the solids volume fraction approaches one. However, from the molecular dynamic simulation data reported by Alder and Wainright [101] the RDF should diverge as the solids volume approaches close packing because particles are in close contact [46, 102, 103]. Alternative expressions have been proposed that tend to infinity at close packing, such as, those proposed by Iddir and Arstoopour [8] and van Wachem *et al*. [46]. These authors modify the expressions of Lebowitz and Mansoori/Boublick, respectively, by incorporating a maximum volume fraction at close packing (ε_s^{max}).

A few additional items are worth noting. Estimating the value of ε_s^{max} used in several of the above referenced expressions is an important problem. As discussed in section 3.4.2.1, ε_s^{max} may be specified as a constant or estimated using correlations that are available to describe the packing of polydisperse systems. As evident, for polydisperse systems the radial distribution functions depends on the volume fraction and diameter of each phase (ε_m and d_m respectively), while for monodisperse systems the radial distribution function depends only on the volume

[40] Note that simply replacing the RDF with a value of 1 in the kinetic equation does not result in the Boltzmann equation; the Enskog equation also evaluates the distribution functions at different locations. The latter results in non-zero collisional transfer of quantities that are conserved during collision (e.g., momentum) ([80, 69]).

[41] Principles from statistical mechanics may be used to estimate the equation of state from a suitable intermolecular potential model but the calculations quickly become complex. A different approach to developing the equation of state involves the introduction of the radial distribution function. The radial distribution function is directly related to the interaction potential, but computing the former from the latter is still a non-trivial task. Nevertheless, the equation of state and the radial distribution function are related. Knowing the RDF, the equation of state can be derived in two different ways, that is, one can obtain the corresponding equation of state through the virial equation or through the use of the isothermal compressibility relation [93, 91, 92].

fraction. Finally, simply swapping one RDF expression for another in a given polydisperse kinetic theory may not be appropriate. Instead, the diffusion force should be re-evaluated as it is derived from the expression used for the RDF at contact (greater see Hrenya [72]). Here it is worth noting that SET and RET result in different expressions for the diffusion force due to their different treatment for the RDF at contact (i.e., as a function or functional) (e.g., [104, 105]).

Table 3-5. Radial distribution functions at contact available in MFIX

Reference	Expression[1]
Carnahan & Starling [97][2]	$g_{mm} = \frac{2-\varepsilon_m}{2(1-\varepsilon_s)^3}$ or equivalently $g_{mm} = \frac{1}{(1-\varepsilon_s)} + \frac{3}{2}\frac{\varepsilon_m}{(1-\varepsilon_s)^2} + \frac{1}{2}\frac{\varepsilon_m^2}{(1-\varepsilon_s)^3}$
Lebowitz [96]	$g_{ml} = \frac{1}{(1-\varepsilon_s)} + \frac{3}{2}\frac{\xi}{(1-\varepsilon_s)^2}\frac{d_m d_l}{d_{ml}}$ where $d_{ml} = \frac{d_m + d_l}{2}$, $\xi = \sum_{p=1}^{M}\frac{\varepsilon_p}{d_p}$
Mansoori et al [100] and Boublick [99]	$g_{ml} = \frac{1}{(1-\varepsilon_s)} + \frac{3}{2}\frac{\xi}{(1-\varepsilon_s)^2}\frac{d_m d_l}{d_{ml}} + \frac{1}{2}\frac{\xi^2}{(1-\varepsilon_s)^3}\left(\frac{d_m d_l}{d_{ml}}\right)^2$
Iddir and Arastoopour [8] (modified Lebowitz [96])	$g_{ml} = \frac{1}{\left(1-\frac{\varepsilon_s}{\varepsilon_s^{max}}\right)} + \frac{3}{2}\frac{\xi}{\left(1-\frac{\varepsilon_s}{\varepsilon_s^{max}}\right)^2}\frac{d_m d_l}{d_{ml}}$
van Wachem et al. [46] (modified Mansoori et al. [100])	$g_{ml} = \frac{1}{\left(1-\frac{\varepsilon_s}{\varepsilon_s^{max}}\right)} + \frac{3}{2}\frac{\xi}{\left(1-\frac{\varepsilon_s}{\varepsilon_s^{max}}\right)^2}\frac{d_m d_l}{d_{ml}} + \frac{1}{2}\frac{\xi^2}{\left(1-\frac{\varepsilon_s}{\varepsilon_s^{max}}\right)^3}\left(\frac{d_m d_l}{d_{ml}}\right)^2$

1) Here it is convenient to introduce the notation ε_s, which represents the total volume fraction of all dispersed M phases, or total *solids* volume fraction: $\varepsilon_s = \sum_{m=1}^{M}\varepsilon_m$.
2) While this expression is presented in terms of the m^{th} phase, it is intended for a monodisperse fluid of hard spheres so that $\varepsilon_s = \varepsilon_m$.

3.4.3.3.7 Corrections In Dilute Limit

Early research on an *infinite* shearing system of particles (i.e., unbounded) observed the shear stress asymptotes to infinity as the solids volume fraction approaches zero [106, 107]. This was

observed in computer simulation data and in those theoretical predictions based on a kinetic theory treatment which included collisional and kinetic contributions.[42] The physical reasoning for this behavior is described by Campbell [107]; in short, temperature dissipation decays faster than temperature production resulting in infinite temperature and therefore infinite stress.. Nevertheless, the author questions the plausibility of the $\varepsilon_s \to 0$ asymptote in any realistic application and that unaccounted dissipation mechanisms may forestall such behavior as these works only accommodate dissipation due to particle-particle collisions. In reality, particle-wall collisions and/or aerodynamic forces on the particles should also act to dampen the granular temperature independently of the inter-particle collision rate.

Sinclair and Jackson [73] and Louge *et al.* [108] proposed a heuristic correction to shear stress to ensure it vanishes as the volume fraction approaches zero. More specifically, the modification involved an adjustment to the calculation of shear viscosity and thermal conductivity. They attributed the problem to the calculation of the mean free path of the particle which tended toward infinity as $\varepsilon_s \to 0$. The modification constrained the mean free path by a characteristic dimension of the physical system. Namely as the solids volume fraction becomes small, particle-wall collisions begin to play an increasing role. This is consistent with the idea that all wall-bounded flows contain a Knudsen layer adjacent to the wall where particle-wall collisions as opposed to particle-particle collisions dictate the behavior [109, 110]. That said, particle-particle collisions are still important to consider in these dilute systems and may not necessarily be ignored [111, 112]. The applied correction is a rough attempt to capture a transition to Knudsen flow. If the Knudsen layer is small then the effects of the Knudsen layer need not be incorporated (a continuum regime can be expected; see section 3.4.3.2.1). However, at higher Knudsen numbers a more rigorous mathematical description may become necessary.

In the context of gas-solid flows, as is discussed in more depth below, Balzar *et al*. [113] provides insight using through three characteristic time scales: inter-particle collision time, particle relaxation time due to drag, and time scale of fluid turbulence as viewed by the particle. For a granular system without an interstitial fluid phase the characteristic time scale is that of the inter-particle collision time (as discussed above). However, the fluid introduces the latter two time scales. When the interparticle collision time is large (as can be expected in dilute flows), the gas may be expected to play a dominate role in the fluctuating motion of particles and may shorten the particle mean free path.

3.4.3.3.8 Interstitial Fluid Effects

Up to now the discussion has focused on developing a hydrodynamic description for a *fluid* of particles. Other important effects, such as, an interstitial fluid phase (e.g., gas) were not

[42] If the kinetic contribution is ignored then the predictions would tend to zero as solids volume fraction goes to zero [43].

included. When the fluid phase does impact the movement of the particles, then the systems are referred to as fluid-solids (or multiphase or two-phase) flows. Efforts to incorporate the effects of the fluid into the solids phase hydrodynamic description have advanced over time. Some of these advancements are discussed briefly here given their relevance to several options available in MFIX-TFM. The interested reader is referred to Hrenya [72] and Garzo *et al*. [11] for additional discussion, and to the original sources for greater detail.

In early efforts to describe two phase flows the effects of the fluid were simply described through the addition of a *mean* drag force (given simply by a mean drag coefficient times a mean relative velocity difference)[43] into the momentum balance (see sections 3.3.3.1 and 3.4.4.2) (e.g., [73]). A refinement of this implementation considered the *fluctuation* in particle velocity in the interaction (drag) force [114]. This treatment leads to an additional sink term in the granular energy balance that has been referred to as dissipation due to viscous drag (i.e., viscous dampening). Incorporation of the effects of the local fluid fluctuation on the particle velocity in the interaction force, a further refinement, was also considered during the derivation of the granular energy balance. This disturbance results in an additional source that has been referred to as production due to slip. These terms are also found in the granular energy equations presented by Louge [108] and Gidaspow [74]. Sangani *et al*. [115] proposed a more comprehensive expression for the additional sink due to viscous effects of the interstitial gas, and similarly, Koch and Sangani [116] for the additional source.

While these aforementioned treatments lead to modification of the balance equation they did not consider how the incorporating such effects might influence the constitutive relations for the solids phases. Efforts in this regard have also been undertaken with varying levels of rigor. For example, Ma & Ahamdi [117] and Balzer, Boelle & Simonin [113] accounted for the effects of velocity fluctuations in the gas phase arising from fluid-phase turbulence into the solids phase description.

One of the limitations of these earlier works to incorporate gas and/or solids phase fluctuations is that they tend to maintain that the same basic form of the fluid interaction force (drag coefficient times a relative velocity difference) in terms of mean hydrodynamic fields also holds in terms of local fluctuating (instantaneous) quantities. In contrast, Garzo *et al*. [11] employ a more generalized model for the interaction force to cover a wide range of conditions. This model is then used to derive the solids phase balance equations and constitutive relations. Thus, gas-phase effects are incorporated more systematically on the most fundamental level through its incorporation in the starting kinetic equation (see section 3.4.3.1)

[43] Here mean refers to the value associated with the faraway fluid field as opposed to the instantaneous or fluctuating value.

3.4.3.4 Summary

As discussed earlier and summarized in Table 3-4, there are several kinetic theory options available in MFIX-TFM. Monodisperse kinetic theory models include those of Lun *et al*. [71], Garzo and Dufty [7], Garzo *et al*. [11]. In MFIX-TFM, the theory of Lun *et al*. [71] has been extended to describe polydisperse systems. Also available are the theory of Simonin [78] and Balzer *et al*. [113] and the theory of Cao and Ahmadi [77]. Both of these treatments include kinetic theory stresses as well as gas-phase turbulence models that account for the exchange of turbulence energy between the gas and solids phases (see section 3.4.6). Similar to the implementation of Lun *et al*. [71] these theories have been extended for polydisperse systems.

Two kinetic theories developed specifically for describing poly-dispersed systems have been implemented in MFIX-TFM (Iddir and Arastoopour [8]; and Garzo *et al*, [9, 10]). See Hrenya [72] for a critical comparison of kinetic theories for poly-dispersed systems. Benyahia [92] also compared four different kinetic theories for poly-dispersed systems in a simple shear flow setup, and of those, found Iddir and Arastoopour [8] theory to provide the most accurate predictions.

An examination of the MFIX implementation of the Lun *et al*. [71] kinetic theory follows. A similar analysis of each kinetic theory model available in MFIX is not included here at this time.

3.4.3.5 Lun *et al*. (1984) [71]

In this section the monodisperse kinetic theory of Lun *et al*. [71] as implemented into MFIX-TFM is described. It is worth noting that the implementation of this theory in MFIX includes a number of *ad hoc* modifications to extend the theory beyond its original scope. The modifications target generalizing the monodisperse description for polydispersity and including effects of the fluid phase.

The monodisperse model is generalized and made consistent for *M* number of solids phases to enable description of realistic industrial systems characterized by particle size/density distributions (see section 3.4.3.3.1). To accommodate polydispersity, solids specific quantities (e.g., diameter, density, volume fraction) in the theory of Lun *et al*. are now denoted with subscript m to indicate the specific m^{th} solids phase. And occurrences of $\varepsilon_m g_0$ are *generally* replaced with $\sum_{l=1}^{M} \varepsilon_l g_{ml}$ to maintain consistency.

Incorporating the effects of the fluid phases is accomplished in two ways (see section 3.4.3.3.8). First, the viscosity and granular conductivity are modified as indicated in Agrawal *et al*. [76]. Second, two additional terms are included in the granular energy balance, discussed below, that describes the effects of velocity fluctuations of the gas and those of the individual particles. The result is a term that describes production due to gas-particle slip and another to describe dissipation due to viscous damping. These modifications will be highlighted as they are introduced below.

The solids pressure contribution from the kinetic theory is described as follows:

$$P_m^{kin} = \varepsilon_m \rho_m \Theta_m \left[1 + 4\eta \sum_{l=1}^{M} \varepsilon_l g_{ml}\right] \tag{3-39}$$

For convenience the total stress tensor introduced earlier in equation 3-19 is re-written here in terms of its kinetic contribution:

$$\tau_{mij}^{kin} = 2\mu_m^{kin} S_{mij} + \mu_{bm}^{kin} D_{mkk} \delta_{ij} \tag{3-40}$$

As before, μ_m^{kin} is the kinetic contribution to viscosity, μ_{bm}^{kin} is the kinetic contribution to bulk viscosity, S_{mij} is the deviatoric rate-of-strain tensor, and D_{mij} is the rate-of-strain tensor. The solids viscosities arising from kinetic theory are represented by the equations below:

$$\mu_m^{kin} = \left(\frac{2+\alpha}{3}\right)\left[\frac{\mu_m^*}{(2-\eta)g_{mm}\eta}\left(1 + \frac{8}{5}\eta \sum_{l=1}^{M} \varepsilon_l g_{ml}\right)\left(1 + \frac{8}{5}\eta(3\eta - 2)\sum_{l=1}^{M} \varepsilon_l g_{ml}\right) + \frac{3}{5}\mu_{bm}^{kin}\right] \tag{3-41}$$

where

$$\mu_m^* = \frac{\rho_m \varepsilon_m g_{mm} \Theta_m \mu_m^{**}}{\rho_m \sum_{l=1}^{M} \varepsilon_l g_{ml}\, \Theta_m + \left(\frac{2\beta_{gm}\mu_m^{**}}{\rho_m \varepsilon_m}\right)} \tag{3-42}$$

$$\mu_m^{**} = \frac{5}{96}\rho_m d_m \sqrt{\pi \Theta_m} \tag{3-43}$$

$$\mu_{bm}^{kin} = \eta \frac{256}{5\pi} \mu_m^{**} \varepsilon_m \sum_{l=1}^{M} \varepsilon_l g_{ml} \tag{3-44}$$

$$\eta = \frac{1 + e_{mm}}{2} \tag{3-45}$$

The leading multiplicative factor, $\frac{1}{3}(2+\alpha)$, that appears in the kinetic contribution to the m^{th} solids phase viscosity is not in the work of Lun *et al*. As described by Johnson and Jackson [48] it is effectively an adjustable parameter in which α is a constant of order unity. The quantity u_m^* also represents a modification to that of Lun *et al.* and incorporates the role of the interstitial fluid into the granular viscosity as indicated by Agrawal [76]. Here, the term β_{gm} represents the drag coefficient as discussed in section 3.4.4.2. Inelasticity is introduced through the coefficient of restitution e_{mm}. Finally, Θ_m is the granular temperature or pseudo-thermal energy of the m^{th} phase, which has dimensions of the square of velocity (see section 3.4.3.3.2 and for additional discussion see section 3.4.3 along with Table 3-4). Like traditional thermal energy this quantity has its own balance equation (see sections 3.4.3.3.5).

In MFIX-TFM, the monodisperse theory of Lun *et al.* is re-written in terms of each solids phase. So, instead of a single granular energy equation describing the system, a granular energy associated with each solids phase emerges. Here, the m^{th} phase granular temperature is calculated from the following granular energy balance equation:

$$\frac{3}{2}\varepsilon_m\rho_m\left[\frac{\partial\Theta_m}{\partial t}+U_{mj}\frac{\partial\Theta_m}{\partial x_j}\right]=\frac{\partial}{\partial x_j}\left(\kappa_m\frac{\partial\Theta_m}{\partial x_j}\right)+\tau_{mij}\frac{\partial \mathrm{U}_{mi}}{\partial x_j}-J_m+\Pi_m \tag{3-46}$$

The first term on the right-hand side stands for the granular temperature diffusion or conduction, the second term represents production by shear, the third term denotes the collisional dissipation and the final term encompasses the effects of gas-particle slip and viscous dissipation. Closures for these are presented below.

The granular conductivity, associated with the conduction of granular temperature, is

$$\kappa_m=\left(\frac{\kappa_m^*}{g_{mm}}\right)\left[\left(1+\frac{12}{5}\eta\sum_{l=1}^{M}\varepsilon_l g_{ml}\right)\left(1+\frac{12}{5}\eta^2(4\eta-3)\sum_{l=1}^{M}\varepsilon_l g_{ml}\right)+\frac{64}{25\pi}(41-33\eta)\eta^2\left(\sum_{l=1}^{M}\varepsilon_l g_{ml}\right)^2\right] \tag{3-47}$$

where

$$\kappa_m^*=\frac{\rho_m\varepsilon_m g_{mm}\Theta_m\kappa_m^{**}}{\rho_m\sum_{l=1}^{M}\varepsilon_l g_{ml}\,\Theta_m+\left(\frac{6\beta_{gm}\kappa_m^{**}}{5\rho_m\varepsilon_m}\right)} \tag{3-48}$$

$$\kappa_m^{**}=\frac{75\rho_m d_m\sqrt{\pi\Theta_m}}{48\eta(41-33\eta)} \tag{3-49}$$

Like u_m^* above, κ_m^* represents a modification to that of Lun *et al.* for the effects of the interstitial fluid [76]. Note that the original expression for the granular heat flux also contains an additional term proportional to the gradient in the number density of the solids phase (the Dufour effect). This quantity is, by default, ignored in the MFIX-TFM implementation of this theory.

The expression for the collisional dissipation term is

$$J_m=\frac{48}{\sqrt{\pi}d_m}\eta(1-\eta)\varepsilon_m\rho_m\left(\sum_{l=1}^{M}\varepsilon_l g_{ml}\right)\Theta_m^{3/2} \tag{3-50}$$

The final term in equation (3-46) incorporates the effects of the interstitial fluid and includes production of granular energy due to gas-particle slip and dissipation by viscous damping. These

two terms are not present in purely granular systems and they serve as a modification to that of Lun *et al*. Koch [114] developed expressions for both viscous dissipation and production due to gas particle slip for dilute systems. Louge *et al.* [108], and later Gidaspow [74], present equivalent versions of the former, which is given here by the first term of equation (3-51). This model for viscous dissipation is extended in a later work [115]. The second term in equation (3-50) is also effectively given by Koch [114], but without the quantity g_{mm} appearing in the denominator [76]. Koch and Sangani [116] later extend their source term due to gas particle interactions. For further discussion see section 3.4.3.3.8.

$$\Pi_m = -3\beta_{gm}\Theta_m + \frac{81\varepsilon_m\mu_g^2\left|U_g - U_m\right|^2}{g_{mm}d_m^3\rho_m\sqrt{\pi\Theta_m}}. \tag{3-51}$$

As indicated previously, in MFIX-TFM the monodisperse theory of Lun *et al.* is generalized as a polydisperse theory. In addition to assuring consistency (see section 3.4.3.3.1), an additional term is also included to describe the momentum transfer between particles of different phases. Here it should be noted that when two particles of a given phase collide, no overall momentum change occurs for that phase (overall momentum is conserved during a collision). In this case, however, the single momentum balance has been generalized and written for each distinct phase. So a gain in momentum for one phase and a loss in that of the other may occur, while the net momentum change for both combined is zero. This new term, and how it is closed, is described in more detail in section 3.4.5.

3.4.3.5.1 Algebraic

Rather than solving the complete granular energy balance given in equation (3-46), a simplified algebraic expression for the granular energy has also been proposed (see [55] and later in [56]). In this approach, granular energy is assumed to dissipate locally, hence convection and diffusion are neglected. Assuming steady state, the rate of production is balanced by dissipation and an algebraic form of the energy equation is obtained:

$$\Theta_m = \left\{ -\frac{K_{1m}\varepsilon_m D_{mii}}{2\varepsilon_m K_{4m}} + \frac{\sqrt{K_{1m}^2(D_{mii})^2\varepsilon_m^2 + 4K_{4m}\varepsilon_m\left[K_{2m}(D_{mii})^2 + 2K_{3m}(D_{mij}D_{mji})\right]}}{2\varepsilon_m K_{4m}} \right\}^2 \tag{3-52}$$

$$K_{1m} = 2(1 + e_{mm})\rho_m g_{0mm} \tag{3-53}$$

$$K_{2m} = \frac{4 d_m \rho_m (1 + e_{mm}) \varepsilon_m g_{mm}}{3\sqrt{\pi}} - \frac{2}{3} K_{3m} \tag{3-54}$$

$$K_{3m} = \frac{d_m \rho_m}{2} \left\{ \frac{\sqrt{\pi}}{3(3 - e_{mm})} [0.5(3e_{mm} + 1) + 0.4(1 + e_{mm})(3e_{mm} - 1)\varepsilon_m g_{mm}] + \frac{8 \varepsilon_m g_{mm} (1 + e_{mm})}{5\sqrt{\pi}} \right\} \tag{3-55}$$

$$K_{4m} = \frac{12(1 - e_{mm}^2) \rho_m g_{mm}}{d_m \sqrt{\pi}} \tag{3-56}$$

This approach is considered reasonable in dense flow regions wherein granular energy is expected to be generated and dissipated locally (transport is negligible). For example, researchers have used this in their simulation of bubbling beds (e.g., [118, 119]). The algebraic form may reduce the computational cost of simulations as faster convergence is obtained [119, 46].

3.4.4 Momentum Transfer Between the Fluid and m^{th} Phase

As indicated in section 3.3.3.1, $\mathcal{S}_{gi}$ and $\mathcal{S}_{mi}$ are redefined for convenience and to distinguish the contribution due to interphase momentum transfer between the gas and m^{th} phase:

$$\mathcal{S}_{gi} = -\sum_{m}^{M} I_{gmi} + \mathcal{S}_{gi}' \tag{3-5}$$

$$\mathcal{S}_{mi} = I_{gmi} + \mathcal{S}_{mi}' \tag{3-6}$$

Here I_{gmi} represents the contribution due to interphase momentum transfer between the gas and m^{th} phase, M represents the number of additional phases beyond the fluid phase and $\mathcal{S}_{gi}'$ and $\mathcal{S}_{mi}'$ are general gas and m^{th} phase momentum source terms excluding that due to the interphase momentum transfer between the gas and m^{th} phase, respectively.

Several different mechanisms for gas-solids interphase momentum transfer have been identified from studies of the motion of a single particle in a fluid [120]: *drag force*, caused by velocity differences between the phases; *buoyancy*, caused by the fluid pressure gradient; *virtual or added mass effect*, caused by relative acceleration between phases; *Saffman lift force*, caused by fluid-velocity gradients; *Magnus force*, caused by particle spin; *Basset force*, originating from the history of the particle's motion through the fluid; *Faxen force*, a correction applied to the virtual

mass effect; and forces caused by temperature and density gradients. The mechanisms and formulation of momentum transfer have been reviewed in detail [121, 122].

3.4.4.1 Buoyancy

The buoyancy force is the result of the fluid stress acting on the m^{th} phase [19]. This force is generally considered as the result of the vertical pressure gradient that is induced by the gravitational body force although other contributions to the pressure gradient may occur. Accordingly, different mathematical interpretations of the buoyancy force are possible [19, 39]. In MFIX the default form of the buoyancy force is defined as

$$I_{gmi,Bouy} = -\varepsilon_m \frac{\partial P_g}{\partial x_i} \tag{3-57}$$

This form leads to the multiphase momentum equations presented in 3-8 and 3-9. It has been termed Model A [123], and it leads to an ill-posed set of equations in a canonical problem involving simplified two-phase flow. In particular, 1D incompressible, inviscid-flow equations without virtual-mass effects are ill-posed as an initial value problem [36]. The ill-posed nature prompted researchers to develop modifications to the momentum equations that ensure a well-posed model for this simplified case. One approach has been to simply remove the gas pressure gradient term in the m^{th} phase momentum equation [123], which those authors refer to as Model B. However, such a formulation ignores buoyancy. Alternatively, buoyancy may be accounted for as

$$I_{gmi,Bouy} = -\varepsilon_m \rho_g g_i \tag{3-58}$$

which results in the body force terms appearing as $\rho_g g_i$ and $\varepsilon_m(\rho_m - \rho_g)g_i$ in the gas and m^{th} phase momentum equations, respectively. This form of the momentum equations is referred to as Model B in MFIX, but it has its own limitations [124]. While the Model B formulation is available in MFIX, the Model A formulation is generally used in practice and is seen as a good approximation of the well-posed model.

Jackson [39] presents different definitions of the buoyancy force along with a discussion on the remaining contributions in the interphase interaction term and the corresponding form of the governing equations for gas solids systems. Two of those definitions are discussed here for context and comparison with the above formulations. The first formulation was presented earlier (see equation 3-10) but is repeated here for convenience:

$$I_{gmi,Bouy} = -\varepsilon_m \left(\frac{\partial P_g}{\partial x_i} - \frac{\partial \tau_{gij}}{\partial x_j} \right) \tag{3-59}$$

This form leads to the multiphase momentum equations presented in 3-11 and 3-12, which are available in MFIX. As evident, this definition is similar to the MFIX default shown in equation 3-57 that led to the momentum equations designated Model A. The primary difference is the

appearance of the gas phase stress tensor in Jackson's definition (see [19, 39] for details). The second formulation [39] is given as

$$I_{gmi,Bouy} = -\rho_g \varepsilon_m \left(g_i - \left(\frac{\partial U_{gi}}{\partial t} + U_{gj} \frac{\partial U_{gi}}{\partial x_j} \right) \right) \tag{3-60}$$

This second formulation is not currently available in MFIX. However, it is worth noting that this definition is similar to MFIX's alternative definition shown in equation 3-58 that led to the momentum equations designated Model B. The difference is that Jackson's form is re-written to accommodate acceleration.

Regardless of the formulation for the buoyancy force, the value of the *total* interaction force (I_{gmi}) should remain the same. That is, if one is to consider decomposing the interface interaction force into the sum of a buoyancy force and all remaining contributions, then when different interpretations of the buoyancy force are used the latter terms should be formulated such that the *total* interface interaction force remains the same. Using the two different interpretations of buoyancy discussed above, Jackson shows that the remaining interaction terms must be related by a factor of void fraction (ε_g). For example, consider decomposing the interphase transfer term into buoyancy and drag due to relative velocity differences (see below). To ensure that the total interaction force is the same, then the drag force coefficients are related as: $\beta_{gm,B} = \beta_{gm,A}/\varepsilon_g$. Here $\beta_{gm,A}$ corresponds to the drag coefficient in the total interaction force when the first formulation for buoyancy is used (equation 3-59), while $\beta_{gm,B}$ corresponds to the drag coefficient when the second formulation for buoyancy is used (equation 3-60). This same practice is used in the MFIX implementation of Model A and Model B. These different definitions and their relation are also discussed by Van der Hoef [125].

The buoyancy force is added to the gas and m^{th} phase momentum balances (equation 3-3 and 3-4, respectively) through their corresponding general source terms S_{gi} and S_{mi} as a component of the interphase momentum transfer term (see equations 3-5 and 3-6).

3.4.4.2 Drag Force

The drag force results from relative motion between the phases. The gas-solids drag force encompasses skin friction and form drag arising from small scale distortions of the fluid streamlines in the neighborhood of the particle [19]. In MFIX, the gas-solids drag force is assumed to be a function of the difference in velocities,

$$I_{gmi,Drag} = \beta_{gm}(U_{gi} - U_{mi}) \tag{3-61}$$

where $\beta_{gm}$is the drag coefficient. Drag coefficients available in MFIX are presented in Appendix B. Their presented form assumes Model A form of the momentum equations,

otherwise division by void fraction is necessary for Model B (for further detail see section 3.4.4.1).

The drag force is added to the gas and solids phase momentum balances (equation 3-3 and 3-4, respectively) through their corresponding general source terms S_{gi} and S_{mi} as a component of the gas-solids interphase momentum transfer term (see equations 3-5 and 3-6).

3.4.4.3 Virtual (Added) Mass Effect

The added (virtual) mass force results from relative acceleration and is the force required to displace the fluid surrounding the accelerating body (e.g. particle) [122]. As noted by Anderson and Jackson [19], the relative acceleration term, like the buoyancy force, is not necessarily a well-defined quantity. As a result, different but acceptable definitions are possible. In MFIX, the virtual mass force is defined as follows.

$$I_{gmi,VM} = C_{vm}\varepsilon_m\varepsilon_g\rho_g\left[\left(\frac{\partial U_{gi}}{\partial t} + U_{gj}\frac{\partial U_{gi}}{\partial x_j}\right) - \left(\frac{\partial U_{mi}}{\partial t} + U_{mj}\frac{\partial U_{mi}}{\partial x_j}\right)\right]. \quad (3\text{-}62)$$

where C_{vm} is the virtual mass coefficient defined with a constant value $C_{vm} = \frac{1}{2}$.[44] When the particle has a lower density compared to the fluid, the virtual mass force generally becomes relatively important to the corresponding solids momentum balance [122]. In MFIX, it acts to increase the inertia of the dispersed phase, which generally stabilizes numerical simulation of bubbly flows.[45] For gas-solids flows, however, the added mass term is generally negligible.

The virtual mass force is added to the gas and m^{th} phase momentum balances (equation 3-3 and 3-4, respectively) through their corresponding general source terms S_{gi} and S_{mi} as a component of the gas-solids interphase momentum transfer term (see equations 3-5 and 3-6, respectively). In MFIX, the added mass force may only be invoked between the gas phase and a single user-designated dispersed phase M. No additional phases are involved in the calculation.

3.4.5 Momentum Transfer Between the m^{th} and l^{th} Dispersed Phases

In section 3.3.3.1, $\mathcal{S}_{gi}$ and $\mathcal{S}_{mi}$ are redefined to distinguish the contribution(s) due to interphase momentum transfer between the gas and m^{th} phase (see equations 3-5 and 3-6). For systems containing more than one dispersed phase (i.e. $M > 1$), interphase momentum transfer between M dispersed phase may also arise. This contribution is included in the term $\mathcal{S}_{mi}$ and, like interphase momentum transfer between the gas and m^{th} phase, a constitutive closure is needed.

---

[44] For a single perfect sphere accelerating through a fluid medium a virtual mass coefficient of 1/2 can be derived.
[45] In this scenario, the fluid phase is treated as liquid while the *solids* phase (dispersed phase) becomes a gaseous phase.

As with interphase momentum transfer between the gas and m^{th} phase, different mechanisms may contribute to the interphase momentum transfer between the dispersed phases. For example, drag arises due to relative motion between the m^{th} and l^{th} dispersed phases and is represented in MFIX-TFM as

$$S_{mi,Drag} = \sum_{m=1,m\neq l}^{M} F_{ml}(U_{li} - U_{mi}) \tag{3-63}$$

where F_{ml} is the drag coefficient. The force is added to the m^{th} phase momentum equation (equation 3-4) through the general source term, S_{mi}.

This term acts to hinder relative motion between phases (e.g. inhibit segregation) and has been found important for modeling solids-solids segregation [126]. Recall granular flows are often classified into frictional and kinetic regimes as discussed in section 3.4.1. In terms of the kinetic regime, this term arises due to particle-particle collisions and so is referred to as the collisional momentum source. Note that when two particles of a given phase collide, no momentum change occurs for that phase since total momentum is conserved during a collision. However, when particles of different phases collide, a gain in momentum for one phase and a loss in that of the other may occur such that the net momentum change (for both combined) is zero. Kinetic theory based models for polydisperse solids provide for this term inherently, and so, such descriptions are not discussed here, but are instead included in context of the individual kinetic theory as appropriate. In the case of a generalized multiphase model based on monodisperse theory, however, such a term must be provided.

Expressions for solids-solids drag have been determined experimentally and theoretically [127, 128, 129, 130, 131]. Syamlal [129] used a simplified version of kinetic theory to derive an expression for the drag coefficient F_{ml}:

$$F_{ml} = 3(1 + e_{mm})\left(\frac{\pi}{2} + C_f\frac{\pi^2}{8}\right)\frac{(d_m + d_l)^2}{2\pi(\rho_m d_m^3 + \rho_l d_l^3)}\rho_m\rho_l g_{ml}|U_{mi} - U_{li}| \tag{3-64}$$

Here C_f represents the coefficient of friction between particles of phase m and l.

Gera et al. [132] later modified this expression by incorporating a "hindrance effect" caused by particles in enduring contact, where S_{coef} is an adjustable parameter and P_c represents the close-packed solids pressure (see section 3.4.2):

$$F_{ml} = 3(1 + e_{mm})\left(\frac{\pi}{2} + C_f\frac{\pi^2}{8}\right)\frac{(d_m + d_l)^2}{2\pi(\rho_m d_m^3 + \rho_l d_l^3)}\rho_m\rho_l g_{ml}|U_{mi} - U_{li}| + S_{coef}P_c \tag{3-65}$$

Owoyemi et al. [126] examined the influence of several different models for the solids-solids drag relation on mixing and segregation in a bi-disperse fluidized bed. For the different models examined they observed similar results in regard to overall mixing, overall segregation, bubbling

dynamics and bulk properties (average bed height and bed voidage). However, removal of the term resulted in excessive segregation in contrast to experiment observation.

MFIX-TFM also has several polydisperse kinetic theory based models with their own solids-solids interphase momentum transfer term that includes solids-solids drag due to relative velocity (e.g., Iddir and Arastoopour [8]). If one of the polydisperse theories is invoked then the above formula is changed accordingly.

3.4.6 Turbulence Effects

As mentioned in section 2.5.4 on turbulence, a modified k-ϵ theory [4] is available in MFIX to model the influence of gas phase turbulence in multiphase gas-solids flow. This modified theory is based on the formulations of Simonin [78] and Balzer [79]. Similarly, another modified k-ϵ theory description is available based on the work of Cao and Ahmadi [77]. Both efforts involve some kinetic theory formalism in their derivation, but as indicated in [4], they generally do not distinguish kinetic theory contributions (see sections 3.4.3.3.7 and 3.4.3.3.8 in section 3.4.3) from those of turbulence. As discussed in [133] the lack of distinction between turbulent kinetic energy and granular energy is erroneous and will lead to an incorrect or incomplete formulation for multiphase turbulence.

In general, the modified version(s) in MFIX-TFM involve the same k-ϵ equations as those for single phase except for the inclusion of additional exchange terms. In particular, the Simonin-based implementation incorporates a new source term to both the kinetic energy and dissipation transport equations, whereas the Ahmadi based implementation only includes new source term to the kinetic energy transport equation. For greater detail on the development of either of these theories the reader is referred back to the original sources as well as those of Ma & Ahamdi [117, 134, 135] and Balzer *et al.* [113].

3.4.7 Diffusive Mass Transfer

Species mass flux through the m^{th} solids phase is based on a form of Fick's first law of diffusion [27] (*§17.1, pp 514-520*):

$$j_{mj} = \rho_m \mathcal{D}_{mn} \frac{\partial X_{mn}}{\partial x_j} \tag{3-66}$$

where $\mathcal{D}_{mn}$ is the n^{th} solids phase species diffusion coefficient described in section 3.5.7 and the other quantities are defined as before.

3.4.8 Conductive Heat Transfer

Similar to that of the fluid phase (section 2.5.6), the conductive heat flux in the m^{th} phase (first term on the RHS of equation (3-15) is assumed to follow a standard Fourier Law [27] form:

$$q_{mj} = -\kappa_m \frac{\partial T_m}{\partial x_j} \tag{3-67}$$

where κ_m is the m^{th} phase thermal conductivity described in section 3.5.6. For a solids phase representing a collection of particles, κ_m cannot simply be considered the material conductivity of the particle itself, but instead represents an effective m^{th} phase solids conductivity [136, 137] as described in section 3.5.6.

3.4.9 Radiative Heat Transfer

Radiative heat transfer is modeled by the simple relation,

$$\mathcal{S}_{m,rad} = \gamma_{Rm}(T_{Rm}^4 - T_m^4), \tag{3-68}$$

where T_{Rm} and γ_{Rm} are the radiative temperature and heat transfer coefficient. By default radiative heat transfer is not considered, that is, T_{Rm} and γ_{Rm} are taken as zero. The radiation source term is added in the m^{th} phase internal energy equation (3-15) through the general source term, S_m.

3.4.10 Convective Heat Transfer

Interphase convective heat transfer in MFIX [46] is assumed to be a function of the temperature difference,

$$\mathcal{S}_{m,conv} = \gamma_{gm}(T_m - T_g) \tag{3-69}$$

where $\gamma_{gm}$is the coefficient of heat transfer between the gas phase and the m^{th} phase. Convective heat transfer is added to the gas phase internal energy equation (2-6) through the general source term, S_g, and subtracted from the m^{th} phase internal energy equation (3-15) through the general source term, S_m.

The interphase heat transfer coefficient, γ_{gm}, includes a correction in the heat transfer caused by interphase mass transfer. This correction follows from a film theory analysis presented in reference (See §21.5 Transfer Coefficients at High Mass-Transfer Rates: Film Theory, p658-668 [31]):

$$\gamma_{gm} = \frac{C_{pg} R_{gm}}{\left[\exp\left(\frac{C_{pg} R_{gm}}{\gamma_{gm}^0}\right) - 1\right]} \tag{3-70}$$

[46] Interphase convective heat transfer refers strictly to heat transfer between the gas phase and m disperse phases. MFIX-TFM does not contain any sub-models that account for the direct transfer of heat between separate continuous solids phases.

Here, γ_{gm}^0 represents an intrinsic, or uncorrected, heat transfer coefficient. As is frequently done in more complex heat transfer problems, γ_{gm}^0 is determined using a suitable correlation for the Nusselt number, Nu:

$$\gamma_{gm}^0 = \frac{6\varepsilon_m \kappa_g}{d_m^2}\,\mathrm{Nu} \tag{3-71}$$

Here, the dimensionless Nusselt number is defined as $\mathrm{Nu} = \frac{\gamma_{gm}^0 d_m}{\kappa_g}$.[47] Nusselt number correlations available in MFIX are presented in Appendix C. By default the correlation of Gunn [138] is used in equation (3-71). This correlation was developed to describe heat transfer to particles in fixed and fluidized beds over varying Reynolds number and void fraction. Finally, it is worth pointing out that in the limit of zero interphase mass transfer ($R_{gm} \to 0$) equation (3-71) reduces to intrinsic heat transfer ($\gamma_{gm} = \gamma_{gm}^0$).

3.4.11 Chemical Reaction Source Terms

Source terms associated with chemical reactions are zero by default in MFIX. To incorporate chemical reactions, users must define chemical equations (stoichiometry) in the input deck in addition to specifying reaction rates via user-defined functions[48]. Subsequent subsections present how user-provided information is used to calculate source terms that contribute to the species mass and internal energy conservation equations.

3.4.11.1 Production and Consumption of Species Mass

Change in species mass is evaluated identically for homogeneous and heterogeneous chemical reactions. Specifically, for the p^{th} reaction, let $\mathcal{R}_p$ be the user-defined reaction rate,[49] and $\alpha_{mn,p}$ be the signed stoichiometric coefficient of the m^{th} phase's n^{th} species. The sign of the stoichiometric coefficient is positive for products (i.e., the p^{th} reaction produces the m^{th} phase's n^{th} species) and negative for reactants (the m^{th} phase's n^{th} species is consumed by the p^{th} reaction). Then, the total rate of change of species mass per unit volume for the p^{th} reaction is given by

[47] The additional factor of $6\varepsilon_m/d_m$ corresponds to the specific area or surface area per unit volume for a bed of uniform spheres. It provides the conversion from heat flux to the heat transfer rate per unit volume. Therefore, the implementation implies a system wherein the m^{th} phase is comprised of dispersed spheres.

[48] Details on how to specify chemical equations and reaction rates is provided in the MFIX User Guide available online at https://mfix.netl.doe.gov/doc/mfix/latest

[49] The unit systems adopted in MFIX are not consistent with the general definitions, and as such, MFIX uses units of $kmole/kg$ for molecular weight in SI and $mole/gram$ in CGS units. A consequence of these units is that user-defined reaction rates have units of $kmole/cm^3 sec$ in SI and $mole/m^3 sec$ in CGS units.

$$[R_{mn}]_p = \frac{\alpha_{mn,p}\mathcal{R}_p}{\mathrm{MW}_{mn}} \tag{3-72}$$

where MW_{mn} is the molecular weight of the m^{th} phase n^{th} species. Here, the phase index m ranges from zero to the total number of additional phases (M) beyond the fluid phase ($m = 0$), that is, $m = 0$ represents the fluid (or gas) phase (i.e., $R_{0n} = R_{gn}$)[50]. The total rate of production (or consumption),

$$R_{mn} = \sum_p [R_{mn}]_p \tag{3-73}$$

is substituted into equations (2-3) and (2-4) for $m = 0$, and (3-1) and (3-2) otherwise to account for changes in species mass.

3.4.11.2 Energy Change Due to Mass Production and/or Consumption

The p^{th} chemical reactions contributes to the general source term in the m^{th} phase internal energy equation due to the production or consumption of m^{th} phase species. This contribution may be specified[51] or computed as

$$\left[\mathcal{S}_{m,I}\right]_p = -\sum_{n=1}^{N_m} h_{mn}[R_{mn}]_p \tag{3-74}$$

N_m is the total number of species comprising the m^{th} phase mixture, and h_{mn} is the specific enthalpy of the n^{th} species of the m^{th} phase, , defined in section 3.5.5. The total source term arising from mass production and/or consumption is added in the m^{th} phase internal energy equation (3-15) through the general source term, $\mathcal{S}_m$:

$$\mathcal{S}_{m,I} = \sum_p \left[\mathcal{S}_{m,I}\right]_p \tag{3-75}$$

3.4.11.3 Energy Change Accompanying Interphase Mass Transfer

The energy transfer accompanying interphase mass transfer, specifically transfer between the gas and m^{th} phase (i.e., a heterogeneous reaction between the gas and m^{th} phase), is given by [139]:

---

[50] Observe that equations (3-72) and (3-72) are consistent with equations (2-20) and (2-21) provided in section 2.5.8.1 for gas phase reactions. Specifically, these are the same equations with (2-20) and (2-21) having the index $m = 0 = g$.

[51] If a constant heat of reaction is specified, then the evaluation of enthalpy defined in equation (3-83) is not performed so that the sensible heat contribution is not incorporated. Additionally, the partitioning of the specified heat of reaction between phases must also be provided.

$$\mathcal{S}_{m,rxn} = \sum_{p} \left(\sum_{n=1}^{N_g} \left(h_{gn}(T_{gm}) \left[R_{gn} \right]_p \right) \right). \tag{3-76}$$

Here, $\left[R_{gn}\right]_p$ represents the rate of production (or consumption) of the n^{th} gas phase species attributed to the p^{th} reaction between the gas phase and the m^{th} phase and is given by equation (2-20). The quantity $h_{gn}(T_{gm})$ is the specific enthalpy of the n^{th} gas phase species at temperature, T_{gm}, identified by

$$T_{gm} = \begin{cases} T_g \text{ for } \left[R_{gn}\right]_p \leq 0 \text{ (i.e., consumption of } n^{th} \text{ gas species)} \\ T_m \text{ for } \left[R_{gn}\right]_p > 0 \text{ (i.e., production of } n^{th} \text{ gas species)} \end{cases}. \tag{3-77}$$

where T_g and T_m and the gas and m^{th} phase temperatures, respectively. Energy transfer accompanying interphase mass transfer is added to the gas phase internal energy equation (2-6) through the general source term, $\mathcal{S}_g$, and subtracted from the m^{th} phase internal energy equation (3-15) through the general source term, $\mathcal{S}_m$.

3.5 Solids Phase Physical Properties

This section defines the m^{th} phase physical properties.

3.5.1 Mixture Solids Density

The m^{th} phase (solids) density is either specified as constant, calculated using a user-defined function, or calculated as a function of the chemical species mass fractions. In case of the latter, a variable solids phase density is calculated from a baseline solids density, ρ_m^B, defined as

$$\frac{1}{\rho_m^B} = \sum_{n=1}^{N_m} \frac{X_{mn}^B}{\rho_{mn}^B}, \tag{3-78}$$

where X_{mn}^B and ρ_m^B are the m^{th} solids phase baseline n^{th} chemical species mass fraction and material density. The term *baseline* is used to assert that these values are specific to the solids phase description and may differ from the *initial conditions* used in setting up a simulation. For example, consider a solids phase defined to represent coal particles and taken to be composed of four pseudo-species; char, ash, volatiles and moisture. The baseline mass fractions would likely reflect the *proximate analysis* of the coal and the material densities would reflect the densities of the four components; char, coal-ash, volatile matter, and liquid water.

Equation (3-78) is only valid when calculating the baseline solids density because its derivation uses the assumption that the volume of a particle is equivalent to the total mass of the particle divided by the material density; however, as mass is lost or gained, this assumption no longer holds. Xue *et al.* [6] observed this phenomenon and suggested that the apparent solids density

should be related to the baseline density by a multiplier accounting for increased porosity. This can be avoided by exploiting the notion that the mass of an inert chemical species is constant so that the mass of the m^{th} solids phase, m_m, is given by

$$m_m = (\rho_m^B V_m^B)\frac{X_{mI}^B}{X_{mI}}, \tag{3-79}$$

where the subscript I is the index of the inert solids phase species. Given that the solids phase volume is constant, $V_m = V_m^B = m_m^B/\rho_m^B$, the apparent m^{th} solids phase density is

$$\rho_m = \rho_m^B \frac{X_{mI}^B}{X_{mI}}. \tag{3-80}$$

This model requires users identify one solids phase chemical species as inert. This is a reasonable approach given that the solids diameter is invariant to mass loss and therefore an inert material is needed to provide a rigid matrix to support reactants and/or products.

3.5.2 Viscosity, Bulk Viscosity, and Pressure

As discussed previously, the m^{th} phase stress, τ_{mij}, is cast in the form provided in equations (3-16)-(3-18). This model requires two transport coefficients for closure: viscosity, μ_m, and bulk viscosity, μ_{bm}. Three options are available for defining these quantities. 1) The m^{th} phase viscosity, μ_m, may be specified as a constant at which point the m^{th} phase bulk viscosity, μ_{bm}, and the m^{th} phase stress, P_m, are set to zero. 2) It may be calculated using a user-defined function, which also allows for specification of the bulk viscosity and pressure. 3) It may be calculated based on a selected solids model, wherein the bulk viscosity and pressure are defined accordingly. The latter is the default approach as discussed in section 3.4.1 along with sections 3.4.2 and 3.4.3.

3.5.3 Mixture Molecular Weight

The m^{th} phase mixture molecular weight, MW_m, is either specified as constant or calculated as

$$\frac{1}{\mathrm{MW}_m} = \sum_{n=1}^{N_m} \frac{X_{mn}}{\mathrm{MW}_{mn}} \tag{3-81}$$

where X_{mn} and MW_{mn} are the mass fraction and elemental molecular weight of the m^{th} phase n^{th} chemical species.

3.5.4 Mixture Specific Heat

The m^{th} phase mixture specific heat, C_{pm}, is either specified as constant[52] or calculated as

[52] Specifying a constant specific heat for the m^{th} phase is only permissible for non-reacting flows.

$$C_{pm} = \sum_{n=1}^{N_m} X_{mn} C_{pmn} \tag{3-82}$$

where $C_{pmn}$is the specific heat of the m^{th} phase n^{th} chemical species. The species specific heat is obtained from either the BURCAT database [30] or from a user provided entry following the same format.

3.5.5 Species Specific Enthalpy

The specific enthalpy each species is calculated by combining the heat of formation, $H_{fn}^{\circ}(T_{ref})$, and integrating the specific heat of that species from the reference temperature, T_{ref}, to the gas phase temperature.

$$h_{mn} = H_{fn}^{\circ}(T_{ref}) + \int_{(T_{ref})}^{T_g} C_{pmn}(T)\, dT \tag{3-83}$$

The species heat of formation is obtained from either the BURCAT database [30] or as a user provided entry following the same format.

3.5.6 Thermal Conductivity

The m^{th} phase thermal conductivity, κ_m, is either specified as constant, calculated using a user-defined function, or calculated using a thermal resistance model that is based on heat transfer in a dispersed medium. The latter model is described here.

Formulating the conductive heat transfer between particles is a challenging problem and various approaches have been used. For particles dispersed in a continuous medium, heat transfer is commonly considered through a mixture, or effective bed, conductivity approach, wherein different mechanisms [140, 141] are considered simultaneously. Such mechanisms may include heat transfer between particles in contact, through the fluid (gas) gap between particles and radiation between particles. An effective thermal conductivity is then used to simultaneously describe the influence of these distinct mechanisms.

In MFIX-TFM, the model of Bauer and Schlunder [140] is used to approximate the m^{th} phase thermal conductivity [136, 56]. Their model examines the total heat transfer through a unit cell separated into two contributions: 1) heat transfer only through the surrounding fluid phase and 2) heat transfer through both the fluid and solids. These are considered to act in parallel or as additive fluxes [140, 142] and several mechanisms of heat transfer are considered including

conduction, radiation between particles and the contribution to gas conductivity due to the Smoluchowski or Knudsen effect.[53]

As discussed, this model [140] considers the total effective thermal conductivity of the system as the sum of two contributions. Since MFIX considers heat transfer through the fluid phase separately (section 2.6.5), it is only the second contribution[54] that is used to formulate an approximate m^{th} phase thermal conductivity. This contribution is further simplified by 1) neglecting the influence of the Smoluchowski effect to the gas phase conductivity[55], and 2) dropping radiation[56] since radiative heat transfer is also treated separately (section 3.4.9) [136]. Finally, the original model of Bauer & Schlunder also provides for a modified or mean particle conductivity that incorporates the influence of an oxidation layer on the thermal conductivity of the particle. This aspect[57] is not incorporated. The resulting simplified equation effectively encompasses direct conduction through a factional contact area and indirect conduction through the gas wedge between contacting particles. As in Kuipers et al [137], a *solids phase* thermal conductivity is obtained from Bauer and Schlunders' model for *effective bed* conductivity via the following relation:

$$\kappa_s = \frac{\kappa_b}{\left(1-\varepsilon_g\right)} \tag{3-84}$$

where in MFIX, the quantity κ_b is defined as

$$\kappa_b = \kappa_g \sqrt{1-\varepsilon_g}\,\left(\varphi R + (1-\varphi)\Gamma\right) \tag{3-85}$$

and

$$\Gamma = \frac{-2}{1-\frac{B}{R}}\left[\frac{B(R-1)}{R\left(1-\frac{B}{R}\right)^2}\ln\left(\frac{B}{R}\right) + \frac{B-1}{1-\frac{B}{R}} + \frac{1}{2}(B+1)\right] \tag{3-86}$$

Here, κ_g is the fluid phase conductivity defined in Equation (2-28). The quantity φ represents the fraction of the heat transfer surface area that is in contact (compared to the remaining surface

[53] The thermal conductivity of an unconfined gas is independent of pressure. When the mean free path approaches or exceeds the distance between bounding solid surfaces (Kn>0.001), then heat transfer depends on pressure which reflects the number of molecules participating in heat transfer with the mean free path inversely proportional to pressure. For more details see [214, 215].

[54] Expression 3 in Bauer and Schlunder [138] is assumed to contain a typo. The first term in the parenthesis on the right-hand-side should reflect the quantity λ/λ_D but the expression is missing the numerator λ – only the denominator λ_D is written.

[55] The term $\frac{\lambda}{\lambda_D} = 1$ in the expressions of Bauer and Schlunder [138].

[56] The term $\frac{\lambda_R}{\lambda} = 0$ in the expressions of Bauer and Schlunder [138].

[57] The term $\lambda_S^* = \lambda_S$ in the expressions of Bauer and Schlunder [138].

area through the two particles that are the gas wedges). A value for φ is found from a combination of theoretical computation and fitting of experimental data:

$$\varphi = \frac{23\rho_K^2}{1 + 22\rho_K^{\frac{4}{3}}} = 7.26x10^{-3} \tag{3-87}$$

Here ρ_k^2 was determined experimentally. Specifically, a value of $\rho_k^2 = 3.5x10^{-4}$ was found to work equally well for several different instances of uniformly sized spherical packings of ceramic particles, in which values of diameter ranged from 0.05mm to 2mm. The quantity B is described as a deformation factor that is determined on the basis of geometric considerations and for uniform spherical particles it is written as:

$$B = 1.25\left(\frac{1-\varepsilon_g}{\varepsilon_g}\right)^{\frac{10}{9}} \tag{3-88}$$

Finally, the quantity R is the ratio of the microscopic, or material, thermal conductivity of the solids particle to that of the gas:

$$R = \frac{k_p}{\kappa_g} \tag{3-89}$$

For the default model, k_p is assigned a constant value of 1.0 $W/(m \cdot K)$ taken from Mills [143], Table A.3, dry-soil, p912.

While the model of Bauer and Schlunder allows for incorporating the influence of a particle size distribution through the quantity B (see Bauer and Schlunder equation 6), a uniform spherical distribution is assumed in the expression shown here. For systems with more than one solids phase (differing in size, density or other material property), MFIX employs an ad-hoc extension by replacing κ_s with κ_m for the m^{th} solids phase in Equation (3-84) and k_p with k_m in Equation (3-89):

$$\kappa_m = \frac{\kappa_{bm}}{(1-\varepsilon_g)} = \frac{\kappa_g}{\sqrt{1-\varepsilon_g}}\left(\varphi R_m + (1-\varphi)\Gamma_{\mathrm{m}}\right) \tag{3-90}$$

$$R_m = \frac{k_m}{\kappa_g} \tag{3-91}$$

As evident, the same model is applied separately to each m^{th} phase. Conduction between different solids phases is not considered.

Finally, this conductivity model was developed based on the depiction of particles in a packed configuration. However, this is the default model regardless of the flow regime (i.e., fluidized or

packed). For the default values given here, the bed conductivity, κ_b, is plotted in Figure 3-4 where the gas phase thermal conductivity is calculated using equation (2-28) with temperatures ranging from 300K to 2100K. The bed thermal conductivity is bounded above by the solids material (microscopic) thermal conductivity for physical fluid volume fractions ($\varepsilon_g > 0.25$), and decreases with increasing ε_g becoming comparable to κ_g for dilute flows.

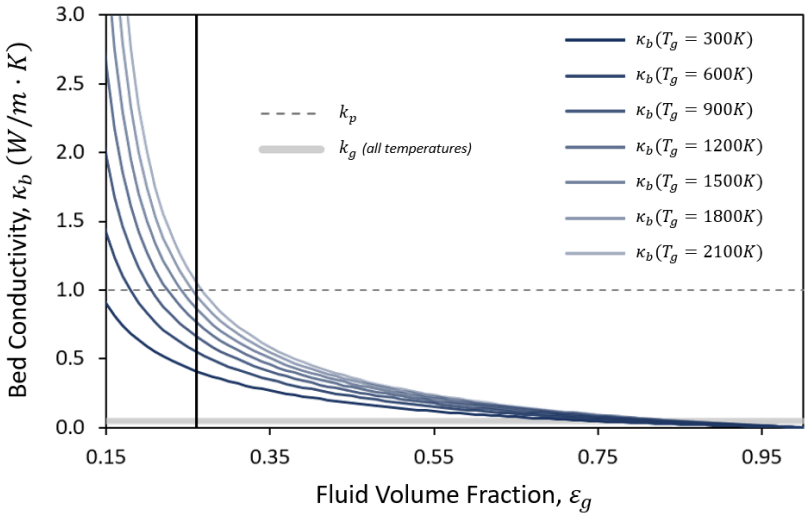

Figure 3-4: Bed thermal conductivity, κ_b given by equation (3-85), is shown as a function of gas phase volume fraction. The gas phase thermal conductivity, k_g is evaluated at several temperatures (300K – 2100K) using equation (2-28) and with all values shown as a single gray line. The constant solids material conductivity, $k_p = 1.0\ W/(m.K)$, is plotted as a dashed line. The bed conductivity is bounded above by k_p, for physical volume fractions ($\varepsilon_g > 0.25$), and decreases with increasing gas volume fraction.

3.5.7 Diffusivity

The m^{th} phase species diffusivity, $\mathcal{D}_{mn}$, is either specified as constant, calculated using a user-defined function, or taken as zero.

References

[1] M. Syamlal, "Multiphase Hydrodynamics of Gas-Solids Flow," Ph.D. dissertation, Illinois Institute of Technology, 1985.

[2] D. Gidaspow and B. Ettehadieh, "Fluidization in Two-Dimensional Beds with a Jet; 2. Hydrodynamic Modeling," *Industrial & Engineering Chemistry Fundamentals,* vol. 22, pp. 193-201, 1983.

[3] M. Syamlal, T. O'Brien, S. Benyahia, A. Gel and S. Pannala, "Open-Source Software in Computational Research: A Case Study," *Modelling and Simulation in Engineering,* vol. 937542, 2008.

[4] S. Benyahia, M. Syamlal and T. O'Brien, "Evaluation of boundary conditions used to model dilute, turbulent gas/solids flows in a pipe," *Powder Technology,* vol. 156, pp. 62-72, 2005.

[5] J.-F. Dietiker, C. Guenther and M. Syamlal, "A Cartesian cut cell method for gas/solids flows," in *AIChE annual meeting,* Nashville, 2009.

[6] Q. Xue, T. Heindel and R. Fox, "A CFD model for biomass fast pyrolysis in fluidized-bed reactors," *Chemical Engineering Science,* vol. 66, pp. 2440-2452, 2011.

[7] V. Garzó and J. Dufty, "Dense fluid transport for inelastic hard spheres," *Physical Review E,* vol. 59, pp. 5895-5911, 1999.

[8] H. Iddir and H. Arastoopour, "Modeling of multitype particle flow using the kinetic theory approach," *AIChE Journal,* vol. 51, p. 1620–1632, 2005.

[9] V. Garzó, J. Dufty and C. Hrenya, "Enskog theory for polydisperse granular mixtures. I. Navier-Stokes order transport," *Physical Review E,* vol. 76, p. 031303, 2007.

[10] V. Garzó, J. W. Dufty and C. Hrenya, "Enskog theory for polydisperse granular mixtures. II. Sonine polynomial approximation," *Physical Review E,* vol. 76, p. 031304, 2007.

[11] V. Garzó, S. Tenneti, S. Subramaniam and C. Hrenya, "Enskog kinetic theory for monodisperse gas–solid flows," *Journal of Fluid Mechanics,* vol. 712, pp. 129-168, 2012.

[12] D. S. Boyalakuntla, "Simulation of Granular and Gas-Solid Flows using Discrete Element Model (DEM) Implemented in MFIX," Ph.D. Dissertation, Carnegie Mellon University, 2003.

[13] R. Garg, J. Galvin, T. Li and S. Pannala, "Open-source MFIX-DEM software for gas–solids flows: Part I—Verification studies," *Powder Technology,* vol. 220, p. 122–137, 2012.

[14] T. Li, R. Garg, J. Galvin and S. Pannala, "Open-source MFIX-DEM software for gas–solids flows: Part II—Validation studies," *Powder Technology,* vol. 220, p. 138–150, 2012.

[15] J. Musser, "Modeling of heat transfer and reactive chemistry for particles in gas-solid flow utilizing continuum-discrete methodology (CDM)," Ph.D. Dissertation, West Virginia University, 2011.

[16] P. Gopalakrishnan and D. Tafti, "Development of parallel DEM for the open source code MFIX," *Powder Technology,* vol. 235, pp. 33-41, 2013.

[17] H. Liu, D. Tafti and T. Li, "Hybrid parallelism in MFIX CFD-DEM using OpenMP," *Powder Technology,* vol. 259, pp. 22-29, 2014.

[18] R. Garg and J. Dietiker, "Documentation of open-source MFIX-PIC software for gas-solids flows," 2013.

[19] T. B. Anderson and R. Jackson, "A Fluid Mechanical Description of Fluidized Beds," *Industrial & Engineering Chemistry Fundamentals,* vol. 6, no. 4, pp. 527-534, 1967.

[20] F. Harlow and A. Amsden, "Numerical Calculation of Multiphase Fluid Flow," *Journal of Computational Physics,* vol. 17, no. 19, pp. 19-52, 1975.

[21] W. Rivard and M. Torrey, "K-FIX: a computer program for transient, two-dimensional, two-fluid flow," United States: N. p., 1976.

[22] H. Versteeg and W. Malalasekera, An Introduction to Computational Fluid Dynamics: The Finite Volume Method, 2nd ed., London: Pearson Education Limited, 2007.

[23] D. C. Wilcox, Turbulence Modeling for CFD, California: DCW Industries, 1994.

[24] L. Prandtl, "Bericht über Untersuchungen zur Ausgebildeten Turbulenz," *Zeitschrift für angewandte Mathematik und Mechanik,* vol. 5, no. 2, pp. 136-139, 1925 [Translated into English as "Report on Investigation of Developed Turbulence", NACA Technical Memorandum No. 1231, 1949].

[25] F. M. White, Viscous Fluid Flow, New York, NY: McGraw-Hill, 2006.

[26] A. Bedford and D. S. Drumheller, "Theories Of Immiscible And Structured Mixtures," *International Journal of Engineering Science,* vol. 21, no. 8, pp. 863-960, 1983.

[27] R. B. Bird, W. E. Stewart and E. N. Lightfoot, Transport Phenomena (Second ed.), New York: John Wiley & Sons, 2006.

[28] W. Sutherland, "The viscosity of gases and molecular force," *Philosophical Magazine Series 5,* vol. 36:223, pp. 507-531, 1893.

[29] F. Morey, "Dry Air (Ideal Gas State); The NBS-NACA Tables of Thermal Properties of Gases," Table: 2.39, U.S. Department of Commerce, National Bureau of Standards, 1950.

[30] A. Burcat and B. Ruscic, "Third millenium ideal gas and condensed phase thermochemical database for combustion (with update from active thermochemical tables) (No. ANL-05/20)," Argonne National Lab (ANL), Argonne, IL (United States), 2005.

[31] B. Bird, W. Stewart and E. Lightfoot, Transport Phenomena, New York: John Wiley & Sons, 1960.

[32] E. Fuller, P. Schettler and J. Giddings, "A new method for prediction of binary gas phase diffusion coefficients," *Industrial and Engineering Chemistry,* vol. 58, no. 5, pp. 19-27, 1966.

[33] C. Curtiss and J. Hirschfelder, "Transport properties of multicomponent gas mixtures," *The Journal of Chemical Physics,* vol. 17, no. 6, p. 550, 1949.

[34] R. J. Atkin and R. E. Craine, "Continuum Theories of Mixtures: Basic Theory and Historical Development," *The Quarterly Journal of Mechanics and Applied Mathematics,* vol. 29, no. 2, pp. 209-244, 1976.

[35] R. M. Bowen, "PartI. Theory of Mixtures," in *Continuum Physics, Volume III: Mixtures and EM Field Theories* , New York, Academic Press, 1976, pp. 2-122.

[36] D. A. Drew, "Mathematical-Modeling of 2-Phase Flow," *Annual Review of Fluid Mechanics,* vol. 15, pp. 261-291, 1983.

[37] M. Ishii and K. Mishima, "2-Fluid Model And Hydrodynamic Constitutive Relations," *Nuclear Engineering and Design,* vol. 82, no. 2-3, pp. 107-126, 1984.

[38] R. Jackson, "Locally averaged equations of motion for a mixture of identical spherical particles and a Newtonian fluid," *Chemical Engineering Science,* vol. 52, no. 15, pp. 2457-2469, 1997.

[39] R. Jackson, The dynamics of fluidized particles, Cambridge: Cambridge University Press, 2000.

[40] D. D. Joseph, T. S. Lundgren, R. Jackson and D. A. Saville, "Ensemble Averaged and Mixture Theory Equations for Incompressible Fluid Particle Suspension," *International Journal of Multiphase Flow,* vol. 16, no. 1, pp. 35-42, 1990.

[41] A. Prosperetti, "Averaged equations for multiphase flow," in *Computational Methods for Multiphase Flow*, Cambridge, Cambridge University Press, 2007.

[42] D. Z. Zhang and A. Prosperetti, "Averaged Equations for Inviscid Disperse 2-Phase Flow," *Journal of Fluid Mechanics*, vol. 267, pp. 185-219, 1994.

[43] D. Z. Zhang and A. Prosperetti, "Ensemble Phase-Averaged Equations for Bubbly Flows," *Physics of Fluids,* vol. 6, no. 9, pp. 2956-2970, 1994.

[44] H. Jakobsen, Chemical Reactor Modeling: Multiphase Reactive Flows, 2nd ed., Gewerbestrasse: Springer International Publishing, 2014.

[45] M. Ishii, Thermo-fluid dynamic theory of two-phase flow, Paris: Eyrolles, 1975.

[46] B. van Wachem, J. Schouten, C. van den Bleek, R. Krishna and J. Sinclair, "Comparative analysis of CFD models of dense gas–solid systems," *AIChE Journal*, vol. 47, no. 5, pp. 1035-1051, 2001.

[47] J. Jenkins and S. Cowin, "Theories for flowing granular materials," in *Mechanics Applied to the Transport of Bulk Materials*, Niagara Falls, N.Y., 1979.

[48] P. C. Johnson and R. Jackson, "Frictional Collision Constitutive Relations for Granular Materials, with Application to Plane Shearing," *Journal of Fluid Mechanics,* vol. 176, pp. 67-93, 1987.

[49] C. S. Campbell, "Granular material flows - An overview," *Powder Technology,* vol. 162, pp. 208-229, 2006.

[50] F. Radjai, J. N. Roux and A. Daouadji, " Modeling granular materials: century-long research across scales," *Journal of Engineering Mechanics,* vol. 143, no. 4, pp. 1-64, 2017.

[51] M. Syamlal and S. Pannala, "Multiphase continuum formulation for gas-solids reacting flows," in *Computational Gas-Solids Flows and Reacting Systems: Theory, Methods and Practice*, S. Pannala, M. Syamlal and T. J. O'Brien, Eds., Hershey, PA, IGI Global, 2011.

[52] S. Savage, "Analyses of slow high-concentration flows of granular materials," *Journal of Fluid Mechanics,* vol. 377, pp. 1-26, 1998.

[53] S. Savage, "Granular flows down rough inclines - review and extension," *Mechanics of Granular Materials: New models and constitutive relations,* pp. 261-282, 1983.

[54] A. Srivastava and S. Sundaresan, "Analysis of a fractional-kinetic model for gas-particle flow," *Powder Technology,* vol. 129, no. 1-3, pp. 72-85, 2003.

[55] Syamlal, M., "A review of granular stress constitutive relations," Technical Report DOE/MC 21343-2372, Morgantown, WV, 1987.

[56] M. Syamlal, W. Rogers and T. O'Brien, "MFIX Documentation: Theory Guide," Morgantown Energy Technology Center, Morgantown, West Virginia, 1993.

[57] R. Jackson, "Some Mathematical and Physical Aspects of Continuum Models for the Motion of Granular Materials," in *Theory of Dispersed Multiphase Flow; Proceedings of an Advanced Seminar, Conducted by the Mathematics Research Center, the University of Wisconsin–Madison,* R. E. Meyer, Ed., Madison, Wisconsin, Academic Press, 1983, pp. 291-337.

[58] D. Schaeffer, "Instability in the evolution equations describing incompressible granular flow," *Journal of Differential Equations,* vol. 66, no. 1, pp. 19-50, 1987.

[59] E. B. Pitman and D. G. Schaeffer, "Stability of time dependent compressible granular flow in two dimensions," *Communications on Pure and Applied Mathematics,* vol. 40, no. 4, pp. 421-447, 2006.

[60] S. Pannala, C. Daw, C. Finney, S. Benyahia, M. Syamlal and T. O'Brien, "Modeling the Collisional-Plastic Stress Transition for Bin Discharge of Granular Material," in *Proceedings Of The 6th International Conference On Micromechanics Of Granular Media,* Golden, Colorado, 2009.

[61] N. Xie, "Computational analyses for modeling fluidized bed gasification processes," Ph.D. Dissertation, Iowa State University, 2007.

[62] N. Xie, F. Battaglia and S. Pannala, "Effects of using two- versus three-dimensional computational modeling of fluidized beds Part I, Hydrodynamics," *Powder Technology,* vol. 182, no. 1, pp. 1-13, 2008.

[63] S. Pannala, C. Daw, C. Finney, S. Benyahia, M. Syamlal and T. O'Brien, "Modeling the Collisional-Plastic Stress Transition for Bin Discharge of Granular Material," in

Proceedings Of The 6th International Conference On Micromechanics Of Granular Media, Golden, Colorado, 2009.

[64] A. Srivastava, "Dense phase gas-solid flows in circulating fluidized beds," Dissertation, Princeton University, Princeton, NJ, 2002.

[65] G. I. Tardos, "A fluid mechanistic approach to slow, frictional flow of powders," *Powder Technology,* vol. 92, no. 1, pp. 61-74, 1997.

[66] J. Prakash and K. Rao, "Steady compressible flow of granular materials through a wedge-shaped hopper: The smooth wall, radial gravity problem," *Chemical Engineering Science,* vol. 43, no. 3, pp. 479-494, 1988.

[67] S. Benyahia, "Validation Study of Two Continuum Granular Frictional Flow Theories," *Industrial & Engineering Chemistry Research,* vol. 47, no. 22, pp. 8926-8932, 2008.

[68] P. C. Johnson, P. Nott and R. Jackson, "Frictional Collisional Equations of Motion for Particulate Flows and Their Application to Chutes," *Journal of Fluid Mechanics,* vol. 210, pp. 501-535, 1990.

[69] S. Chapman and T. Cowling, The mathematical theory of non-uniform gases: an account of the kinetic theory of viscosity, thermal conduction and diffusion in gases, Cambridge: Cambridge University Press, 1970.

[70] S. Savage and D. Jeffrey, "The stress tensor in a granular flow at high shear rates," *Journal of Fluid Mechanics,* vol. 110, pp. 255-272, 1981.

[71] C. Lun, S. Savage, D. Jeffrey and N. Chepurniy, "Kinetic theories for granular flow: inelastic particles in Couette flow and slightly inelastic particles in a general flowfield," *Journal of Fluid Mechanics,* vol. 140, pp. 223-256, 1984.

[72] C. Hrenya, "Kinetic Theory for Granular Materials: Polydispersity," in *Computational Gas-Solids Flows and Reacting Systems,* Hershey, Pa, IGI Global, 2011, pp. 102-127.

[73] J. L. Sinclair and R. Jackson, "Gas-Particle Flow in a Vertical Pipe with Particle-Particle Interactions," *AIChE Journal,* vol. 35, no. 9, pp. 1473-1486, 1989.

[74] D. Gidaspow, Multiphase Flow and Fluidization: Continuum and Kinetic Theory Descriptions, Boston: Academic Press, 1994.

[75] E. Peirano and B. Leckner, "Fundamentals of turbulent gas-solid flows applied to circulating fluidized bed combustion," *Progress In Energy And Combustion Science,* vol. 24, no. 4, pp. 259-296, 1998.

[76] K. Agrawal, P. N. Loezos, M. Syamlal and S. Sundaresan, "The role of meso-scale structures in rapid gas-solid flows," *Journal of Fluid Mechanics,* vol. 445, pp. 151-185, 2001.

[77] J. Cao and G. Ahmadi, "Gas-particle two-phase turbulent flow in a vertical duct," *International Journal of Multiphase Flow,* vol. 21, pp. 1203-1228, 1995.

[78] O. Simonin, "Continuum modeling of dispersed two-phase flows," in *Combustion and Turbulence in Two-Phase Flows*, Belgium, von Karman Institute for Fluid Dynamics, 1996, pp. 1-47.

[79] G. Blazer, O. Simonin, A. Boelle and J. Lavieville, "A unifying modelling approach for the numerical prediction of dilute and dense gas– solid two phase flow," in *CFB5; 5th International Conference on Circulating Fluidized Beds*, Beijing, 1996.

[80] J. J. Brey, J. W. Dufty, C. S. Kim and A. Santos, "Hydrodynamics for granular flow at low density," *Physical Review E,* vol. 58, no. 4, pp. 4638-4653, 1998.

[81] N. Sela and I. Goldhirsch, "Hydrodynamic equations for rapid flows of smooth inelastic spheres, to Burnett order," *Journal of Fluid Mechanics,* vol. 361, pp. 41-74, 1998.

[82] H. van Beijeren and M. H. Ernst, "The modified Enskog equation," *Physica,* vol. 68, no. 3, pp. 437-456, 1978.

[83] J. W. Dufty and A. Baskaran, "Hydrodynamic Equations from Kinetic Theory: Fundamental Considerations," in *Computational Gas-Solids Flows and Reacting Systems*, Hershey, PA, IGI Global, 2011, pp. 66-101.

[84] J. T. Jenkins and M. W. Richman, "Kinetic-theory for plane flows of a dense gas of identical, rough, inelastic, circular disks," *Physics of Fluids,* vol. 28, no. 12, pp. 3485-3494, 1985.

[85] P. Zamankhan, "Kinetic Theory of Multicomponent Dense Mixtures of Slightly Inelastic Spherical Particles," *Physical review. E,* vol. 52, pp. 4877-4891, 1995.

[86] J. T. Jenkins and M. Mancini, "Balance Laws and Constitutive Relations for Plane Flows of a Dense, Binary Mixture of Smooth, Nearly Elastic, Circular Disks," *Journal of Applied Mechanics,* vol. 54, no. 1, pp. 27-34, 1987.

[87] I. Goldhirsch, "Rapid granular flows," *Annual Review of Fluid Mechanics,* vol. 35, pp. 267-293, 2003.

[88] M. Y. Louge, "The surprising relevance of a continuum description to granular clusters," *Journal of Fluid Mechanics,* vol. 742, pp. 1-4, 2014.

[89] P. P. Mitrano, J. R. Zenk, S. Benyahia, J. E. Galvin, S. R. Dahl and C. M. Hrenya, "Kinetic-theory predictions of clustering instabilities in granular flows: beyond the small-Knudsen-number regime," *Journal of Fluid Mechanics,* vol. 738, p. R2, 2014.

[90] J. T. Jenkins, "Kinetic Theory for Nearly Elastic Spheres," in *Physics of Dry Granular Media*, Dordrecht, Springer Netherlands, 1998, pp. 353-370.

[91] V. Mathiesen, T. Solberg and B. H. Hjertager, "An experimental and computational study of multiphase flow behavior in a circulating fluidized bed," *International Journal of Multiphase Flow,* vol. 26, pp. 387-419, 2000.

[92] S. Benyahia, "Verification and validation study of some polydisperse kinetic theories," *Chemical Engineering Science*, vol. 63, no. 23, pp. 5672-5680, 2008.

[93] H. van Beijeren and M. H. Ernst, "Kinetic Theory of Hard Spheres," *Journal of Statistical Physics,* vol. 21, no. 2, pp. 125-167, 1979.

[94] J. W. Tester and M. Modell, Thermodynamics and its Applications, 3rd edition, Upper Saddle River: Prentice Hall, 1997.

[95] S. B. Yuste, M. L. de Haro and A. Santos, "Structure of hard-sphere metastable fluids," *Physical Review E,* vol. 53, no. 5, pp. 4820-4826, 1996.

[96] J. L. Lebowitz, "Exact Solution of Generalized Percus-Yevick Equation for a Mixture of Hard Spheres," *Physical Review,* vol. 133, no. 4A, p. A895, 1964.

[97] N. F. Carnahan and K. E. Starling, "Equation of State for Nonattracting Rigid Spheres," *Journal of Chemical Physics,* vol. 51, pp. 635-636, 1969.

[98] L. Verlet and J. J. Weis, "Equilibrium Theory of Simple Liquids," *Physical Review A,* vol. 5, no. 2, pp. 939-952, 1972.

[99] T. Boublík, "Hard-Sphere Equation of State," *The Journal of Chemical Physics,* vol. 53, no. 1, pp. 471-472, 1970.

[100] G. A. Mansoori, N. F. Carnahan, K. E. Starling and T. W. Leland, "Exact Solution of Generalized Percus-Yevick Equation for a Mixture of Hard Spheres," *Journal of Chemical Physics,* vol. 54, pp. 1523-1525, 1971.

[101] B. J. Alder and T. E. Wainwright, "Studies in Molecular Dynamics. II. Behavior of a Small Number of Elastic Spheres," *Journal of Chemical Physics,* vol. 33, no. 5, pp. 1439-1451, 1960.

[102] Y. Song, R. M. Stratt and E. A. Mason, "The equation of state of hard spheres and the approach to random closest packing," *The Journal of Chemical Physics,* vol. 88, no. 2, pp. 1126-1133, 1988.

[103] J. Tobochnik and P. M. Chapin, "Monte Carlo simulation of hard spheres near random closest packing using spherical boundary conditions," *The Journal of Chemical Physics,* vol. 88, no. 9, pp. 5824-5830, 1988.

[104] M. López de Haro, E. G. D. Cohen and J. M. Kincaid, "The Enskog theory for multicomponent mixtures. I. Linear transport theory," *The Journal of Chemical Physics,* vol. 78, no. 5, pp. 2746-2759, 1983.

[105] B. O. Arnarson and J. T. Jenkins, "Particle Segregation in the Context of the Species Momentum Balances," in *Traffic and Granular Flow '99,* D. Helbing, H. J. Herrmann, M. Schreckenberg and D. E. Wolf, Eds., Berlin, Heidelberg, Springer Berlin Heidelberg, 2000, pp. 481-487.

[106] C. S. Campbell, "The stress tensor for simple shear flows of a granular material," *Journal of Fluid Mechanics,* vol. 203, pp. 449-473, 1989.

[107] C. S. Campbell, "Rapid Granular Flows," *Annual Review of Fluid Mechanics,* vol. 22, no. 1, pp. 57-90, 1990.

[108] M. Y. Louge, E. Mastorakos and J. T. Jenkins, "The role of particle collisions in pneumatic transport," *Journal of Fluid Mechanics,* vol. 231, pp. 345-359, 1991.

[109] J. E. Galvin, C. M. Hrenya and R. D. Wildman, "On the role of the knudsen layer in rapid granular flows," *Journal of Fluid Mechanics,* vol. 585, pp. 73-92, 2007.

[110] C. M. Hrenya, J. E. Galvin and R. D. Wildman, "Evidence of higher-order effects in thermally driven rapid granular flows," *Journal of Fluid Mechanics,* vol. 598, pp. 429-450, 2008.

[111] C. K. K. Lun and H. S. Liu, "Numerical simulation of dilute turbulent gas-solid flows in horizontal channels," *International Journal of Multiphase Flow*, vol. 23, pp. 257-605, 1997.

[112] C. K. K. Lun, "Numerical simulation of dilute turbulent gas-solid flow," *International Journal of Multiphase Flow*, vol. 26, pp. 1707-1736, 2000.

[113] G. Balzer, A. Boelle and O. Simonin, "Eulerian gas-solid flow modelling of dense fluidized bed," in *Fluidization VIII: Proceedings of the Eighth Engineering Foundation Conference on Fluidization*, Tours, France, 1995.

[114] D. L. Koch, "Kinetic theory for a monodisperse gas–solid suspension," *Physics of Fluids A: Fluid Dynamics*, vol. 2, no. 10, pp. 1711-1723, 1990.

[115] A. S. Sangani, G. Mo, H.-K. Tsao, and D. L. Koch, "Simple shear flows of dense gas-solid suspensions at finite Stokes numbers," *Journal of Fluid Mechanics*, vol. 313, pp. 309-341, 1996.

[116] D. L. Koch and A. S. Sangani, "Particle pressure and marginal stability limits for a homogenous monodisperse gas-fluidized bed: kinetic theory and numerical simulations," *Journal of Fluid Mechanics*, vol. 400, pp. 229-263, 1999.

[117] D. Ma and G. Ahmadi, "A kinetic model for rapid granular flows of nearly elastic particles including interstitial fluid effects," *Powder Technology*, vol. 56, pp. 191-207, 1988.

[118] A. Boemer, H. Qi, U. Renz, S. Vasquez and F. Boysan, "Eulerian computation of fluidized bed hydrodynamics -- A comparison of physical models," in *Proceedings of the International Conference on FBC*, Orlando, FL, 1995.

[119] B. van Wachem, J. Schouten, R. Krishna and C. van den Bleek, "Eulerian simulations of bubbling behaviour in gas-solid fluidised beds," *Computers & Chemical Engineering*, vol. 22, no. Supplement 1, pp. S299-S306, 1998.

[120] M. R. Maxey and J. J. Riley, "Equation of Motion for a Small Rigid Sphere in a Nonuniform Flow," *Physics of Fluids*, vol. 26, no. 4, pp. 883-889, 1983.

[121] M. Massoudi, "Constitutive relations for the interaction force in multicomponent particulate flows," *International Journal of Non-Linear Mechanics*, vol. 38, no. 3, pp. 313-336, 2003.

[122] G. Johnson, K. R. Rajagopal and M. Massoudi, "A review of interaction mechanisms in fluid-solid flows," U.S. Department of Energy, Pittsburgh, PA, 1990.

[123] J. X. Bouillard, R. W. Lyczkowski, S. Folga, D. Gidaspow and G. F. Berry, "Hydrodynamics of erosion of heat exchanger tubes in fluidized-bed combustors," *Canadian Journal of Chemical Engineering,* vol. 67, p. 218–229, 1989.

[124] M. Syamlal, "A hyperbolic model for fluid–solids two-phase flow," *Chemical Engineering Science,* vol. 66, pp. 4421-4425, 2011.

[125] M. van der Hoef, R. Beestra and J. Kuipers, "Lattice-Boltzmann simulations of low-Reynolds-number flow past mono- and bidisperse arrays of spheres: Results for the permeability and drag force," *Journal of Fluid Mechanics,* vol. 528, pp. 233-254, 2005.

[126] O. Owoyemi, L. Mazzei and P. Lettieri, "CFD modeling of binary-fluidized suspensions and investigation of role of particle-particle drag on mixing and segregation," *AIChE Journal,* vol. 53, no. 8, pp. 1924-1940, 2007.

[127] S. L. Soo, Fluid Dynamics of Multiphase Systems, Waltham, MA: Blaisdell Publishing Corp., 1967.

[128] K. Nakamura and C. E. Capes, "Vertical Pneumatic Conveying of Binary Particle Mixtures," in *Fluidization Technology,* D. L. Keairns, Ed., Washington, DC, Hemisphere Publishing Corp., 1976, pp. 159-184.

[129] M. Syamlal, " The Particle-Particle Drag Term in a Multiparticle Model of Fluidization," DOE/MC 21353 2373, NTIS/DE 87006500, Morgantown, WV, 1987.

[130] M. G. Srinivasan and E. D. Doss, "Momentum-Transfer Due to Particle Particle Interaction in Dilute Gas Solid Flows," *Chemical Engineering Science,* vol. 40, no. 9, pp. 1791-1792, 1985.

[131] H. Arastoopour, C.-H. Wang and S. Wei, "Particle-particle interaction force in a dilute gas—solid system," *Chemical Engineering Science,* vol. 37, no. 9, pp. 1379-1386, 1982.

[132] D. Gera, M. Syamlal and T. J. O'Brien, "Hydrodynamics of particle segregation in fluidized beds," *International Journal Of Multiphase Flow,* vol. 30, no. 4, pp. 419-428, 2004.

[133] R. Fox, "On multiphase turbulence models for collisional fluid–particle flows," *Journal of Fluid Mechanics,* vol. 742, pp. 368-424, 2014.

[134] G. Ahmadi and D. Ma, "A thermodynamical formulation for dispersed multiphase turbulent flows - 1: Basic theory," *International Journal of Multiphase Flow,* vol. 16, no. 2, pp. 323-340, 1990.

[135] D. Ma and G. Ahamdi, " thermodynamical formulation for dispersed multiphase turbulent flows II: Simple shear flow for dense Mixtures," *International Journal of Multiphase Flow,* vol. 16, no. 2, pp. 341-351, 1990.

[136] M. Syamlal and D. Gidaspow, "Hydrodynamics of Fluidization: Prediction of Wall to Bed Heat Transfer Coefficients," *AIChE Journal,* vol. 31, no. 1, pp. 127-135, 1985.

[137] J. A. M. Kuipers, W. Prins and W. Van Swaaij, "Numerical calculation of wall-to-bed heat-transfer coefficients in gas-fluidized beds," *AIChE Journal,* vol. 38, no. 7, pp. 1079-1091, 1992.

[138] D. J. Gunn, "Transfer of heat or mass to particles in fixed and fluidised beds," *International Journal of Heat and Mass Transfer,* vol. 21, no. 4, pp. 467-476, April 1978.

[139] J. Musser, M. Syamlal, M. Shahnam and D. E. Huckaby, "Constitutive equation for heat transfer caused by mass transfer," *Chemical Engineering Science,* vol. 123, pp. 436-443, 2015.

[140] R. Bauer and E. U. Schlunder, "Effective radial thermal conductivity of packings in gas flow. Part II. Thermal conductivity of the packing fraction without gas," *International Chemical Engineering,* vol. 18, no. 2, pp. 189-204, 1978.

[141] S. Yagi and D. Kunii, "Studies on Effective Thermal Conductivities in Packed Beds," *AIChE Journal,* vol. 3, no. 3, pp. 373-381, 1957.

[142] A. Griesinger, K. Spindler and E. Hahne, "Measurements and theoretical modelling of the effective thermal conductivity of zeolites," *International Journal of Heat and Mass Transfer,* vol. 42, pp. 4363-4374, 1999.

[143] A. Mills, Basic Heat & Mass Transfer, Upper Saddle River, N.J, USA: Prentice Hall; 2 edition, 1998.

[144] A. R. Khan, R. L. Pirie and J. F. Richardson, "Hydraulic Transport of Solids in Horizontal Pipelines—Predictive Methods for Pressure-Gradients," *Chemical Engineering Science,* vol. 42, no. 4, pp. 767-778, 1987.

[145] S. Ergun, "Fluid Flow Through Packed Columns," *Chemical Engineering Progress,* vol. 48, no. 6, pp. 89-94, 1952.

[146] J. F. Richardson and W. N. Zaki, "Sedimentation and Fluidization: Part I," *Transactions of the Institution of Chemical Engineers,* vol. 32, 1954.

[147] C. Y. Wen and Y. H. Yu, "Mechanics of fluidization," *Chemical Engineering Progress Symposium Series,* vol. 62, p. 100, 1966.

[148] R. Beetstra, M. A. van der Hoef and J. A. Kuipers, " Drag force of intermediate Reynolds number flow past mono- and bidisperse arrays of spheres," *AIChE Journal,* vol. 53, p. 489–501, 2007.

[149] R. Beestra, M. A. van der Hoef and J. A. Kuipers, "Erratum," *AIChE Journal,* vol. 2007, no. 53, p. 3020, 2007.

[150] R. J. Hill, D. L. Koch and J. C. Ladd, "The first effects of fluid inertia on flows in ordered and random arrays of spheres," *Journal of Fluid Mechanics,* vol. 448, p. 213–241, 2001.

[151] R. J. Hill, D. L. Koch and J. C. Ladd, "Moderate-Reynolds-number flows in ordered and random arrays of spheres," *Journal of Fluid Mechanics,* vol. 448, pp. 243-278, 2001.

[152] S. Benyahia, M. Syamlal and T. J. O'Brien, "Extension of Hill-Koch-Ladd drag correlation over all ranges of Reynolds number and solids volume fraction," *Powder Technology,* vol. 162, no. 2, pp. 166-174, 2006.

[153] X. Yin and S. Sundaresan, "Drag Law for Bidisperse Gas-Solid suspensions Containing Equally Sized Spheres," *Industrial & Engineering Chemistry Research,* vol. 48, p. 227–241, 2009.

[154] X. Yin and S. Sundaresan, "Fluid-particle drag in low-Reynolds-number polydisperse gas-solid suspensions," *AIChE Journal,* vol. 55, p. 1352–1368, 2009.

[155] L. Schiller and A. Naumann, "A drag coefficient correlation," *Zeitschrift des Vereines deutscher Ingenieure,* vol. 77, pp. 318-320, 1933.

[156] H. Arastoopour and D. Gidaspow, "Vertical Pneumatic Conveying Using Four Hydrodynamic Models," *Industrial & Engineering Chemistry Fundamentals,* vol. 18, no. 2, pp. 123-130, 1979.

[157] M. Ishii and N. Zuber, "Drag coefficient and relative velocity in bubbly, droplet or particulate flows," *AIChE Journal,* vol. 25, no. 5, pp. 843-855, 1979.

[158] Z. Duan, B. He and Y. Duan, "Sphere Drag and Heat Transfer," *Scientific Reports,* vol. 5, no. 1, p. 12304, 2015.

[159] J. Almedeij, "Drag coefficient of flow around a sphere: matching asymptotically the wide trend," *Powder Technology,* vol. 186, no. 3, pp. 218-223, 2008.

[160] R. Clift, J. Grace and M. Weber, Bubbles, Drops and Particles, London: Academic Press, 1978.

[161] D. Gidaspow, B. Ettehadieh, C. Lin, A. Goyal and R. Lyczkowski, "Solids circulation around a jet in a fluidized bed gasifier. Final technical report, September 1, 1978-September 30, 1980," United States, N. p., 1980.

[162] D. Lathouwers and J. Bellan, "Modeling of dense gas-solid reactive mixtures applied to biomass pyrolysis in a fuidized bed," in *Proceedings of the 2000 U.S. DOE Hydrogen Program Review NREL/CP-570-28890*, San Ramon, California, 2000.

[163] J. Leboreiro, G. Joseph and C. Hrenya, "Revisiting the standard drag law for bubbling, gas-fluidized beds," *Powder Technology,* vol. 183, no. 3, pp. 385-400, 2008.

[164] D. Lathouwers and J. Bellan, "Modeling and simulation of bubbling fluidized beds containing particle mixtures," *Proceedings of the Combustion Institute,* vol. 28, no. 2, pp. 2297-2304, 2000.

[165] S. Dahl and C. Hrenya, "Size segregation in gas-solid fluidized beds with continuous size distributions," *Chemical Engineering Science,* vol. 60, no. 23, pp. 6658-6673, 2005.

[166] L. Huilin and D. Gidaspow, "Hydrodynamics of binary fluidization in a riser: CFD simulation using two granular temperatures," *Chemical Engineering Science,* vol. 58, no. 16, pp. 3777-3792, 2003.

[167] J. Leboreiro, G. Joseph, C. Hrenya, D. Snider, S. Banerjee and J. Galvin, "The influence of binary drag laws on simulations of species segregation in gas-fluidized beds," *Powder Technology,* vol. 184, no. 3, pp. 275-290, 2008.

[168] M. Syamlal and T. J. O'Brien, "A Generalized Drag Correlation for Multiparticle Systems," U.S. Department of Energy, Office of Fossil Energy, Morgantown, WV, 1987.

[169] J. Garside and M. R. Aldibouni, "Velocity-Voidage Relationships for Fluidization and Sedimentation in Solid-Liquid Systems," *Industrial & Engineering Chemistry Process Design and Development,* vol. 16, no. 2, pp. 206-214, 1977.

[170] W. E. Ranz and W. R. Marshall, "Evaporation from drops, Part 1 & 2," *Chemical Engineering Progress,* vol. 48, pp. 141-146; 173-180, 1952.

[171] N. I. Gelperin, V. G. Einstein and Toskubay, "Heat Transfer Coefficient between a Surface and a Fluid Bed," *British Chemical Engineering and Process Technology,* vol. 16, no. 10, p. 922, 1971.

[172] S. S. Zabrodsky, Hydrodynamics and Heat Transfer in Fluidized Beds, Cambridge, MA: MIT Press, 1966.

[173] A. Yu and N. Standish, "Porosity calculation of multicomponent mixtures of spherical particles," *Powder Technology,* vol. 52, p. 233–241, 1987.

[174] R. Fedors and R. Landel, "An empirical method of estimating the void fraction in mixtures of uniform particles of different size," *Powder Technology*, vol. 23, p. 225–231, 1979.

[175] J. M. Vedovoto, A. da Silveira Neto, A. Mura and L. da Silva, "Application of the method of manufactured solutions to the verification of a pressure-based finite-volume numerical scheme," *Computers & Fluids,* vol. 51, no. 1, pp. 85-99, 2011.

[176] C. J. Roy, "Review of code and solution verification procedures for computational simulation," *Journal of Computational Physics*, vol. 205, no. 1, pp. 131-156, 2005.

[177] P. J. Roache, Fundamentals of Verification and Validation, Socorro, NM: Hermosa Publishers, 2009.

[178] P. J. Roache and S. Steinberg, "Symbolic manipulation and computational fluid dynamics," *AIAA Journal,* vol. 22, no. 10, pp. 1390-1394, October 1984.

[179] W. L. Oberkampf and C. J. Roy, Verification and validation in scientific computing, Cambridge: Cambridge University Press, 2010.

[180] A. Choudhary, C. Roy, J. Dietiker, M. Shahnam and R. Garg, "Code Verification for Multiphase Flows Using the Method of Manufactured Solutions," in *ASME 2014 4th Joint US-European Fluids Engineering Division Summer Meeting collocated with the ASME 2014 12th International Conference on Nanochannels, Microchannels, and Minichannels*, Chicago, Illinois, USA, August 3–7, 2014.

[181] AIAA, "Guide for the Verification and Validation of Computational Fluid Dynamics Simulations (AIAA G-077-1998(2002))," American Institute of Aeronautics and Astronautics (AIAA), 1998.

[182] D. Gidaspow, "Hydrodynamics of fluidization and heat transfer: supercomputer modeling," *Applied Mechanical Review,* vol. 39, pp. 1-23, 1986.

[183] J. M. Dalla Valle, Micromeritics : the technology of fine particles, New York ; Toronto ; London: Pitman Publishing Corp, 1948.

[184] M. Syamlal and T. J. O'Brien, "Fluid dynamic simulation of O3 decomposition in a bubbling fluidized bed," *AIChE Journal,* vol. 49, no. 11, pp. 2793-2801, 2003.

[185] W. Holloway, X. Yin and S. Sundaresan, "Fluid-Particle Drag in Inertial Polydisperse Gas–Solid Suspensions," *AIChE Journal,* vol. 56, pp. 1995-2004, 2010.

[186] M. C. Roco, Ed., "Analytical modeling of multiphase flow," in *Particulate Two-Phase Flow (Butterworth-Heinemann Series in Chemical Engineering)*, Boston,MA, Butterworth-Heinemann, 1993.

[187] B. A. Kashiwa and R. M. Rauenzahn, "A multimaterial formalism," in *Numerical Methods in Multiphase Flows*, C. T. Crowe, Ed., U.S., ASME, 1994, p. 149–157.

[188] G. B. Wallis, One-Dimensional Two-Phase Flow, New York: McGraw-Hill, 1969.

[189] M. Andrews and P. O'Rourke, "The multiphase particle-in-cell (MP-PIC) method for dense particulate flows," *International Journal of Multiphase Flow,* vol. 22, no. 2, pp. 379-402, 1996.

[190] D. M. Snider, "Three-Dimensional Multiphase Particle-in-Cell Model for Dense Particle Flows," *Journal of Computational Physics,* vol. 170, no. 2, pp. 523-549, 2001.

[191] P. J. O'Rourke, P. Zhao and D. Snider, "A model for collisional exchange in gas/liquid/solid fluidized beds," *Chemical Engineering Science,* vol. 64, no. 8, pp. 1784-1797, 2009.

[192] P. J. O'Rourke and D. M. Snider, "An improved collision damping time for MP-PIC calculations of dense particle flows with applications to polydisperse sedimenting beds and colliding particle jets," *Chemical Engineering Science,* vol. 65, no. 22, pp. 6014-6028, 2010.

[193] H. J. Herrmann and S. Luding, "Modeling granular media on the computer," *Continuum Mechanics and Thermodynamics,* vol. 10, no. 4, pp. 189-231, 1998.

[194] L. Silbert,, D. Ertas, G. Grest, T. Halsey, D. Levine and S. Plimpton, "Granular flow down an inclined plane: Bagnold scaling and rheology," *Physical Review E,* vol. 64, no. 5, p. 051302, 2001.

[195] J. Shäfer, S. Dippel and D. Wolf, "Force Schemes in Simulations of Granular Materials," *Journal de Physique I (France),* vol. 6, no. 1, pp. 5-20, 1996.

[196] ,. G. K. Batchelor and R. W. O'Brien, "Thermal or Electrical Conduction Through a Granular Material," *Proceedings of the Royal Society of London. Series A, Mathematical and Physical Sciences,* vol. 355, no. 1682, pp. 313-333, July 1977.

[197] C. Y. Wen and T. M. Chang, "Particle-to-particle heat transfer in air-fluidized beds," in *Proceedings of the International symposium on fluidization*, Eindhoven, June 6-9, 1967.

[198] D. Rong and M. Horio, "DEM simulation of char combustion in a fluidized bed," in *Second International Conference on CFD in the Minerals and Process Industries*, Melbourne, 1999.

[199] C. Delvosalle and J. Vanderschuren, "Gas-to-particle and particle-to-particle heat transfer in fluidized beds of large particles," *Chemical Engineering Science,* vol. 40, no. 5, pp. 769-779, 1985.

[200] A. M. Xavier and J. F. Davidson, "Heat transfer to surfaces immersed in fluidised beds, particularly tube arrays," in *Fluidization: Proceedings of the Second Engineering Foundation Conference*, Cambridge, England, 2-6 April, 1978.

[201] P. N. Dwivedi and S. N. Upadhyay, "Particle-fluid mass transfer in fixed and fluidized beds," *Industrial & Engineering Chemistry Process Design and Development,* vol. 16, no. 2, pp. 157-165, April 1977.

[202] N. Wakao, S. Kaguei and T. Funazkri, "Effect of fluid dispersion coefficients on particle-to-fluid heat transfer coefficients in packed beds : Correlation of Nusselt numbers," *Chemical Engineering Science,* vol. 34, no. 3, pp. 325-336, 1979.

[203] P. K. Agarwal, "Transport phenomena in multi-particle systems--II. Particle-fluid heat and mass transfer," *Chemical Engineering Science,* vol. 43, no. 9, pp. 2501-2510, 1988.

[204] J. E. Galvin and S. Benyahia, "The effect of cohesive forces on the fluidization of aeratable powders," *AIChE Journal,* vol. 60, no. 2, p. 473–484, 2014.

[205] A. Jenike, "A Theory of Flow of Particulate Solids in Converging and Diverging Channels Based on a Conical Yield Function," *Powder Technology,* vol. 50, no. 3, pp. 229-236, 1987.

[206] J. Arnold, "Vapor viscosities and the Sutherland equation," *The Journal of Chemical Physics,* vol. 1, no. 2, pp. 170-176, 1933.

[207] P. Bhatnagar, E. Gross and M. Krook, "A Model for Collision Processes in Gases. I. Small Amplitude Processes in Charged and Neutral One-Component Systems," *Physical Review,* vol. 94, no. 3, pp. 511-525, 1954.

[208] W. Vincenti and C. Kruger, Jr., Introduction to Physical Gas Dynamics, New York: John Wiley and Sons, 1965.

[209] F. Auzerais, R. Jackson and W. Russel, "The resolution of shocks and the effects of compressible sediments in transient settling," *Journal of Fluid Mechanics,* vol. 195, no. 1, pp. 437-462, 1988.

[210] D. Snider, P. O'Rourke and M. Andrews, "An Incompressible Two-Dimensional Multiphase Particle-In-Cell Model for Dense Particle Stress," Los Alamos National Laboratory, Los Alamos, June 1997.

[211] D. Snider, "Three fundamental granular flow experiments and CPFD predictions," *Powder Technology,* vol. 176, no. 1, pp. 36-45, 2007.

[212] D. Snider, C. S.M. and P. O'Rourke, "Eulerian-Lagrangian method for three-dimensional thermal reacting flow with application to coal gasifiers," *Chemical Engineering Science,* vol. 66, no. 6, pp. 1285-1295, 2011.

[213] P. O'Rourke and S. D.M., "Inclusion of collisional return-to-isotropy in the MP-PIC method," *Chemical Engineering Science,* vol. 80, pp. 39-54, 2012.

[214] P. O'Rourke and D. Snider, "A new blended acceleration model for the particle contact forces induced by an interstitial fluid in dense particle/fluid flows," *Powder Technology,* vol. 256, pp. 39-51, 2014.

[215] S. Pannala, M. Syamlal and T. O'Brien, "Multiphase Continuum Formulation for Gas-Solids Reacting Flows," in *Computational Gas-Solids Flows and Reacting Systems: Theory, Methods and Practice*, Hershey, PA, IGI Global, 2011, pp. 1-65.

[216] S. Benyahia, M. Syamlal and T. J. O'Brien, "Study of the ability of multiphase continuum models to predict core-annulus flow," *AIChE Journal,* vol. 53, no. 10, pp. 2549-2568, 2007.

[217] K. R. Rajagopal, G. Johnson and M. Massoudi, "Averaged equations for an isothermal, developing flow of a fluid- solid mixture," U.S. Department of Energy, Pittsburgh, 1996.

[218] H. Schlichting, Boundary-Layer Theory, 6th ed., New York: McGraw-Hill Book Company, 1968.

[219] C. Campbell, "Granular shear flows at the elastic limit," *Journal of Fluid Mechanics,* vol. 465, pp. 261-291, 2002.

[220] S. Bharathraj and V. Kumaran, "Effect of particle stiffness on contact dynamics and rheology in a dense granular flow," *Physical Review E,* vol. 97, pp. 012902-15, 2018.

[221] C. Campbell, "Stress-controlled elastic granular shear flows," *Journal of Fluid Mechanics,* vol. 539, pp. 273-297, 2005.

[222] J. Capecelatro and O. Desjardins, "An Euler–Lagrange strategy for simulating particle-laden flows," *Journal of Computational Physics,* vol. 238, pp. 1-31, 2013.

[223] N. G. Deen, M. Van Sint Annaland, M. A. Van Der Hoef and J. A. M. Kuipers, "Review of discrete particle modeling of fluidized beds," *Chemical Engineering Science,* vol. 62, pp. 28-44, 2007.

[224] D. Lathouwers and J. Bellan, "Modeling of dense gas-solid reative mixtures applied to biomass pyrolysis in a fluidized bed," *International Journal of Mulitphase Flow,* vol. 27, pp. 2155-2187, 2001.

[225] M. Syamlal, "MFIX Documentation: Numerical Technique," Morgantown Energy Technology Center, Morgantown, West Virginia, 1998.

[226] M. Moscardini, Y. Gan, S. Pupeschi and M. Kamlah, "Discrete element method for effective thermal conductivity of packed pebbles accounting for the Smoluchowski effect," *Fusion Engineering and Design,* vol. 127, pp. 192-201, 2019.

[227] M. G. Kaganer, Thermal Insulation in Cryogenic Engineering, Jerusalem: Israel Program for Scientific Translations Ltd., 1969.

[228] M. Leva., "Chapter 4 The Expanded Bed," in *Fluidization*, New York, McGraw-Hill, 1959, pp. 78-113.

Appendix A: Internal Energy Equations Derivation

Simplifying assumptions have been made in the formulation of internal energy equations:

(1) The irreversible rate of increase of internal energy due to viscous dissipation and interphase momentum transfer has been neglected. Such terms are negligible except in the case of very large relative velocities;
(2) Interfacial work terms are negligible;
(3) Energy transfer accompanying species diffusion is negligible.

A.1 Gas Phase Energy Equation.

The gas phase internal energy equation is [20, 21]

$$\frac{\partial}{\partial t}\left(\varepsilon_g \rho_g I_g\right) + \frac{\partial}{\partial x_i}\left(\varepsilon_g \rho_g U_{gi} I_g\right) = -\frac{\partial}{\partial x_i}\left(\varepsilon_g q_{gi}\right) - p_g\left(\frac{\partial \varepsilon_g}{\partial t} + \frac{\partial \varepsilon_g U_{gi}}{\partial x_i}\right) + \mathcal{S}_g' \qquad \text{(A-1)}$$

where I_g is the specific internal energy of the gas phase. The terms on the left hand side are the rate of internal energy accumulation and the net rate of convective internal energy flux. The three terms on the right hand side are the conductive heat flux, work done by the gas to change the volume fraction, and a generalized source term whereby contributions from additional models are incorporated.[58]

The gas phase enthalpy is defined as

$$H_g = I_g + \left(\frac{p_g}{\rho_g}\right) \qquad \text{(A-2)}$$

which is used to recast (A-1) as

$$\begin{aligned} &\varepsilon_g \rho_g \left(\frac{\partial H_g}{\partial t} + U_{gi}\frac{\partial H_g}{\partial x_i}\right) + H_g\left(\frac{\partial}{\partial t}\left(\varepsilon_g \rho_g\right) + \frac{\partial}{\partial x_i}\left(\varepsilon_g \rho_g U_{gi}\right)\right) \\ &\qquad = -\frac{\partial}{\partial x_i}\left(\varepsilon_g q_{gi}\right) + \varepsilon_g\left(\frac{\partial p_g}{\partial t} + U_{gi}\frac{\partial p_g}{\partial x_i}\right) + \mathcal{S}_g' \end{aligned} \qquad \text{(A-3)}$$

Here we can see the left hand side of the continuity equation (2-3) multiplied by H_g such that (A-3) can be written as

[58] Several terms defined in the referenced works (i.e., equation 2.3 in [21]) are omitted. Specifically, equation (A-1) does not include changes in internal energy due to interphase momentum and mass transfer, nor does it include changes in internal energy due to viscous dissipation. The remaining omitted terms, such as interphase convective heat transfer and changes in internal energy arising from phase change and/or chemical reactions, are covered in section 3.4.

$$\varepsilon_g \rho_g \left(\frac{\partial H_g}{\partial t} + U_{gi} \frac{\partial H_g}{\partial x_i} \right) = -\frac{\partial}{\partial x_i}(\varepsilon_g q_{gi}) + \varepsilon_g \left(\frac{\partial p_g}{\partial t} + U_{gi} \frac{\partial p_g}{\partial x_i} \right) - H_g \sum_{n=1}^{N_g} R_{gn} + \mathcal{S}'_g \quad \text{(A-4)}$$

The enthalpy of the gas mixture is defined as the sum of the enthalpies of the individual species,

$$H_g = \sum_{n=1}^{N_g} h_{gn} X_{gn} \quad \text{(A-5)}$$

The specific enthalpy each species is calculated by combining the heat of formation and integrating the specific heat of that species from the reference temperature to the gas phase temperature,

$$h_{gn} = H_{fn}^{\circ}(T_{ref}) + \int_{(T_{ref})}^{T_g} C_{pgn}(T)\, dT \quad \text{(A-6)}$$

Differentiating (A-5) and (A-6) yields

$$dH_g = \sum_{n=1}^{N_g} \left(dh_{gn} X_{gn} + h_{gn} dX_{gn} \right) \quad \text{(A-7)}$$

and

$$dh_{gn} = C_{pgn} dT_g \quad \text{(A-8)}$$

Substituting (A-8) into (A-7) gives

$$dH_g = \sum_{n=1}^{N_g} \left(X_{gn} C_{pgn} dT_g + h_{gn} dX_{gn} \right) \quad \text{(A-9)}$$

Substituting the definition of the gas phase mixture specific heat (2-26) into (A-9)

$$dH_g = C_{pg} dT_g + \sum_{n=1}^{N_g} h_{gn} dX_{gn} \quad \text{(A-10)}$$

Substituting (A-10) into (A-4) and expanding the derivatives results in the energy equation in terms of temperatures and enthalpies,

$$\varepsilon_g \rho_g C_{pg} \left(\frac{\partial T_g}{\partial t} + U_{gi} \frac{\partial T_g}{\partial x_i} \right) = -\frac{\partial}{\partial x_i}(\varepsilon_g q_{gi}) + \varepsilon_g \left(\frac{\partial p_g}{\partial t} + U_{gi} \frac{\partial p_g}{\partial x_i} \right) - \sum_{n=1}^{N_g} h_{gn} \left(\varepsilon_g \rho_g \left[\frac{\partial X_{gn}}{\partial t} + U_{gi} \frac{\partial X_{gn}}{\partial x_i} \right] + X_{gn} \sum_{n'=1}^{N_g} R_{gn'} \right) + \mathcal{S}'_g \quad \text{(A-11)}$$

Combining the gas phase continuity and n^{th} gas phase species equations gives (to obtain the non-conservative form of the species equation),

$$\varepsilon_g \rho_g \left(\frac{\partial X_{gn}}{\partial t} + U_{gi} \frac{\partial X_{gn}}{\partial x_i} \right) = \frac{\partial}{\partial x_j} \left(\mathcal{D}_{gn} \frac{\partial X_{gn}}{\partial x_j} \right) + R_{gn} - X_{gn} \sum_{n=1}^{N_g} R_{gn} \quad \text{(A-12)}$$

Substituting (A-12) into (A-11),

$$\varepsilon_g \rho_g C_{pg} \left(\frac{\partial T}{\partial t} + U_{gi} \frac{\partial T}{\partial x_i} \right) = -\frac{\partial}{\partial x_i}(\varepsilon_g q_{gi}) + \varepsilon_g \left(\frac{\partial p_g}{\partial t} + U_{gi} \frac{\partial p_g}{\partial x_i} \right) - \left(\sum_{n=1}^{N_g} h_{gn} \left(\frac{\partial}{\partial x_j} \left(\mathcal{D}_{gn} \frac{\partial X_{gn}}{\partial x_j} \right) + R_{gn} \right) \right) + \mathcal{S}'_g \quad \text{(A-13)}$$

Neglecting expansion effects and diffusive enthalpy transfer yields,

$$\varepsilon_g \rho_g C_{pg} \left(\frac{\partial T}{\partial t} + U_{gi} \frac{\partial T}{\partial x_i} \right) = -\frac{\partial}{\partial x_i}(\varepsilon_g q_{gi}) - \sum_{n=1}^{N_g} h_{gn} R_{gn} + \mathcal{S}'_g. \quad \text{(A-14)}$$

Finally, we obtain the gas phase energy equation, shown below as well as equation (2-6), by combining the change in enthalpy due to the production and/or consumption of species mass[59] with the general source term.

$$\varepsilon_g \rho_g C_{pg} \left(\frac{\partial T}{\partial t} + U_{gi} \frac{\partial T}{\partial x_i} \right) = -\frac{\partial}{\partial x_i}(\varepsilon_g q_{gi}) + \mathcal{S}_g \quad \text{(A-15)}$$

[59] The source term for change in enthalpy due to the production and/or consumption of species mass is defined separately from the energy equation (see section 2.5.8.2).

Note that the prime superscript is removed from the source term to indicate that the final source term is not identical to the source term identified initially in equation (A-1). Although this last modification to the energy equation is not necessary, it casts the final equation into the same form as the other conservation equations whereby specific models and sub-models are presented separately from the conservation equation.

A.2 Continuum Solids Phase Energy Equation.

The m^{th} phase internal energy equation is [20, 21]

$$\frac{\partial}{\partial t}(\varepsilon_m \rho_m I_m) + \frac{\partial}{\partial x_i}(\varepsilon_m \rho_m U_{mi} I_m) = -\frac{\partial}{\partial x_i}(\varepsilon_m q_{mi}) + \mathcal{S}'_m \tag{A-16}$$

where I_m is the specific internal energy of the m^{th} solids phase. The terms on the left hand side are the rate of internal energy accumulation and the net rate of convective internal energy flux. The terms on the right hand side include the conductive heat flux described by Fourier's Law and a general source term S_m.

The m^{th} solids phase enthalpy is defined as

$$H_m = I_m \tag{A-17}$$

is used to recast(A-17) as

$$\begin{aligned} \varepsilon_m \rho_m \left(\frac{\partial H_m}{\partial t} + U_{mi}\frac{\partial H_m}{\partial x_i}\right) + H_m \left(\frac{\partial}{\partial t}(\varepsilon_m \rho_m) + \frac{\partial}{\partial x_i}(\varepsilon_m \rho_m U_{mi})\right) \\ = -\frac{\partial}{\partial x_i}(\varepsilon_m q_{mi}) + \mathcal{S}'_m \end{aligned} \tag{A-18}$$

Here we can see the left hand side of the continuity equation (3-1) multiplied by H_m such that (A-18) can be written as

$$\varepsilon_m \rho_m \left(\frac{\partial H_m}{\partial t} + U_{mi}\frac{\partial H_m}{\partial x_i}\right) = -\frac{\partial}{\partial x_i}(\varepsilon_m q_{mi}) - H_m \sum_{n=1}^{N_m} R_{mn} + \mathcal{S}'_m \tag{A-19}$$

The enthalpy of the solids is defined as the sum of the enthalpies of the individual species,

$$H_m = \sum_{n=1}^{N_m} h_{mn} X_{mn} \tag{A-20}$$

The specific enthalpy of each species is calculated by combining the heat of formation and integrating the specific heat of that species from the reference temperature to the gas phase temperature,

$$h_{mn} = H_{fn}^{\circ}(T_{ref}) + \int_{(T_{ref})}^{T_m} C_{pmn}(T)\, dT \tag{A-21}$$

Differentiating (A-20) and (A-21) yields

$$dH_m = \sum_{n=1}^{N_m} (dh_{mn} X_{mn} + h_{mn} dX_{mn}) \tag{A-22}$$

and

$$dh_{mn} = C_{pmn} dT_m \tag{A-23}$$

Substituting (A-23) into (A-22) gives

$$dH_m = \sum_{n=1}^{N_m} \left(X_{mn} C_{pmn} dT_m + h_{mn} dX_{mn}\right) \tag{A-24}$$

Substituting the definition of the solids phase mixture specific heat (3-82) into (A-24)

$$dH_m = C_{pm} dT_m + \sum_{n=1}^{N_m} h_{mn} dX_{mn} \tag{A-25}$$

Substituting (A-25) into (A-19) and expanding the derivatives results in the energy equation in terms of temperatures and enthalpies,

$$\begin{aligned} \varepsilon_m \rho_m C_{pm} \left(\frac{\partial T_m}{\partial t} + U_{mi} \frac{\partial T_m}{\partial x_i}\right) & \\ = -\frac{\partial}{\partial x_i}(\varepsilon_m q_{mi}) & \\ - \sum_{n=1}^{N_m} h_{mn} \left(\varepsilon_m \rho_m \left[\frac{\partial X_{mn}}{\partial t} + U_{mi} \frac{\partial X_{mn}}{\partial x_i}\right] + X_{mn} \sum_{n'=1}^{N_m} R_{mn'} \right) + \mathcal{S}'_m & \end{aligned} \tag{A-26}$$

Combining the m^{th} solids phase continuity and species mass equations gives,

$$\varepsilon_m \rho_m \left(\frac{\partial X_{mn}}{\partial t} + U_{mj} \frac{\partial X_{mn}}{\partial x_j}\right) = R_{mn} - X_{mn} \sum_{n'=1}^{N_m} R_{mn'} \tag{A-27}$$

Substituting (A-27) into (A-26) gives the solids energy equation in terms of temperature.

$$\varepsilon_m \rho_m C_{pm} \left(\frac{\partial T_m}{\partial t} + U_{mi} \frac{\partial T_m}{\partial x_i}\right) = -\frac{\partial}{\partial x_i}(\varepsilon_m q_{mi}) - \sum_{n=1}^{N_m} h_{mn} R_{mn} + \mathcal{S}'_m \tag{A-28}$$

Finally, we obtain the gas phase energy equation, shown below as well as equation (2-6), by combining the change in enthalpy due to the production and/or consumption of species mass[60] with the general source term.

$$\varepsilon_m \rho_m C_{pm} \left(\frac{\partial T_m}{\partial t} + U_{mi} \frac{\partial T_m}{\partial x_i} \right) = -\frac{\partial}{\partial x_i} (\varepsilon_m q_{mi}) - \mathcal{S}_m \qquad \text{(A-29)}$$

As in the previous section, the prime superscript is removed from the source term to indicate that the final source term is not identical to the source term identified initially in equation (A-16)(A-1). Although this last modification to the energy equation is not necessary, it casts the final equation into the same form as the other conservation equations whereby specific models and sub-models are presented separately from the conservation equation.

[60] The source term for change in enthalpy due to the production and/or consumption of species mass is defined separately from the energy equation (see section 3.4.11.2).

Appendix B: Drag coefficients

An expression for the interaction force is necessary to close the averaged equation of motion (Section 3.3.3). While providing closure models for the interaction force is an active area of research, it is a complex problem and precise evaluation is possibly in only certain very limited circumstances. As discussed in Section 3.4.4 several different physical mechanisms responsible for gas-solids interphase momentum transfer have been identified. By default, MFIX accounts for buoyancy and drag in its formulation for this term.

Several well-known formulas accurately represent the drag force on a single-sphere as a function of the Reynolds number [144]. In a multi-particle system, the nearness of other particles makes the drag force on each particle significantly greater than that given by the single-particle drag formula. Thus, the formula for multi-particle drag force must include the gas volume fraction as an additional parameter to account for the effect of neighboring particles. For practical purposes an expression(s) that describes the phenomena of interest over the whole range of Reynolds and Stokes numbers and up to high solids volume fraction [39] is desirable.

Traditionally, experimental information has been used to derive empirical correlations for the drag force. One type, valid for high values of the solids volume fraction, is the packed-bed pressure drop correlation, such as the Ergun equation [145]. Another type of experimental data is the terminal velocity in fluidized or settling beds, given as correlations for the ratio of the terminal velocity of a multi-particle system to that of a single particle [146]. Deducing a drag model capable of spanning the whole range of Reynolds numbers from this approach, however, is also not clear-cut [39]. To this end, the ratio of the drag force in a multi-particle system to that on a single particle was used to encompass the entire regions of flow [147]. In recent years, models for the drag force have been derived from accurate numerical experiments. Several of these models have been incorporated into MFIX over the years [148, 149, 150, 151, 152, 148, 149, 153, 154], however a detailed analysis of their formulation and implementation are not included here at this time.

Since the drag force arises due to relative motion between the phases, its general form is often represented in terms of a drag coefficient and relative velocity difference. MFIX follows this approach, and the expression given in Chapter 3 is repeated here for convenience:

$$I_{gmi,Drag} = \beta_{gm}\left(U_{gi} - U_{mi}\right) \tag{3-61}$$

β_{gm} is referred to as the drag coefficient and is generally taken as a scalar function that depends on a number of factors, such as, size and shape of the particle, properties of the fluid, the solids volume fraction and magnitude of the relative velocity difference.

The traditional drag force correlations (Ergun [145], Wen and Yu [147]) are effectively limited to describing a monodisperse system. However, systems found in nature or in industry are typically characterized by nonuniform solids. As a result, these monodisperse drag force models are generalized in an *ad hoc* manner for application to polydisperse systems. Namely, the particle diameter is replaced with the m^{th} phase particle diameter (d_m) and the solids velocity is replaced with the m^{th} phase solids velocity. Finally, in the multi-fluid model (MFIX-TFM), the monodisperse drag coefficient expression is also scaled by the ratio of the m^{th} phase solids volume fraction to total solids volume fraction, or equivalently, by $\varepsilon_m/(1-\varepsilon_g)$ as:

$$\beta_{gm} = \frac{\varepsilon_m}{1-\varepsilon_g}\beta'_{gm} \tag{B-1}$$

In the discrete element model (MFIX-DEM), these same expressions for the drag coefficient are used to find the drag force on the particle:

$$\beta_g^{(i)} = \frac{\mathcal{V}^{(i)}}{1-\varepsilon_g}\beta'_{gm} \tag{B-2}$$

Finally, as noted in Section 3.4.4.1, some ambiguity can also occur in regard to the definition of the different interaction terms and how they are carried through into the averaged equations. Thus sufficient care must be taken to ensure the total interaction force remains the same regardless of the decomposition. Since MFIX has two definitions for the buoyancy force (pressure gradient versus Archimedean form), the definition of the drag force must reflect those changes. The drag coefficients presented in this Appendix assume that buoyancy is given by the pressure gradient (i.e., equation 3-59). Thus, the drag coefficient does not include the effect of relative motion on the local pressure gradient. Otherwise, if the Archimedean formulation for buoyancy is used (equation 3-60), then MFIX automatically divides the expressions given here for β_{gm} by the void fraction to ensure equivalency of the total interaction force [39].

B.1 Wen-Yu [147]

Wen and Yu [147] extend the work of Richardson and Zaki [146] to derive an expression for the drag force in a particulate system to encompass a wide range of Reynolds number. They measured pressure drop and void fraction data in single sized particle fluidization experiments starting at high flow rates and decreasing until fixed bed conditions were achieved. Their tabulated data, along with additional literature data, was used to correlate a voidage function defined as the ratio of force on a particle in a multiparticle system to that in single particle system. The force in a single particle system was expressed using Schiller and Naumann [155] correlation for the single particle drag coefficient, which is valid for Reynolds numbers ranging from 0.001 to 1000. Following some manipulation their correlation for the average drag force

exerted on a particle in a multiparticle system by the fluid can be expressed in terms of a drag coefficient as:

$$\beta_{gm}^{'WenYu} = \frac{3}{4} C_{Ds} \frac{\rho_g \varepsilon_g (1-\varepsilon_g) |U_{gi} - U_{mi}|}{d_{pm}} \varepsilon_g^{-2.65} \tag{B-3}$$

where

$$C_{Ds} = \begin{cases} \frac{24}{\mathrm{Re}}(1 + 0.15\mathrm{Re}^{0.687}) & \mathrm{Re} \le 1000 \\ 0.44 & \mathrm{Re} > 1000 \end{cases} \tag{B-4}$$

$$\mathrm{Re} = \frac{\rho_g \varepsilon_g |U_g - U_m| d_{pm}}{\mu_g} \tag{B-5}$$

Here, as done elsewhere (e.g., [156, 157]), the expression for the single particle drag coefficient is extended for Reynold numbers greater than 1000.[61] Specifically, in the range of Reynold numbers between about 1000 to $2x10^5$, the drag coefficient for a smooth sphere remains relatively constant (c.f. [158, 159] and Chapter 5 and Figure 5.12 in [160]). Here it is held at a constant value of 0.44. At even higher Re a transition to turbulent flow occurs resulting in immediately lower values of C_{Ds} followed by increasing C_{Ds} with Re. This behavior is not captured here.

B.2 Gidaspow [74]

A drag model is formulated that is a combination of Ergun [145] and Wen and Yu [147] correlations stitched together based on void fraction. Here it is referred to as the Gidaspow [2, 161] drag model. Ergun proposed a comprehensive correlation for pressure drop through a *packed* bed of granular solids using data from the literature and his own experimental data which recognized the importance of simultaneous consideration of viscous and inertial energy loss. More specifically, he measured pressure drop through packed beds involving crushed solids materials (e.g., sand, pulverized coke) with different void fractions and over different gas flows. The drag force is then related to the pressure drop over the system so that the drag coefficient is written as:

[61] In determining their correlation the particle Reynold number was defined as a function of the *superficial* fluid velocity. Here it is replaced with the relative velocity difference of the fluid and solids phases.

$$\beta_{gm}^{\prime Ergun} = \frac{150\left(1-\varepsilon_g\right)^2 \mu_g}{\varepsilon_g d_m^2} + \frac{1.75\rho_g\left(1-\varepsilon_g\right)\left|U_{gi}-U_{mi}\right|}{d_m} \tag{B-6}$$

As has been well-noted (e.g., §2.4 in [39]), Ergun's expression is intended for dense flow conditions. To ensure representative behavior is predicted in the dilute limit it is replaced with a new expression. Wen and Yu (see section B.1 of this appendix) derived an expression for the drag force over a wide range of Reynolds number using literature data and their own data from a series of de-fluidization experiments (starting at fluidized state and decreasing the flow rate until a fixed bed condition). In the limit of a single particle ($\varepsilon_g \to 1$), Wen and Yu's expression will reduce to Schiller and Naumann [155] drag relation.

In this combined model, the correlation of Ergun is used for a void fraction less than 0.8 (or solids volume fraction greater than 0.2) otherwise the correlation of Wen and Yu is used:[62]

$$\beta_{gm}^{\prime} = \begin{cases} \beta_{gm}^{\prime\, WenYu} & \varepsilon_g \geq 0.8 \\ \\ \beta_{gm}^{\prime\, Ergun} & \varepsilon_g < 0.8 \end{cases} \tag{B-7}$$

B.3 Gidaspow Blend [162]

The drag model correlation referred to as the Gidaspow model [161, 2] (Appendix B.2) produces a discontinuity in the drag force at a void fraction of 0.8 (e.g., see discussion in [163]). To avoid numerical convergence problems, various approaches have been used to eliminate this discontinuity (e.g., [162, 164, 165, 166]). Lathouwers and Bellan [162, 164] use an inverse tangent function with a stitch point of $\varepsilon_g = 0.8$, that is, the function passes through the point 0.5 at void fraction of 0.8. For void fractions below this point the function becomes zero, and above this point the function becomes one. Later Huilin and Gidapow [166] essentially employ the same continuous function with the only difference between an additional multiplying factor of 1.75 is included within the arctan function. It is this latter version of the continuous stitching function that is implemented in MFIX:

$$\beta_{gm}^{\prime} = \phi_{gs}\beta_{gm}^{\prime\, WenYu} + \left(1-\phi_{gs}\right)\beta_{gm}^{\prime\, Ergun} \tag{B-8}$$

where

[62] Selection of $\varepsilon_g = 0.8$ as the switch point between these two models, likely stems back to discussion in [222] concerning a comparison of the Kozeny-Carman equation to reported experimental data and its inability to capture flow behavior in liquid-fluidized beds for $\varepsilon_g > 0.8$.

$$\phi_{gs} = \tan^{-1}\Big(150 * 1.75\big(\varepsilon_g - 0.8\big)\Big)/\pi + \frac{1}{2} \qquad \text{(B-9)}$$

And the drag coefficients $\beta_{gm}'^{WenYu}$ and $\beta_{gm}'^{Ergun}$ are presented in expressions (B-3) (along with (B-4) and (B-5)) and (B-6), respectively. Leboreiro et al. [167] explored the impact of the value of the transition point (given here by $\varepsilon_g = 0.8$) as well as the stitching function on injected-bubble and freely bubbling beds. They found the transition point itself had more influence in the former system then the latter. For further details see [167].

B.4 Syamlal-O'Brien [168]

Syamlal & O'Brien [168] propose a model for the drag force in multiparticle systems using the correspondence of the force balance relationships found under terminal settling conditions for single and multiple particle systems combined with a velocity-voidage correlation and an expression for the single particle drag coefficient. The applicability of the derived relationship beyond the terminal settling condition is then reasoned. The velocity voidage equation (V_r) expresses the ratio of the terminal settling velocity of a multiparticle system (V_t) to that of a single particle (V_{ts}) as a function of the void fraction. A well-known example is based on the sedimentation work of Richardson-Zaki [146]. Rather than use their expression for determining the drag force, which requires an iterative procedure, the velocity-voidage correlation proposed by Garside and Al-Dibouni [169] is used for which an analytic solution can be obtained. The resulting expression implemented in MFIX is shown below.[63]

$$\beta_{gm} = \frac{3}{4}\frac{(1-\varepsilon_g)\varepsilon_g\rho_g}{V_{rm}^2 d_{pm}}\left(0.63 + 4.8\sqrt{\frac{V_{rm}}{\mathrm{Re}}}\right)^2 \left|U_{gi} - U_{mi}\right| \qquad \text{(B-10)}$$

where

$$V_{rm} = 0.5\left[A - 0.06\mathrm{Re} + \sqrt{(0.06\mathrm{Re})^2 + 0.12\mathrm{Re}(2B - A) + A^2}\right] \qquad \text{(B-11)}$$

$$A = \varepsilon_g^{4.14} \qquad \text{(B-12)}$$

[63] It is worth noting that the velocity-voidage correlation proposed by Garside and Al-Dibouni [166] was defined as a function of the particle Reynolds number based on the terminal velocity of a single particle. In the derivation of Syamlal and O'Brien [165] the Reynolds number is expressed a function of the relative velocity difference of the phases.

$$B = \begin{cases} 0.8\varepsilon_g^{1.28} & \varepsilon_g \leq 0.85 \\ \varepsilon_g^{2.65} & \varepsilon_g > 0.85 \end{cases} \tag{B-13}$$

$$\mathrm{Re} = \frac{\rho_g \left| U_g - U_m \right| d_m}{\mu_g} \tag{B-14}$$

Appendix C: Nusselt Number Correlations

Nusselt number correlations reported in the literature span from single-particle correlations [170] to packed or fluidized beds [171, 137, 172]. The Nusselt number correlations available in MFIX are presented in the following sections. Table C-1 outlines the availability of each correlation with respect to each solids model.

Table C-1: Nusselt number heat transfer correlation availability in MFIX.

Correlation	Availability		
	MFIX-TFM	MFIX-DEM	MFIX-PIC
Gunn, 1978 [137]	(default)		
Ranz and Marshall, 1952 [170]		(default)	(default)

C.1 Gunn [137]

The Nusselt number correlation of Gunn [137],

$$\mathrm{Nu}_m = \left(7 - 10\varepsilon_g + 5\varepsilon_g^2\right)\left(1 + 0.7\mathrm{Re}_m^{0.2}\mathrm{Pr}^{1/3}\right) + \left(1.33 - 2.4\varepsilon_g + 1.2\varepsilon_g^2\right)\mathrm{Re}_m^{0.7}\mathrm{Pr}^{1/3} \tag{C-1}$$

is applicable for a porosity range of 0.35–1.0 and a Reynolds numbers up to 10^5. Here, where Re and Pr are the dimensionless Reynolds and Prandtl numbers given by

$$\mathrm{Re}_m = \frac{\rho_g \varepsilon_g \left|U_g - U_m\right| d_{pm}}{\mu_g} \tag{C-2}$$

$$\mathrm{Pr} = \frac{C_{pg}\mu_g}{\kappa_g} \tag{C-3}$$

C.2 Ranz and Marshall [170]

The Nusselt number correlation of Ranz and Marshall [170],

$$\mathrm{Nu} = 2.0 + 0.6\mathrm{Re}^{1/2}\mathrm{Pr}^{1/3} \tag{C-4}$$

was developed for single, isolated particles where Re and Pr are the Reynolds and Prandtl numbers.

Appendix D: Maximum Packing Correlations

This section provides the empirical correlations for computing the solids maximum packing in polydisperse systems.

D.1 Yu and Standish [173]

The Yu and Standish [173] correlation is used to calculate the solids volume fraction at maximum packing for a solids mixture containing two or more components.

$$\varepsilon_{s,mix}^{max} = \min_{m\in[1,M]} \left\{ \frac{\varepsilon_m^{max}}{\left(1 - \sum_{\substack{j=1 \\ j\neq m}}^{M} \left(1 - \frac{\varepsilon_m^{max}}{p_{ij}}\right) \frac{cx_i}{X_{ij}}\right)} \right\} \tag{D-1}$$

where ε_m^{max} is the maximum packing of the m^{th} solids phase. The remaining terms are defined as follows:

$$cx_i = \frac{\varepsilon_i}{\sum_{j=1}^{M} \varepsilon_j} \tag{D-2}$$

$$X_{ij} = \begin{cases} \dfrac{1 - r_{ij}^2}{2 - \varepsilon_i^{max}} & j < i \\ 1 - \dfrac{1 - r_{ij}^2}{2 - \varepsilon_i^{max}} & j \geq i \end{cases} \tag{D-3}$$

$$p_{ij} = \begin{cases} \varepsilon_i^{max} + \varepsilon_i^{max}(1 - \varepsilon_i^{max})\left(1 - 2.35 r_{ij} + 1.35 r_{ij}^2\right) & r_{ij} \leq 0.741 \\ \varepsilon_i^{max} & r_{ij} > 0.741 \end{cases} \tag{D-4}$$

$$r_{ij} = \begin{cases} d_{p,i}/d_{p,j} & i \geq j \\ d_{p,j}/d_{p,i} & i < j \end{cases} \tag{D-5}$$

D.2 Fedors and Landel [174]

The Fedors and Landel [174] correlation is used to calculate the solids volume fraction at maximum packing for a binary mixture of solids.

For $cx_1 < \frac{\varepsilon_1^{max}}{\varepsilon_1^{max}+(1-\varepsilon_1^{max})\varepsilon_2^{max}}$,

$$\varepsilon_{s,mix}^{max} = \left[(\varepsilon_1^{max} - \varepsilon_2^{max}) + \left(1 - \sqrt{r_{2,1}}\right)(1 - \varepsilon_1^{max})\varepsilon_2^{max}\right] * \left[\varepsilon_1^{max} + (1 - \varepsilon_1^{max})\varepsilon_2^{max}\right]\frac{cx_1}{\varepsilon_2^{max}} + \varepsilon_2^{max} \quad \text{(D-6)}$$

otherwise,

$$\varepsilon_{s,mix}^{max} = \left(1 - \sqrt{r_{2,1}}\right)[\varepsilon_1^{max} + (1 - \varepsilon_1^{max})\varepsilon_2^{max}]cx_2 + \varepsilon_2^{max}. \quad \text{(D-7)}$$

where cx_1 and cx_2 are given by Equation (D-2) and $r_{2,1}$ is obtained from Equation (D-5).

Randall Gentry
Deputy Director & Chief Research Officer
Science & Technology Strategic Plans & Programs
National Energy Technology Laboratory
U.S. Department of Energy

John Wimer
Associate Director
Strategic Planning
Science & Technology Strategic Plans & Programs
National Energy Technology Laboratory
U.S. Department of Energy

Bryan Morreale
Executive Director
Research & Innovation Center
National Energy Technology Laboratory
U.S. Department of Energy

Jimmy Thornton
Associate Director
Computational Science & Engineering
National Energy Technology Laboratory
U.S. Department of Energy